MIT
SEA
GRANT
PROGRAM

MATHEMATICAL MODELS OF THE MASSACHUSETTS BAY

PART III. A MATHEMATICAL MODEL FOR THE DISPERSION OF SUSPENDED SEDIMENTS IN COASTAL WATERS

by
Georgios C. Christodoulou
William F. Leimkuhler
and
Arthur T. Ippen

Massachusetts Institute of Technology
Cambridge, Massachusetts 02139

Report No. MITSG 74-14
January 31, 1974

MATHEMATICAL MODELS OF THE MASSACHUSETTS BAY

PART III. A MATHEMATICAL MODEL FOR THE DISPERSION OF SUSPENDED SEDIMENTS IN COASTAL WATERS

by

Georgios C. Christodoulou

William F. Leimkuhler

and

Arthur T. Ippen

Report No. MITSG 74-14
Index No. 74-314-Cbs

ERRATA - T. R. #179

Page 10: 4th line should read

m = Mass rate of injection of the sediment mixture

Page 12: 10th line should read

ν = Kinematic viscosity

Page 33: Equation (3.10a) should read

$$\alpha = \frac{w_s}{h} [\phi(0) - \phi(1)] + \frac{1}{h^2} [(\varepsilon_\zeta \frac{\partial \phi}{\partial \zeta})_{\zeta=0} - (\varepsilon_\zeta \frac{\partial \phi}{\partial \zeta})_{\zeta=1}]$$

Page 71: 4th line

ν should be λ

Page 80: 2nd line from the bottom should read

predictive capabilities

Page 124: Reference 1 should read

Environmental Equip. Div., EG&G, Waltham, Massachusetts, December 1972

MATHEMATICAL MODELS OF THE MASSACHUSETTS BAY

ABSTRACT - PART III

A MATHEMATICAL MODEL FOR THE DISPERSION OF SUSPENDED SEDIMENTS IN COASTAL WATERS

by

GEORGIOS C. CHRISTODOULOU

WILLIAM F. LEIMKUHLER

and

ARTHUR T. IPPEN

A three-dimensional analytical model is proposed for the description of the dispersion of fine suspended sediments in coastal waters. The model basically predicts the quasi-steady state sediment concentration as a function of space and tidal time and the deposition pattern in the region surrounding a continuous vertical line source. It requires that the sediment settling velocities and the hydrodynamic features of the area, the net drift and the tidal velocities as well as the dispersion coefficients be known. Effects of wave action and vertical stratification are not explicitly considered. A separation of variables technique permits a rather independent treatment of the vertical and horizontal distributions; they are linked primarily through the decay factor, which represents the loss of material to the bottom.

The model is applied to a hypothetical dredging situation in Massachusetts Bay. Values for the hydrodynamic parameters were obtained from the analysis of field data collected during the past year. Laboratory experiments were carried out for the determination of settling rates of clays in seawater, in view of unknown flocculation factors. Stoke's law was considered adequate for silt and very fine sand.

The model results indicated very long and relatively narrow dispersion patterns, under the assumption of constant drift direction. The net drift and the sediment settling velocity seem to be the most important factors controlling the dispersion of fines in coastal waters.

PART III

ACKNOWLEDGEMENTS

This study constitutes a part of a series of investigations in a major environmental research program on the "Sea Environment in Massachusetts Bay and Adjacent Waters". This program consists of theoretical and field investigations and is under the administrative and technical direction of Dr. Arthur T. Ippen, Institute Professor, Department of Civil Engineering and of Dr. Erik L. Mollo-Christensen, Professor, Department of Meteorology as co-principal investigators. Support of the program is provided in part by the Sea Grant Office of NOAA, Department of Commerce, Washington, D.C. through Grant No. NG-43-72, in part by the New England Offshore Mining Environmental Study (NOMES) of NOAA, in part by the Henry L. and Grace Doherty Foundation, Inc., and in part by the Department of Natural Resources, Commonwealth of Massachusetts through Project No. DMR-73-1. The project which is the subject of this report was conducted by staff members of the Ralph M. Parsons Laboratory for Water Resources and Hydrodynamics and was administered under Project No. DSR 80344, 80575 and 81100 at M.I.T.

All computer work was carried out at the M.I.T. Information Processing Center. The authors gratefully acknowledge the work of Ms. Sheila L. Frankel, who contributed laboratory results on background measurements of suspended sediment in Massachusetts Bay; she also assisted in the collection of current and suspended sediment field data along with Dr. Bryan R. Pearce, project coordinator, Mr. Edward F. McCaffrey, chief technician, Mr. Douglas A. Briggs, Mr. Cortis Cooper, Mr. Robert F. Paquette and Mr. John D. Wang.

Appreciation is expressed here to Ms. Susan M. Johnson and Ms. Stephanie M. Demeris for their excellent typing of this manuscript.

TABLE OF CONTENTS

TABLE OF CONTENTS (Ct'd)

LIST OF FIGURES

LIST OF FIGURES (ct'd)

LIST OF TABLES

LIST OF SYMBOLS

a	=	Reference depth for the vertical sediment distribution
A	=	Overall probability that a particle reaching the bottom is deposited there
A	=	Cross-sectional area (in one-dimensional models)
c	=	Concentration of suspended sediments
$\overline{c}$	=	Average concentration over the depth (or the cross section)
c_o	=	Total concentration of sediments in mixture injected
c_{oi}	=	Concentration of a particular group in mixture injected
c_a	=	Reference concentration at depth a for the vertical distribution
c''	=	Spatial deviation of local concentration from the average value over the depth (or the cross section)
d	=	Particle diameter
D	=	Rate of deposition
$\overline{D}$	=	Average value of D over the tidal cycle
E	=	Dispersion coefficient
E_x, E_y	=	Dispersion coefficients in x and y directions, respectively
E_L	=	Longitudinal dispersion coefficient (in one-dimensional models)
E_d	=	Part of the dispersion coefficient associated with the velocity variations over the depth (or the cross-section)
f	=	The Darcy-Weisbach friction factor
g	=	Acceleration of gravity
h	=	Total water depth
H	=	Height of water column in settling tube experiments

k = Von Karman's constant

ℓ = Length scale for diffusion

$2\ell_T$ = Movement due to tide (see Figure 14)

L = Distance from the source

m = Mass rate of injection of the sediment-seawater mixture

m_i = Mass rate of injection of sediment group i

n = Number of tidal cycles to steady state

M = Total mass injected

$P(\zeta)$ = Probability density function of the vertical position of particles, used by Elder (2-7). Analogous to $\phi(\zeta)$

r_o = Pipe radius in Taylor's formula (Equation 2-5)

r_i, r_e = Source and sink terms in general dispersion Equation (2-3)

s = $\overline{c}\, e^{-\alpha(t-\tau)}$, variable used in the transformation of the differential equation for $\overline{c}$ (see Section 5.1)

t = Time

T = Tidal period

T_I = Initial time, after which diffusion modelling is valid

T' = Time scale for mixing, as defined by Fischer

u,v = Local velocities (at depth z) along x and y directions, respectively

u'',v'' = Spatial deviations of u,v from their respective depth-averaged values u,v

u_f = Net drift velocity (at depth z) along x axis

u_T, v_T = Max tidal velocities (at depth z) along x,y axes, respectively

u_* = Shear velocity

U, V = Mean velocities over the depth in x,y directions, respectively

U_s, V_s = Mean-weighted velocities over the depth, i.e. transport rates along x,y directions, respectively (taking into consideration the nonuniform sediment distribution over the vertical)

U_f = Depth-averaged drift velocity along x axis

U_T, V_T = Depth-averaged max tidal velocities along x,y axes

U_{fs} = Mean transport rate along the net drift

U_{TS}, V_{TS} = Transport rates associated with the max tidal velocity in x,y directions

U_m = Representative velocity magnitude for the determination of u_*

$\forall$ = Volume rate of injection of the sediment-seawater mixture

w_s = Sediment settling velocity

x, y = Horizontal coordinates along net drift and normal to it

z = Vertical coordinate, increasing upwards

Z = Exponent in the expression of the vertical sediment distribution $= \frac{w_s}{k\beta u_*}$

α = Decay rate in the two-dimensional dispersion equation for the depth-averaged concentration

β = ϵ_z/ϵ_m

γ_s = Sediment specific weight

γ_w = Seawater specific weight

δ = Thickness of layer of sediment deposited

ε = Horizontal turbulent (eddy) diffusion coefficient

$\varepsilon_x, \varepsilon_y$ = Turbulent diffusion coefficients along x,y directions

$\varepsilon_z, \varepsilon_\zeta$ = Vertical sediment diffusion coefficient

$\overline{\varepsilon}_z$ = Mean value of ε_z over the depth

ε_m = Vertical momentum transfer coefficient

ζ = z/h, non-dimensional depth

η, ξ = Transformation of horizontal coordinates y,x (see Section 5.1)

λ = Constant of proportionality in formulas for the dispersion coefficient

λ_i = c_{oi}/c_o , proportion of group i in initial sediment mixture

r = Kinematic viscosity

ρ = Density

ρ_e = Effective density of loosely deposited sediment

ρ_s = Sediment density

ρ_w = Seawater density

σ^2 = Variance of sediment (or tracer) distribution along an axis

τ = Dummy time variable (see Section 5.1)

τ_o = Bottom shear stress

$\phi(\zeta)$ = Normalized vertical sediment distribution

ω = $\frac{2\pi}{T}$

Note: A prime is used to denote non-dimensional parameters, except for T' (see Section 5.1)

CHAPTER 1

INTRODUCTION

Suspended sediments of inorganic and organic origin exist in most coastal waters in varying small concentrations. Their presence arises either from natural sources or increasingly from man's activities near and off the shores. Natural erosion processes take place inland and produce suspended sediment which eventually reach the estuaries and the sea. Man has contributed to this natural supply by construction, waste disposal, agricultural and irrigation practices, and in more recent years provides additional amounts of sediments by extension of his activities to the shorelines and coastal waters.

The amount of sediment naturally present in the coastal environment must be considered a part of this environment, and all biological activity has in time come to quasi-equilibrium with this as with all other factors present. A drastic change in sediment concentration could hinder some natural processes possibly causing severe damage to many forms of life.

More specifically, suspended solid particles contribute to the turbidity of the waters and hence affect biological processes through the extinction of light. Thus, increased concentrations could impair the growth of many organisms locally as well as some distance away from the disturbance created by man. In addition, these particles, wherever they are deposited, could directly affect plant and animal life on the sea bed.

A growing concern has therefore arisen with regard to this type of pollution and the prediction of the movement and dispersion of the fine sediments introduced into a coastal area by dredging or dumping has become a most important problem. In order to make such a prediction, it is first necessary that the hydrodynamic characteristics of the area be known. Thus the problem requires information concerning dynamic characteristics such as the magnitudes and directions of tidal and non-tidal currents, the distribution of the velocities in the vertical direction, the vertical and horizontal dispersion rates, the effects of wind and waves, and other parameters. All of these depend upon the geometry and the geographical position of the body of water under consideration, in addition to the meteorological conditions. However, the geometry is usually complex and the meteorological conditions cannot be readily forecast. Theoretical approaches to the determination of the velocity field must therefore be based on simplifying assumptions.

The limited knowledge of sediment transport behavior, coupled with the hydrodynamic complexities, makes the problem one of extreme difficulty. The sediments of interest consist typically of very fine material. For the most part they fall into the silt and clay range. In the presence of sea water, electrochemical forces become important, causing flocculation, that is, the individual grains form larger aggregates which have lower density and mostly increased settling rates.

In spite of these complications, theoretical investigations can still lead to some significant results. Even under gross assumptions,

these results provide at least qualitative information, which can form the basis for more sophisticated approaches toward a good understanding of the process.

Previous investigations of the behavior of solid suspensions have dealt for the most part with single aspects of the problem. These studies are briefly reviewed in a following section.

The present study is an attempt to solve the general problem of sediment dispersion in coastal waters by combining the results of previous analytical investigations, field measurements, and laboratory experiments. Several simplifying assumptions were made to this end and a specific three-dimensional analytical model is proposed for a description of the processes involved. Numerical models may be developed as a further step. Nevertheless, it is believed that an analytical solution, relatively simple and generally applicable, can serve as a first approximation for the prediction of sediment transport and dispersion in coastal waters.

This analytical model starts with the general three-dimensional dispersion equations to which a separation of variables technique is applied so that the vertical concentration distribution can be treated independently. A single layer shear flow is then assumed, and the equilibrium concentration profile is found for the vertical direction, as is done in open channel flow. Stokes' law for settling velocities of sediments other than clays is applied. For clays such velocities were determined in a laboratory settling tube, however, without specific examination of the flocculation process.

A velocity field is assumed consisting of the superposition of a net drift and a sinusoidal tidal velocity at any angle to the net drift. Taking into consideration the nonuniform sediment distribution over the vertical, a technique for the analysis of current data was developed to provide values of the advection and dispersion factors in the two-dimensional dispersion equation which is then solved for the quasi-steady state case. It is further shown that in addition to the concentrations of suspended sediment as a function of time and space, deposition patterns on the sea bottom can also be derived.

This work was initiated as a complementary study to the Sea Grant Project, "The Sea Environment of Massachusetts Bay and Adjacent Waters", and to the New England Offshore Mining Environmental Study (NOMES-NOAA) which involved an experimental dredging operation planned in Massachusetts Bay for the summer of 1974. While the actual dredging operation has been cancelled, base line measurements were made during the past year and provided some input for the parameters needed for the application of the analytical model to a natural coastal environment.

The relative importance of the various parameters for predictive purposes is established. Thus field measurements can be planned with better judgement as to whether certain quantities should be determined accurately or can be estimated approximately without serious effects on the ultimate dispersion patterns.

CHAPTER 2

REVIEW OF PREVIOUS RESEARCH

There have been quite a number of studies related to the subject of the present work. Most of these, however, have dealt with only one aspect of the problem.

The relative vertical distribution of suspended sediment in a turbulent stream can be stated in analytical form when a suitable velocity distribution function is introduced into the differential equation for the equilibrium between turbulent upward transport of sediment and downward settling due to gravity. The latter relation was first established by Schmidt (1925) to describe the distribution of dust particles in the air. In the 1930's, Ippen (16) and Rouse (26) introduced the velocity distribution functions by Krey and Von Karman, respectively, with identical results. A linear shear distribution for a steady, two-dimensional flow was also assumed. The well-known solution is:

$$\frac{c}{c_a} = \left[\frac{h-z}{h-a}\ \frac{a}{z}\right]^Z \qquad (2\text{-}1)$$

where

$$Z = \frac{w_s}{k\beta u_*}$$

c_a = the reference concentration at elevation a

h = the total depth

w_s = the settling velocity of the particles

k = the Von Karman constant

β = $\varepsilon_z/\varepsilon_m$, the ratio of the sediment mass exchange coefficient to the momentum transfer coefficient

u_* = $\sqrt{\frac{\tau_o}{\rho}}$, the shear velocity

τ_o = the bottom shear stress

ρ = fluid density

Dobbins (6) investigated the problem of vertical sediment distribution in the transient state, and by a separation of variables technique he obtained a solution as a series expression. He also conducted experiments to verify his results.

Since that time, the parameters appearing in the exponent, Z, of Equation (2-1) have become the subject of research. The Von Karman constant was found to depend upon the near-bed concentration, while $k = 0.4$ applies strictly only to clear water. Furthermore, the velocity distribution changes due to the presence of suspended sediments, as Ippen pointed out (17). These changes, however, are significant only in the case of high sediment concentrations, and therefore are not considered important to the present work.

Another subject of debate was the coefficient β, which has been found to take on values both higher and lower than unity (18). Nevertheless, for fine sediments most investigators agree on a value of β close to 1.

The greatest difficulties arise in estimates of the proper values for the settling velocities of the suspended particles. Stoke's law is adequate for very fine sands, however it is not readily applied to clay particles because the settling rates of clays are altered by flocculation. In this process large groups of particles with high settling rates are formed from collision of smaller ones. Flocculation takes place to a high degree in the sea environment. Partheniades (24,25) and Krone (7,20) have done extensive work in the field of deposition of fine clays in estuaries and generally in salt water. While the mechanism of collision is well understood, the rates of sedimentation are, in general, far from being quantitatively determined. Because of the need for some form of quantitative prediction of settling rates in the present study, it was decided that some laboratory experiments should be performed. Sections 4-4 and 4-5 deal with this problem of flocculation in more detail.

Recently, Jobson and Sayre, in a series of papers have approached the problem of dispersion in a uniform open channel flow with turbulent shear, through a two-dimensional model, i.e. not considering lateral variations of velocity

$$\frac{\partial c}{\partial t} + u(z)\frac{\partial c}{\partial x} = \frac{\partial}{\partial z}\left(\varepsilon_z \frac{\partial c}{\partial z}\right) + w_s \frac{\partial c}{\partial z} + \varepsilon_x \frac{\partial^2 c}{\partial x^2} \qquad (2\text{-}2)$$

where ε_z = the turbulent diffusion coefficient in the vertical direction

ε_x = the turbulent diffusion coefficient in the longitudinal direction which is considered constant

$u(z)$ = the longitudinal velocity at depth z

w_s = the fall velocity of the particles

Sayre (27) worked on the transient distribution of suspended solids in the silt range. He used the method of moments to formulate a finite difference scheme, which provides values for the moments of the distribution of the suspension. He elaborated on the bottom boundary condition, introducing a bed absorbency factor and an entrainment factor. He also investigated their effect upon the dispersion process. Jobson and Sayre (18,19) incorporated these two factors into one coefficient, called A, which effectively represents the overall probability that a particle settling to the bed is deposited there. Its importance was examined, but its value was not determined for any particular sediment. The two-dimensional equation was simplified for the steady state by omitting the term $\frac{\partial c}{\partial t}$, and assuming $\varepsilon_x \frac{\partial^2 c}{\partial x^2}$ as negligible. The resulting numerical solution was compared to experimental results. They stated in their conclusions that the fall velocity is the primary factor for controlling the rate of descent of the sediment matter; the effect of turbulence on the fall velocity was negligible compared to the effects of grouping due to the injection method. The accuracy of the vertical diffusivity (ε_z) distribution was found not to be particularly important for the determination of the vertical concentration profiles.

Other researchers, working mainly on the dispersion of pollutants, tried to estimate the longitudinal dispersion coefficient E_L, appearing

in the general one-dimensional dispersion equation as stated by Harleman (12):

$$\frac{1}{A}\frac{\partial(A\bar{c})}{\partial t} + \frac{1}{A}\frac{\partial}{\partial x}(AU\bar{c}) = \frac{1}{A}\frac{\partial}{\partial x}(AE_L\frac{\partial\bar{c}}{\partial x}) + \frac{r_i}{\rho} + \frac{r_e}{\rho} \qquad (2\text{-}3)$$

where A = the (variable) cross-sectional area of the channel

$U, \bar{c}$ = the cross-sectional averages of velocity and concentration, respectively

$\frac{r_i}{\rho}, \frac{r_e}{\rho}$ = source and sink terms

E_L is the sum of the longitudinal diffusivity and a term accounting for the velocity variations over the cross section:

$$E_L = \varepsilon_x + \frac{\frac{1}{A}\int_A u''c''dA}{-\frac{\partial\bar{c}}{\partial x}} \qquad (2\text{-}4)$$

where u",c" are the spatial deviations of the velocity and concentration from their mean values, U and $\bar{c}$. The second term is normally much greater than the first.

G.I. Taylor first developed in 1954 a theoretical formula for determining E_L in a circular pipe, assuming a logarithmic velocity distribution. His formula was

$$E_L = 10.1\, r_o u_* \qquad (2\text{-}5)$$

where r_o = the radius of the pipe.

Elder in 1959 (8) carried out a similar computation for steady, uniform, two-dimensional (i.e. infinitely wide) open channel flow with a logarithmic velocity distribution and found

$$E_L = 5.9\, hu_* \qquad (2\text{-}6)$$

where h = the depth of the channel.

Both Taylor and Elder verified their results by tracer experiments. Elder, in addition, pointed out that his formula is valid only for suspensions of uniform vertical distribution and that a similar analysis could be done for particles having a non-uniform distribution, by considering the deviations of the local velocity from the mean-weighted velocity, rather than from the average velocity. The mean-weighted velocity is:

$$U_s = \int_0^1 P(\zeta) u \, d\zeta \qquad (2\text{-}7)$$

where $P(\zeta)$ = the probability density function of the position of the particles, analogous to their vertical distribution.

u = the local velocity

ζ = non-dimensional depth z/h

Later on, Fischer (9) suggested that in a natural river lateral variations of velocity are more significant than vertical ones. His formula for finding the longitudinal dispersion based on the lateral depth-averaged velocity distribution gives values of at least an order

of magnitude higher than Taylor's values. Fischer also tried to estimate the "initial time", T_I, after which the dispersion resulting from an instantaneous injection is adequately described by models of the form of Equation (2-3). He defined a time scale for cross-sectional mixing, $T' = \frac{\ell^2}{\epsilon}$, where ℓ is the distance over which diffusion takes place (e.g. the distance from the point of maximum velocity in the cross section to the channel boundary) and ϵ the diffusion coefficient in the corresponding direction. He concluded that for a pollutant initially uniformly distributed over the cross section, $T_I \cong 0.4T'$.

These studies increased the understanding of the dispersion process in natural streams, but the extension of their conclusions to estuaries, where the flow includes a periodic component, and, moreover, to coastal waters is not straightforward.

For estuaries, Harleman (12) proposed that Taylor's basic equation could be used, modified so as to include the hydraulic radius instead of the pipe radius and also have an increased coefficient (by a factor of 2) to account for natural non-uniformities. He suggested using the average value of the absolute magnitude of the velocity over the tidal cycle. More detailed approaches to the problem of sinusoidal tidal velocities were made by Holley and Harleman (15) and Holley, Harleman, and Fischer (14). In the former it was found that the fluctuations of the dispersion coefficient due to the tide become insignificant after 1 to 2 tidal cycles following injection. In the latter it was suggested that two dispersion coefficients could be computed, one from the vertical and one from the lateral velocity variation and the larger

should be used in the dispersion equation. It was found that the "initial time" was approximately $T_I = 0.2T'$, that is, about half its value for steady flow. Finally, it was indicated that an order of magnitude accuracy in the value of the dispersion coefficient was adequate for modelling continuous injections. This conclusion is very important for the present study, in view of the difficulty involved in the determination of this coefficient.

Another approach to the dispersion in periodic flow was made by Okubo (23), who assumed a linear oscillating velocity profile and worked with the method of moments to find the variance σ_x^2 of the longitudinal distribution. From this the dispersion coefficient could be defined as

$$E_x = \frac{\sigma_x^2}{2t} \qquad (2\text{-}8)$$

In periodic flow the coefficient has only half its value for a steady flow of the same velocity.

Okubo also presented an excellent review of previous work relative to the horizontal diffusion coefficient in the ocean. He collected information from numerous experiments and correlated the diffusion coefficient to a characteristic length scale (22). The purely diffusive process, however, does not contribute significantly to the overall dispersion of sediments and therefore is not of great significance to the present study.

Lately, three-dimensional models for dispersion problems began to appear. Wnek and Fochtman (33) combined some of the previous ideas

to develop a mathematical model for dispersion of pollutants in near-shore waters; assuming constant dispersion coefficients in all three directions they found an analytical solution in terms of error functions for the case of infinitely distant boundaries, which they adjusted for a finite depth by the method of images. However, they considered only neutrally buoyant particles. Also, they did not include tidal currents in the model.

Tetra Tech published a report (31) on the dispersion of radioactive debris due to an underwater explosion; this was a detailed study in which a three-layer model was developed to account for the thermocline and the transfer between layers was considered. The vertical profiles of the ocean currents were examined and a vertical density gradient was taken into account. The solution of the model was performed numerically by the method of moments and numerous computer plots of the concentration and other parameters vs. time and space were presented in the report. In this study, the particles were also assumed to be neutrally buoyant. Furthermore, the effect of the bottom was considered negligible, since the model dealt with deep oceans rather than coastal areas.

In addition to mathematical models, major field studies were also carried out in some areas, specifically for estimating the hydrodynamic characteristics of relevance to dispersion of suspended particles. For example, current meter and dye studies were made in the Gulf of Maine (1). The dispersion coefficient was found to be larger in the direction of the stronger current, as expected, but the natural variations of the parameters were too large to establish a reliable

correlation between dispersion and current magnitudes.

Finally, under the NOMES project itself, a discharge of glass beads simulating the sediment entrainment due to offshore mining was performed in June 1973 (21,13). At that time Hess had developed a preliminary model for predicting the dispersion of suspended matter (21). The model was intended to give only rough estimates and thus some factors such as the tide and the vertical diffusion were not considered. He used the same dispersion coefficient for all directions as obtained from a surface dye study combined with aerial photographs taken in the summer of 1972.

CHAPTER 3

THE MATHEMATICAL MODEL

3.1 Basic Assumptions

The analytical solution required several assumptions concerning the geometry of the water body, the velocity field, and the characteristics of the sediments.

The sediments are assumed to be introduced continuously into the water body along a uniform vertical line source, at a constant rate. The sediment is assumed to consist of a number of grain size groups, each having a certain settling velocity, w_s. These settling velocities are considered to be constant over the depth. Flocculation of particles in the clay range is taken into consideration as discussed in Sections 4.4 and 4.5.

The location of the line source is assumed to be far enough from the shore so that problems due to the land-sea boundaries do not arise. Amongst these, for example, is the action of breaking waves. In deeper water the effect of waves is negligible and need not be considered. Wave action may have some influence on sediment suspension, but it affects it only indirectly by increasing vertical diffusion.

The depth of the body of water is assumed to be constant. If the resulting movement of sediments does not extend to areas with significantly different depth, this assumption is justified in view of the great simplification involved.

In the ideal case of a straight shoreline, the velocity field near the shore would normally consist of a longshore current and some tidal component normal to the coast. However, since the area of interest is a considerable distance offshore, this is not necessarily true. Therefore, for purposes of generality, the tidal and net drift directions are not assumed as normal to each other. These directions are not easily determined in any particular coastal region. The difficulties increase as the geometry of the area becomes more complicated and field measurements are necessary for the determination of the prevailing current directions and magnitudes.

The coordinate system is set up with the origin on the bottom at the position of the vertical line source, the x-axis parallel to the net drift, the y-axis normal to the drift, and the z-axis vertical upwards. The flow field is modeled as a one layer system, that is, no thermocline is considered.

The currents are assumed as functions of depth, z, only, and invariable in the horizontal directions. The tidal velocities are, of course, also functions of time. Thus, the flow field may be represented as follows:

x-axis: $u(z,t) = u_T(z) \sin \omega t + u_f(z)$ (3-1.a)

y-axis: $v(z,t) = v_T(z) \sin \omega t$ (3-1.b)

z-axis $w = 0$ (3-1.c)

where

u_f = net drift velocity

u_T, v_T = the components of the maximum tidal velocity, assumed sinusoidal

Since many of the assumptions would not apply near the shore, a detailed shoreline configuration is not essential to the model. For simplicity, it may be represented by a straight line or a set of straight lines.

3.2 Structure of the Model

Under the above assumptions, the mass balance equation for suspended matter is:

$$\frac{\partial c}{\partial t} + u \frac{\partial c}{\partial x} + v \frac{\partial c}{\partial y} - w_s \frac{\partial c}{\partial z} = \frac{\partial}{\partial x}(\varepsilon_x \frac{\partial c}{\partial x}) + \frac{\partial}{\partial y}(\varepsilon_y \frac{\partial c}{\partial y}) + \frac{\partial}{\partial z}(\varepsilon_z \frac{\partial c}{\partial z}) \quad (3\text{-}2)$$

where w_s is the particle settling velocity and ε_x, ε_y, ε_z are the turbulent or eddy diffusivities in the three corresponding directions. The two horizontal diffusivities are normally independent of x and y and equal. Therefore, Equation (3-2) can be written as:

$$\frac{\partial c}{\partial t} + u \frac{\partial c}{\partial x} + v \frac{\partial c}{\partial y} - w_s \frac{\partial c}{\partial z} = \varepsilon_x \frac{\partial^2 c}{\partial y^2} + \varepsilon_y \frac{\partial^2 c}{\partial y^2} + \frac{\partial}{\partial z} \left(\varepsilon_z \frac{\partial c}{\partial z}\right) \qquad (3\text{-}3)$$

The depth, h, in coastal areas is, in general, much smaller than the horizontal dimensions. Therefore, vertical equilibrium is achieved after a relatively short time. In general, this time depends on the depth and the vertical diffusivity, ε_z, provided that the particles are small. Using the definition of "time scale" for diffusion T' (g,14), it is found to be h^2/ε_z. This is believed to be an upper bound for the time to equilibrium, since the settling velocity acts in addition to the vertical diffusivity. It should be noted that the diffusion-type modeling of the process does not hold for short times after the beginning of the injection, as already mentioned in Chapter 2. Also, the model is not expected to be valid in the immediate vicinity of the sediment source, because the time needed for vertical equilibrium implies some excursion of the sediment away from the source, before the model is reliable.

Once vertical equilibrium is established the shape of the vertical profile does not depend upon the magnitude of concentration over some range. This assumption is basic to the solution of the model, for it permits independent treatment of the vertical and horizontal distributions. In fact, the concentration, c, can be represented as the product of a depth-averaged function, $\bar{c}$, and a normalized function of depth, ϕ:

$$c(x,y,z,t) = \bar{c}(x,y,t)\phi(\zeta), \quad \zeta = z/h \tag{3-4}$$

where

$$\int_0^1 \phi(\zeta)d\zeta = 1 \tag{3-4a}$$

The parameters u, v, c can be written

$$\begin{aligned} u &= U + u'' \\ v &= V + v'' \\ c &= \bar{c} + c'' \end{aligned} \tag{3-5}$$

where U, V, $\bar{c}$ are the depth-averaged values of the velocities and concentration, and u'', v'', c'' are the spatial deviations about these average values. Thus, Equation (3.3) becomes

$$\frac{\partial c}{\partial t} + (U + u'') \frac{\partial(\bar{c}+c'')}{\partial x} + (V + v'') \frac{\partial(\bar{c}+c'')}{\partial y} - w_s \frac{\partial c}{\partial z}$$

$$= \varepsilon_x \frac{\partial^2 c}{\partial x^2} + \varepsilon_y \frac{\partial^2 c}{\partial y^2} + \frac{\partial}{\partial z}\left(\varepsilon_z \frac{\partial c}{\partial z}\right) \tag{3-6}$$

Averaging over the depth and taking into account

i) the Leibnitz Rule for differentiation of integrals

ii) the fact that $\int_0^h u'' \, dz = 0$, $\int_0^h v'' \, dz = 0$, $\int_0^h c'' \, dz = 0$

iii) simplifications such as $\frac{\partial}{\partial x} c'' = \frac{\partial}{\partial y} c'' = 0$

the equation takes the form

$$\frac{\partial \bar{c}}{\partial t} + U \frac{\partial \bar{c}}{\partial x} + V \frac{\partial \bar{c}}{\partial y} - \frac{w_s \bar{c}}{h} [\phi(1) - \phi(0)]$$

$$= E_x \frac{\partial^2 \bar{c}}{\partial x^2} + E_y \frac{\partial^2 \bar{c}}{\partial y^2} + \frac{\bar{c}}{h^2} [\varepsilon_\zeta \frac{\partial \phi}{\partial \zeta})_{\zeta=1} - (\varepsilon_\zeta \frac{\partial \phi}{\partial \zeta})_{\zeta=0}] \qquad (3\text{-}7)$$

where

$$E_x = \varepsilon_x + \frac{\int_0^h u''c''dz}{-h \frac{\partial \bar{c}}{\partial x}}, \quad E_y = \varepsilon_y + \frac{\int_0^h u''c''dz}{-h \frac{\partial \bar{c}}{\partial y}} \qquad (3\text{-}7a,b)$$

The coefficients E_x and E_y account for both the turbulent diffusion and the dispersion due to the non-uniform velocity distribution. They are refered to simply as the dispersion coefficients. In the case of heavy particles, which have more variable concentrations over the depth, the mean transport rates should be used (Elder (8)) rather than the mean velocities. That is,

$$U_s = \frac{\int_0^h uc dz}{\int_0^h c dz} = \frac{1}{h}\int_0^h u \frac{c}{\bar{c}} dz = \int_0^1 u\phi d\zeta \qquad (3\text{-}8a)$$

and similarly $V_s = \int_0^1 v\phi d\zeta \qquad (3\text{-}8b)$

These weighted velocities, U_s and V_s, describe the advective motion of the centroid of the dispersing suspended matter. They are the product of the corresponding mean water velocities over the depth and the coefficient a, as defined by Ippen (17). It is evident that

the physical meaning of the dispersion coefficients given by Equations (3.7a,b) is modified accordingly. Their second term should account for the velocity deviations about the weighted-mean values, as defined in Equations (3.8a,b).

Equation (3.7) can be further written

$$\frac{\partial \bar{c}}{\partial t} + U_s \frac{\partial \bar{c}}{\partial x} + V_s \frac{\partial \bar{c}}{\partial y} = E_x \frac{\partial^2 \bar{c}}{\partial x^2} + E_y \frac{\partial^2 \bar{c}}{\partial y^2} - \alpha \bar{c} \qquad (3\text{-}9)$$

where

$$\alpha = \frac{w_s}{h}[\phi(0) - \phi(1)] + \frac{1}{h^2}[(\epsilon_\zeta \frac{\partial \phi}{\partial \zeta}_{\zeta=0} - (\epsilon_\zeta \frac{\partial \phi}{\partial \zeta})_{\zeta=1})] \qquad (3.10a)$$

or

$$\alpha = [\frac{w_s \phi(0)}{h} + \frac{1}{h^2}(\epsilon_\zeta \frac{\partial \phi}{\partial \zeta})_{\zeta=0}] - [\frac{w_s \phi(1)}{h} + \frac{1}{h^2}(\epsilon_\zeta \frac{\partial \phi}{\partial \zeta})_{\zeta=1}] \qquad (3.10b)$$

Equation (3.9) has the familiar form of a two-dimensional dispersion equation, with α representing the decay constant. The meaning of α can also be understood in view of Equation (3.10b). The first term represents the rate of loss of material to the bottom, while the second term expresses the gain of material through the surface. The latter may be assumed zero. These considerations will be discussed in Section 4.2 .

The vertical distribution, represented by the normalized function $\phi(\zeta)$, plays a key role in the determination of the horizontal distribution. It not only readily defines the decay rate α (Equation 3.9, 3.10) but also affects the advective terms (3.8a and b) and the dispersion coefficients.

CHAPTER 4

THE VERTICAL CONCENTRATION DISTRIBUTION

4.1 The Normalized Equilibrium Distribution

Because of the assumption that the shape of the vertical profile does not depend upon the horizontal variations, it is possible to solve for the vertical distribution first. In fact, this order is essential, since important parameters for the solution of the horizontal distribution require knowledge of the normalized function $\phi(\zeta)$. In addition, the main objective of this work is to obtain the quasi-steady state solution of the entire problem. The distribution over the vertical dimension will be the first to come to equilibrium because of the relatively small value of h^2/ε_z. Thus, total equilibrium is obtained when the horizontal (depth-averaged) concentration distribution reaches steady state, provided that the time needed for this is sufficiently larger than h^2/ε_z.

Because of the relatively short duration of the transition period, only the equilibrium state of the vertical distribution will be considered here. The vertical profile of suspended sediments over the depth, under equilibrium conditions, is described by the Schmidt equation:

$$\varepsilon_z \frac{\partial c}{\partial z} + w_s c = 0 \qquad (4\text{-}1)$$

where c = the concentration of suspended matter at depth z

w_s = the settling velocity of the grain size considered

ε_z = the vertical mass diffusivity for sediment

This equation expresses a balance between the tendency of the particles to settle ($w_s c$) and the upward flux of sediments due to diffusion ($\varepsilon_z \frac{\partial c}{\partial z}$). In order to solve for c it is necessary to provide expressions for w_s and ε_z. The latter is a function of z, whereas w_s can be considered constant.

The sediment diffusivity ε_z is related to the turbulent momentum transfer coefficient ε_m by the relation

$$\varepsilon_z = \beta \varepsilon_m \tag{4-2}$$

where β is close to unity for the very small particles with which the present work is concerned. The value of ε_m is obtained from the velocity profile. In the case of a logarithmic velocity distribution and of the related linear shear distribution in a uniform open channel flows, the distribution of ε_m over the depth is parabolic. The solution to the Schmidt equation under the above assumptions is

$$c = c_a \left[\frac{h/z-1}{h/a-1}\right]^Z \tag{4-3}$$

where $Z = \frac{w_s}{\beta k u_*} = 2.5 \frac{w_s}{u_*}$ (for $\beta = 1$, $k = 0.4$) (4-4)

In Equation (4-3) a is a reference depth at which the concentration c_a is supposedly known. The shear velocity, u_*, is related to the mean velocity and the Weisbach-Darcy friction factor, f, by the relation

$$u_* = \sqrt{\frac{f}{8}}\, U_m \tag{4-5}$$

The value of U_m to be used here should represent a mean current magnitude regardless of direction. For flat bed conditions the friction factor may be given an average value close to $f \approx 0.02$, thus $u_* \approx \frac{1}{20} U_m$.

The one-layer shear flow with a logarithmic velocity profile assumed here may be a poor description of coastal currents, especially during the summer season when a definite thermocline exists. Nevertheless, recalling that wave action and density differences have been neglected in the level of sophistication of this model, the shear effects become primary factors of transport and dispersion of suspended matter. Furthermore, the logarithmic velocity profile was adopted in view of the extensive work done in justifying its application to open-channel flow and the lack of adequate field information to propose a different profile. A different assumption about the vertical velocity profile would lead to a different distribution of ϵ_z. However the vertical concentration distribution is not very sensitive to changes in

ε_z, as Jobson has stated (19). The general procedures shown in this model can be easily made to comply with any profile that might be found to prevail in a specific coastal area. Thus, the generality of this study is not restricted by the velocity profile assumption.

It can be seen from Equation (4-3) that the shape of the vertical profile for a particular grain size (i.e. w_s) and certain flow conditions (i.e. u_*) is constant, provided that the concentrations are sufficiently low so that k can be assumed constant (The actual magnitude of the profile depends, of course, on the reference value c_a). Therefore, the assumption made in Chapter 3 regarding the similarity of the vertical profiles is justified.

Recalling that $c = \bar{c}\phi$, Equation (4-3) can be written in terms of $\phi(\zeta)$:

$$\phi(\zeta) = \phi(a/h)\left[\frac{h/z-1}{h/a-1}\right]^{Z} \tag{4-6}$$

Before proceeding to more details, it should be mentioned that the Schmidt equation is not valid very close to the bottom. It is fairly well-established that in the lower 4-5% of the total depth, the concentration is approximately constant, not obeying Equation (4-3) although measurements in that zone are difficult both in the laboratory, because of the size of the instruments, and in the field, because of the interference of the bed-load transport.

In light of this approximation, it is convenient to chose a reference depth a = 0.05 h which yields the following normalized

profile:

$$\phi(\zeta) = \phi(0.05)\left[\frac{1/\zeta-1}{20-1}\right]^{Z} \quad \text{for } \zeta \geq 0.05$$

$$\phi(\zeta) = \phi(0.05) \quad \text{for } \zeta \leq 0.05 \tag{4-7}$$

In most cases the reference concentration c_a for Equation (4-3) has to be determined experimentally. However, due to the fact that $\phi(\zeta)$ is a normalized function, the determination of $\phi(0.05)$ can be performed analytically, by combining (4-7) with Equation (3-4a), i.e. $\int_0^1 \phi(\zeta)d\zeta = 1$. The resulting value of $\phi(0.05)$ is

$$\phi(0.05) = \frac{1}{\left[0.05 + \int_{0.05}^{1} \left[\frac{1/\zeta-1}{19}\right]^{Z} d\zeta\right]} \tag{4-8}$$

The integral can be evaluated numerically for several values of Z, corresponding to different settling velocities. This is done through a computer program, which then finds $\phi(0.05)$ and the whole vertical distribution according to Equation (4-7). This program is presented in Appendix B, as part of the larger program developed for the model and discussed in Chapter 7.

4.2 Boundary Conditions - Determination of the Decay Rate

In order to determine the decay factor α of the depth-averaged distribution, it can be seen from Equation (3.10) that the values of the normalized vertical distribution and its derivative must be known

at the bottom ($\zeta = 0$) and the surface ($\zeta = 1$).

From Equation (4-7) it is evident that $\phi(1) = 0$

Also $\epsilon_\zeta = 0$ at $\zeta = 1$

$$\text{Thus, } \alpha = \frac{w_s}{h}\ \phi(0) + \frac{1}{h^2}\ (\epsilon_\zeta \frac{d\phi}{d\zeta})_{\zeta=0} \tag{4-9}$$

In the general case, the bottom boundary condition may be expressed (18,19) as

$$\epsilon_z \frac{dc}{dz} + (1-A)w_s c = 0 \qquad \text{at} \quad z = 0 \tag{4-10}$$

This can be written

$$\frac{\epsilon_\zeta}{h} \frac{dc}{d\zeta} + (1-A)w_s c = 0 \qquad \text{or}$$

$$\frac{\epsilon_\zeta}{h} \frac{d\phi}{d\zeta} + (1-A)w_s \phi = 0 \qquad \text{at} \quad \zeta = 0 \tag{4-11}$$

The quantity "A" represents the overall probability that a particle reaching the bottom will stay there and will not be resuspended. It refers to a time average of the percentage of particles sticking to the bottom relative to all particles that reach it. In fact, A does not distinguish between those particles that simply "bounce" off the bottom and those that remain at the bottom being replaced by other, newly scoured, particles. It is believed that A is related to the flow conditions, specifically the mean velocity and bottom shear and also to the sediment characteristics, particularly the degree of

cohesion. The lower the flow velocity or bottom shear, the higher A is expected to be, approaching unity.

For fine cohesive sediments, some quantitative relations have been derived. Partheniades (24,25) tried to determine the minimum shear stress under which all suspended matter is deposited, and the equilibrium concentrations of clays in suspension under certain flow conditions. Einstein and Krone (7) conducted experiments with "San Francisco Bay mud" and found a linear relation between the percentage deposited and the bottom shear. These results, however, were derived with specific sediments and experimental techniques and cannot be easily extended.

In general, A is a very uncertain factor to predict and accurate values have to be determined experimentally for every particular problem. For the low velocities prevailing in coastal areas, A is expected to be close to unity. As Jobson and Sayre (19,27) have reported, changes in A seem to affect the vertical profile only very close to the bottom.

Nevertheless, A is very important for the horizontal distribution. It is directly related to the decay constant α. In fact, Equation (4-11) may be written:

$$\frac{1}{h}\left(\varepsilon_\zeta \frac{d\phi}{d\zeta}\right)_{\zeta=0} + w_s\phi(0) = Aw_s\phi(0) \qquad (4\text{-}11a)$$

By comparison of Equations (4-9) and (4-11a) it is evident that

$$\alpha = \frac{Aw_s\phi(0)}{h} \qquad (4\text{-}12)$$

It must be mentioned that the assumption of constant $\phi(\zeta)$ in the interval $0 \leq \zeta \leq 0.05$ (Section 4.1) implies $\left.\frac{d\phi}{d\zeta}\right|_{\zeta=0} = 0$, which is inconsistent with any value of A other than 1, as it can be readily seen from Equation (4-11). For $A < 1 \rightarrow \left.\frac{d\phi}{d\zeta}\right|_{\zeta=0} < 0 \rightarrow \phi(0) > \phi(0.05)$. It would be possible to modify this small lower portion of the vertical profile so that various values of A can be incorporated. The correction, however, would be insigificant in view of the many uncertainties involved in the near-bottom concentrations. Hence, Equations (4-7) are considered herein as giving an adequate description of the vertical profile, regardless of the value of A.

4.3 Sediment Settling Velocities

The settling velocity is the most important sediment characteristic. It affects directly the vertical distribution (Equation 4-4) and indirectly the horizontal distribution, mainly through the decay factor (Equation 4-12).

In the present work only fine particles are of interest. Their fineness is essentially associated with their ability to stay in suspension for a sufficiently long time so that they can travel a reasonable distance away from the source before being deposited. The terms "sufficiently" and "reasonable" are of course vague; it remains for the engineer to estimate appropriate values for every particular problem, based on such factors as depth, magnitude of currents, etc.

In the case of the area of interest in Massachusetts Bay, the depth is approximately 30 meters. If the particles are required to

travel for at least one hour before being deposited, the maximum settling velocity of interest is of the order of 0.8 cm/sec. Particles with such small settling velocities are considered to follow Stoke's law:

$$w_s = \frac{gd^2}{18\nu} (\gamma_s - \gamma_w) \qquad (4\text{-}13)$$

where d = the diameter of the particle

g = the acceleration of gravity

ν = the kinematic viscosity of the water

γ_s = the specific weight of the sediment considered

γ_w = the specific weight of seawater

Substituting, $g = 981$ cm/sec^2

$\gamma_s \simeq 2.65$ for natural sand and silt,

$\gamma_w \simeq 1.025$ for a mean temperature of 10°C and a salinity of 33 $o/_{oo}$

$\nu \simeq 1.31 \times 10^{-2}$ cm^2/sec (at 10°C)

the resulting settling velocity is

$$w_s = 0.68 \times 10^4 d^2 \qquad (4\text{-}13a)$$

Therefore, $w_s = 0.8$ cm/sec corresponds to a particle size of $d = 0.0108$ cm = 108 μ. In the present work particles smaller than 100 μ will be considered.

Stoke's law refers to spherical particles of diameter d. Particles having the same volume and weight but different shapes have significantly different settling velocities. However the settling velocity, not the actual shape and size of a particle, is the sediment characteristic most essential to this study; thus, the particles can be classified in terms of "equivalent Stoke's diameters".

Following the MIT soil classification, the sediments are divided into groups of particle sizes and characterized as "very fine sand", "silt" and "clay" as shown in Table 1. The settling velocities are computed using Equation (4.13a). The mean velocity of the group will be used as the representative value for all sediments belonging to it. The value for the clay group corresponds to d = 1 μ. The distribution of each group can be examined independently if the interaction between various groups is assumed negligible (29). This is true for low concentrations.

Table 1. Separation of Fines into Groups

Group Name	Particle Size range (μ.)	Settling Velocities w_s (cm/sec) lowest	highest	mean
Very fine sand	60-100	0.245	0.680	0.462
Coarse silt	20-60	2.72×10^{-2}	0.245	0.136
Medium silt	6-20	2.45×10^{-3}	2.72×10^{-2}	1.43×10^{-2}
Fine silt	2-6	2.72×10^{-4}	2.45×10^{-3}	1.36×10^{-3}
Clay	< 2		2.72×10^{-4}	0.68×10^{-4}

4.4 Flocculation Characteristics and Effects

While for the sand and silt range the above considerations are adequate for the determination of the settling rates, the phenomenon of flocculation does not allow such a simplified approach for the clay range. Flocculation is the process of formation of large aggregates of particles by the association of many smaller ones. It is due to the collision of individual particles and to the cohesive and electro-chemical nature of clay particles in saline water.

Several investigators have tried in the past to present a comprehensive description of the flocculation process. It is known that collision of particles may be caused by three different mechanisms (20):

i) Brownian motion, in which the rate of collision depends on the temperature

ii) Local shear or velocity gradients, in which the rate of collisions depends on the size of the particles and the magnitude of the gradient

iii) Differences in settling velocities of particles: Larger particles settling through a suspension of smaller particles collide with them at a rate depending on their relative velocities. Commonly, Browian motion contributes to the initial stages of flocculation, while the internal shearing dominates the formation of larger aggregates. It is also known that limiting floc sizes are obtained for certain shearing rates. The collision rates in all mechanisms are directly proportional to the concentration of suspended matter.

Despite the good understanding of these mechanisms, there is very little information concerning the settling rates of flocs. The change of the floc size along with its density during settling and the breaking of flocs in layers of higher shear makes the problem too complicated. Furthermore, the non-uniform composition of natural clay suspensions adds to the complexity. It seems that the problem is more tractable from a "macroscopic" point of view, that is, without trying to fully understand the process, but by simply studying the effective settling velocity of the flocs. Some field and laboratory experiments have been carried out for this purpose. Krone (20) from studies in the Savannah Harbor concludes that the settling velocities of the aggregates are of the order of 1 cm/sec, varying considerably between ebb and flood. These aggregates were found to have a specific weight of about 1.1 gr/cm^3. Because of the high settling velocity, most of the suspended matter was deposited during high or low water slack and resuspended when the tidal velocities, and therefore the shear stress, increased during flood or ebb.

4.5 Settling Tube Experiments on Clay Suspensions

4.5.1 Experimental program and procedures

In order to get an overall quantitative idea of the settling rates of clay suspensions a laboratory experiment was carried out. Specifically, the experiment was intended to provide a set of equivalent settling velocities, without dealing with the details of the flocculation process.

A plexiglass tube, 90 cm high and of 21 cm inner diameter as shown in Figure 1, was initially filled with a uniform suspension of clay in seawater and the decrease of concentration over time was monitored through the extraction of samples by means of valves placed at 15 cm intervals along the tube. The samples were analyzed with respect to their "turbidity" values, by means of a HACH 2100A turbidimeter.

Turbidity measurements were made as an expedient for determining suspended sediment concentrations as opposed to laborious filtering procedures. Field samples from the Massachusetts Bay analyzed by both turbidity and gravimetric techniques provided the opportunity to correlate turbidity with concentration of total suspended matter (both organic and inorganic). This correlation appears to be linear, as can be seen in Figure 2, at least in the range of concentrations encountered, which are generally below 10 mg/ℓ. Since the turbidimeter operates by measuring the scattering of light due to the particles in suspension it is apparent that not only the concentration but also the composition and size distribution of these particles affect the turbidity readings. Also, the presence of plankton increases the turbidity of the water, but does not contribute much to the weight of the matter collected on the filter. Thus, the scattering of the field data is reasonable in view of the variety of locations and conditions under which the samples were taken.

In the settling tube experiment kaolinite suspensions were first used. The material used was "Peerless No. 2 kaolinite" the same as

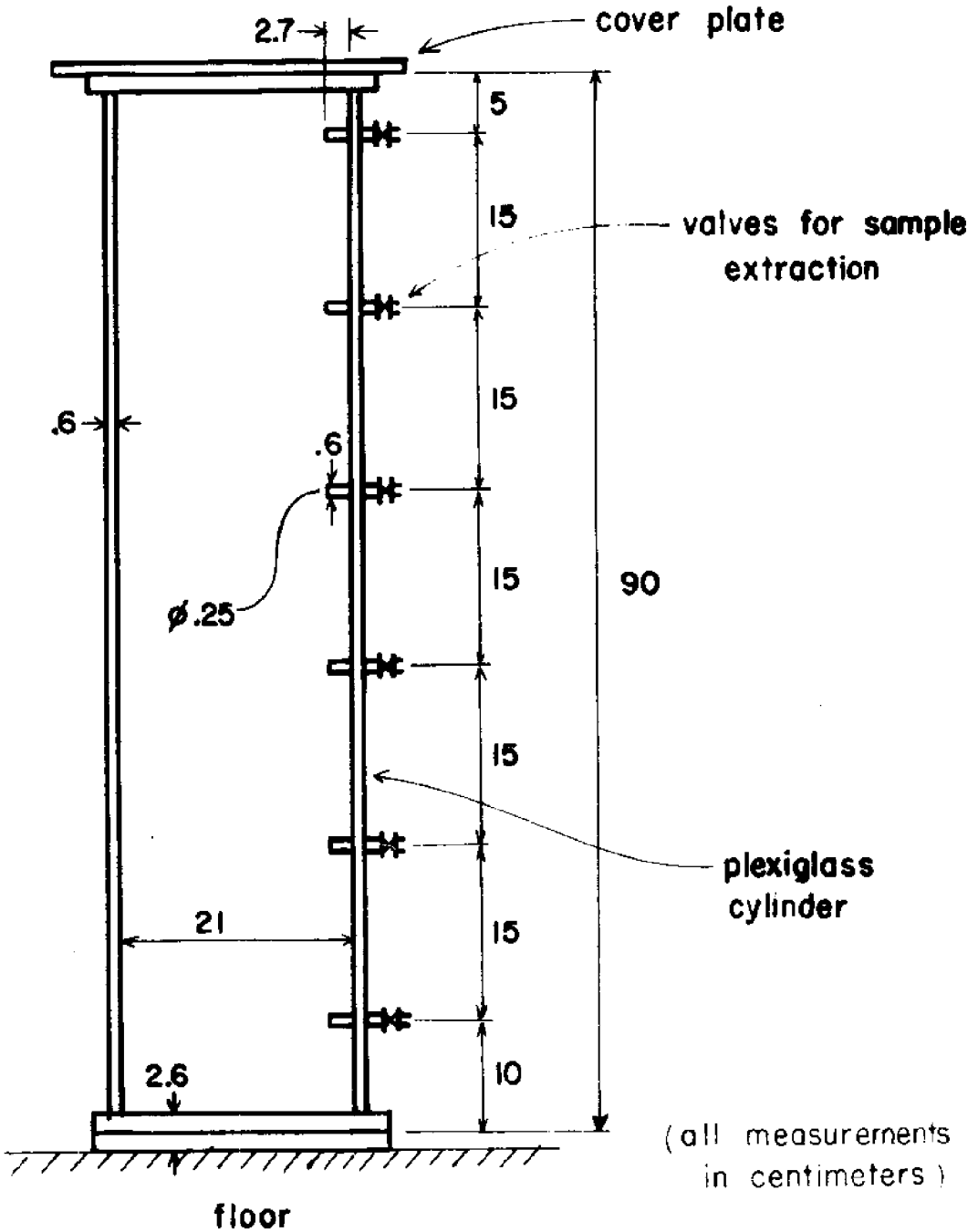

Figure 1

Sediment Settling Tube

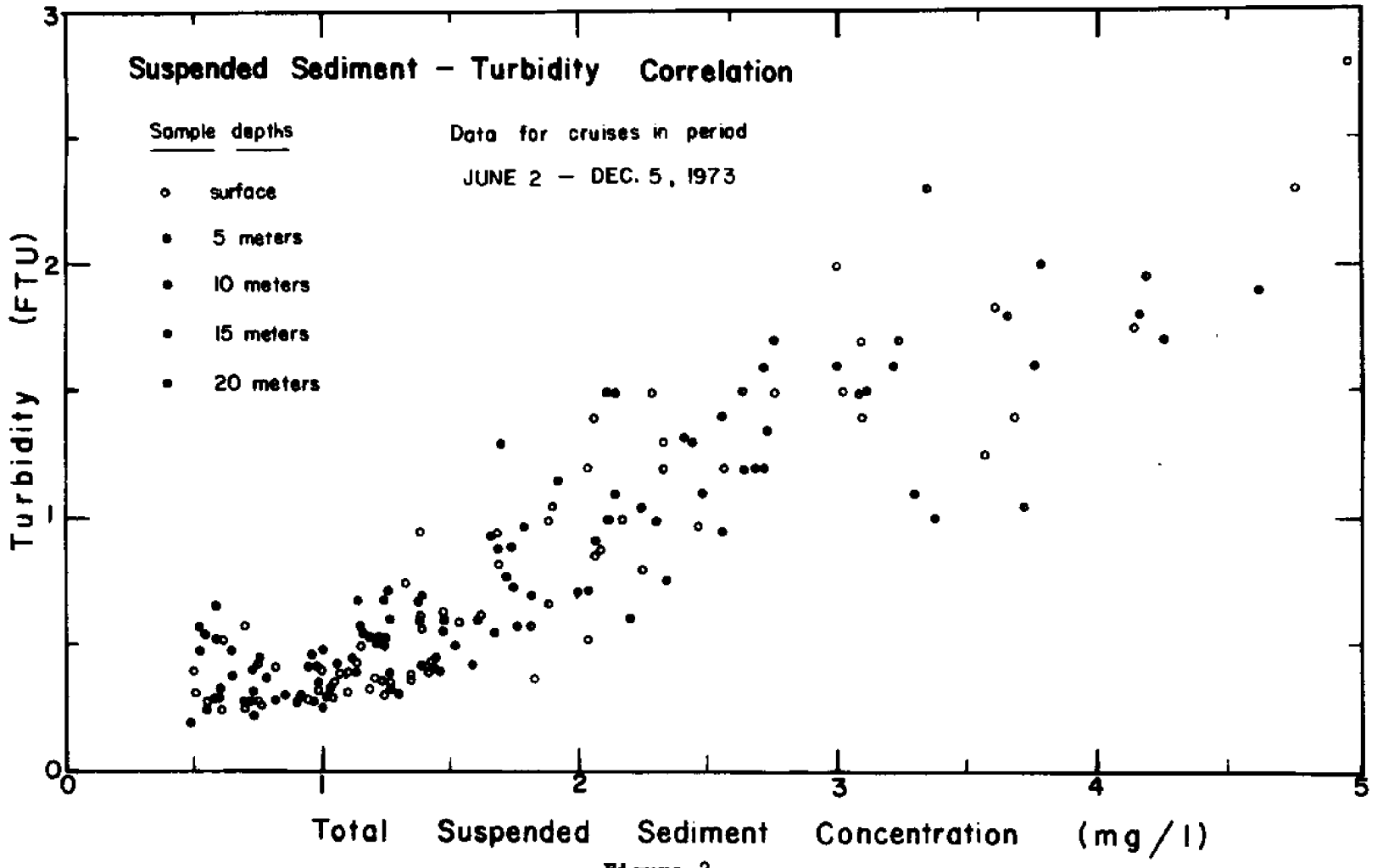

Figure 2

Correlation of Turbidity and Total Suspended Sediment Concentration from Field Data

that used by Partheniades in his experiments in a rotating channel several years ago. The experiment was repeated with illite and Boston Harbor mud. The illite was part of a sample of "Boston blue clay" being used for soil testing in the MIT Soil Mechanics Laboratory. The Boston Harbor mud was taken from the bottom of the harbor near Spectical Island. Both samples were oven-dried at 140°F and powdered before being used in the experiment.

In each run a known weight of sediment was added to a known volume of seawater and the two vigorously mixed so as to achieve a uniform initial concentration. The initial uniformity was checked by taking samples at various depths immediately after the suspension was made. As long as their turbidity readings were approximately the same, the initial concentration was assumed uniform. These initial samples were poured back into the settling tube in order to maintain the original water elevation. A new sample was taken from the mid-depth and its turbidity was checked to see if it agreed with the average of the previous samples. It was then used for calibrating the turbidimeter for the particular suspension under consideration. The background turbidity was subtracted from all readings. The calibration, made with dilutions of this initial sample, indicated a good linear relation between turbidity and concentration in all cases. These calibration curves are presented in Figure 3. The background turbidity of the seawater used was recorded before adding the sediments; it was generally very low, about 0.2 FTU.

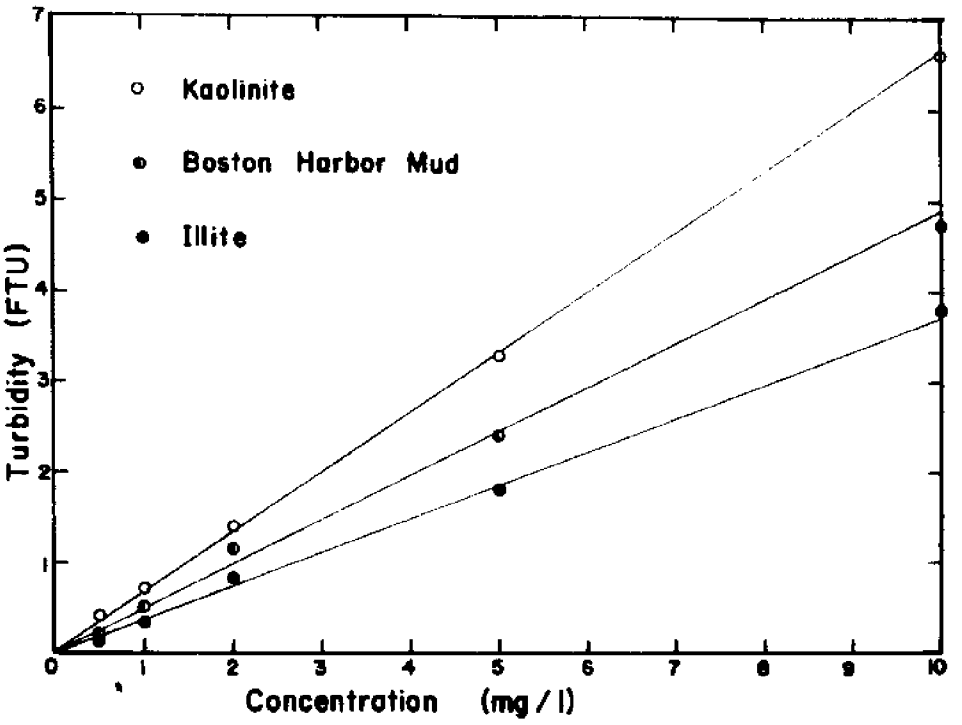

a) 0 – 10 mg/l range

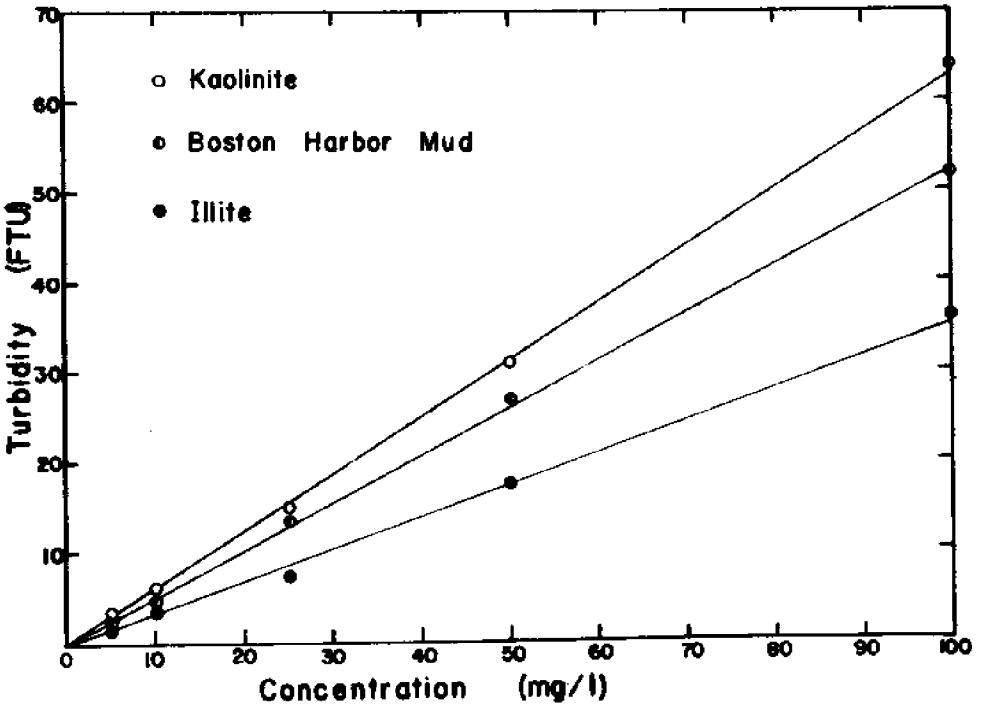

b) 0 – 100 mg/l range

Figure 3

Turbidimeter Calibration Curves for Clay Suspensions

During each run samples were taken at certain times at various depths and their turbidity measured. The number of samples was limited to minimize the disturbance of the water column and to avoid drastic changes in the surface elevation. At first, the measurements indicated a rather rapid decrease in turbidity in all depths, with higher values always at the lower sample depths. For each set of measurements, after subtracting the background value, the average turbidity over the depth was computed. Due to the linearity of the turbidity-concentration relationship, the percent decrease in average turbidity represents the percent of the initial sediments that had settled below the bottom valve. The turbidity measurements are presented in Appendix A. Plots of percentage settled vs. time are shown in Figures 5 and 6.

The percentage of the sediment having an average settling time between t_1 and t_2 can be estimated graphically by drawing tangents to the sedimentation curve (drawn in linear scales) at t_1 and t_2 and finding the difference of the percentages w_1 and w_2 where these tangents intersect the ordinate axis (30). This technique is demonstrated in Figure 4. The corresponding settling velocity will be between H/t_1 and H/t_2, where H is the depth of the water above the lowest valve. If the times are chosen so that they correspond to the settling velocities that separate the groups in Table 1, the respective percentages simply indicate the clay fractions (by weight) that macroscopically behave as if they belonged to one of these groups.

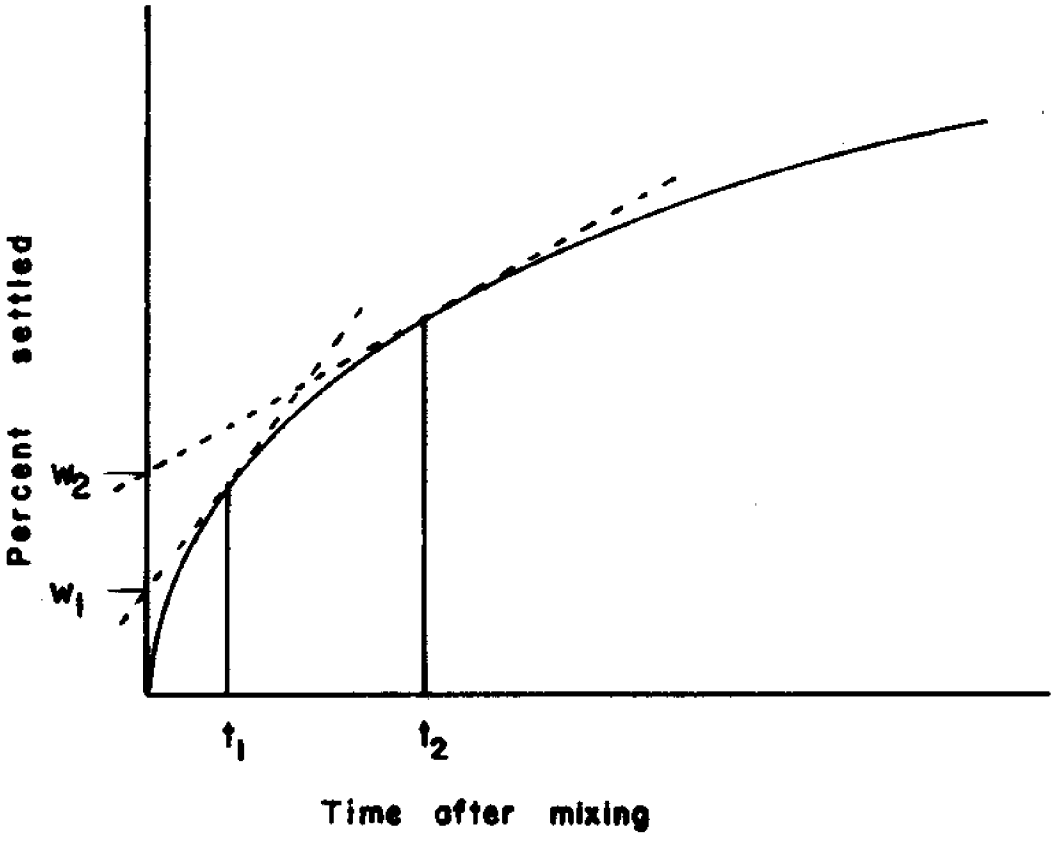

$w_2 - w_1$ = percentage of sediments with settling velocities between H/t_1 and H/t_2 , where H is the total height of the settling tube.

Figure 4

Technique for Sediment Separation into Groups of Settling Velocities (30)

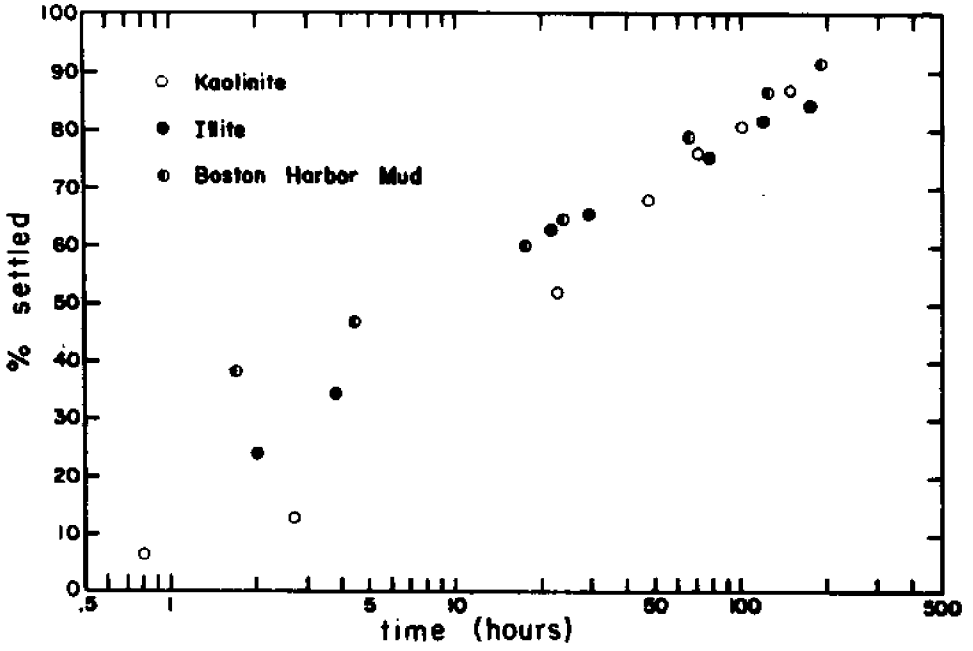

Figure 5 Settling Tube Results for the 10 mg/ℓ Initial Concentration Runs

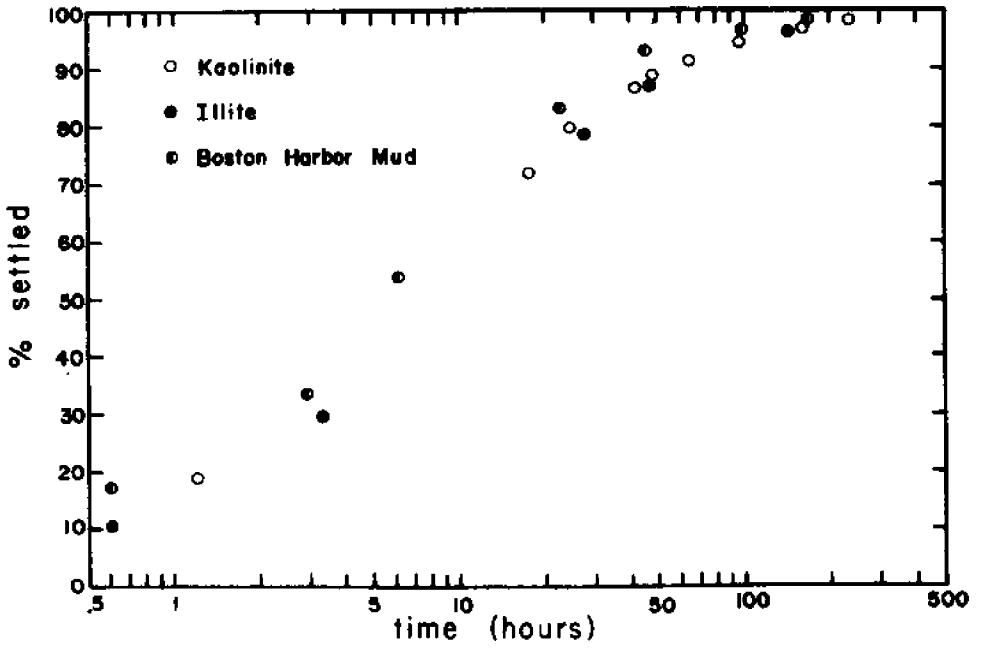

Figure 6 Settling Tube Results for the 100 mg/ℓ Initial Concentration Runs

4.5.2 Discussion of results

The data plotted in Figures 5 and 6 illustrate a rather consistent settling behavior with respect to both the type of clay suspension used and the initial concentration of the suspension. Comparing first the three types of clay, it can be seen that the percentage of Boston Harbor mud settled out with time is higher than that of the kaolinite and of the illite in all cases. This is the result of a high initial deposition rate of the harbor mud, possibly due to the presence of non-clay particles with higher settling rates. The illite and kaolinite agree essentially for the two initial concentrations tested, except during the shorter settling times in the 10 mg/ℓ initial concentration runs.

The dependence of the settling on the initial concentration is more apparent than the dependence on clay type. Plotted on semi-logarithmic scales, the points for the runs with 10 mg/ℓ initial concentration form reasonably straight lines suggesting a relationship of the following form:

$$\% \text{ settled} = a \log(\text{time}) + b$$

where a and b are constants; a is the slope, while b is the value of percent settled at a time of one hour. Thus, for example, the following relationship follows for Boston Harbor mud:

$$\% \text{ settled} = 27 \log(\text{time}) + 30$$

As can be seen in the plot of Figure 5, this relationship does not hold

at values of time less than about 1 hour and obviously at times when the percent settled comes close to 100.

The runs with 100 mg/ℓ initial concentration clearly show higher deposition rates. If there were no flocculation, it would be expected that the curves formed by the data points of a particular type of clay would coincide, because the settling rates and therefore the percent deposition with time would be the same regardless of concentration. However, since flocculation occurs, the percent deposition should be faster for a higher initial concentration due to the higher number of collisions.

The results of these experiments seem to be quite consistent in light of the low degree of scatter in the calibration curves (Figure 3a and Figure 3b). The fact that the lines for 10 mg/ℓ and 100 mg/ℓ initial concentration have almost identical slopes for each particular clay implies that turbidity measurements are appropriate in principle for determining sediment concentrations. However, the different slopes for the different clays mean that some other factors, such as particle size, affect turbidity also. This fact is important to consider in making conclusions about settling rates from the experimental data, for the grain size distribution of the material in suspension continuously changes during the run. This is because the larger particles settle first and also because flocculation forms new particles with different characteristics. This problem may control the reliability in an experiment such as the present one, for it is felt that the experimental techniques and equipment introduce relatively small error (± 5%).

From the technique described in the previous section and illustrated in Figure 4, the results in Table 2 were obtained. These results depend, of course, upon the reliability of this technique and also upon that of the experiment.

Table 2. Distribution of Clays Tested into Groups

Material in Suspension	Initial Concentration (mg/ℓ)	Percentage of Sample with Settling Velocity (cm/sec)		
		$w_s > 2.45 \times 10^{-3}$ (group 3)	$2.72 \times 10^{-4} < w_s < 2.45 \times 10^{-3}$ (group 4)	$w_s < 2.72 \times 10^{-4}$ (group 5)
Kaolinite	100	29%	56%	15%
Illite	100	29%	57%	14%
Boston Harbor Mud	100	41%	51%	8%
Kaolinite	10	14%	48%	38%
Illite	10	29%	40%	31%
Boston Harbor Mud	10	43%	24%	33%

In this tabular form it can again be seen that Kaolinite and Illite behave rather similarly, while Boston Harbor Mud has higher settling rates, that is, a higher percentage is settling at the rate of group 3.

CHAPTER 5

THE HORIZONTAL DISTRIBUTION OF AVERAGE CONCENTRATION

5.1 Solution of the Differential Equation

The distribution of the depth-averaged concentration $\bar{c}(x,y,t)$ is described by Equation (3-9):

$$\frac{\partial \bar{c}}{\partial t} + (U_{fs}+U_{Ts}\sin \omega t)\frac{\partial \bar{c}}{\partial x} + V_{Ts}\sin \omega t \frac{\partial \bar{c}}{\partial y} = E_x \frac{\partial^2 \bar{c}}{\partial x^2} + E_y \frac{\partial^2 \bar{c}}{\partial y^2} - \alpha \bar{c} \tag{5-1}$$

where U_{fs}, U_{Ts}, V_{Ts} represent mean-weighted values over the depth, taking into account the nonuniform sediment distribution. Following Harleman's method (12), by the change of variables:

$$\xi = x - \int_{\tau}^{t} (U_{fs}+U_{Ts}\sin \omega t)dt = x-U_{fs}(t-\tau) + \frac{U_{Ts}}{\omega}(\cos \omega t-\cos \omega \tau)$$

$$= x-U_{fs}(t-\tau) + \frac{U_{Ts}T}{2\pi}\left(\cos 2\pi \frac{t}{T} - \cos 2\pi \frac{\tau}{T}\right) \tag{5-2a}$$

$$\eta = y - \int_{\tau}^{t} V_{Ts}\sin \omega t dt = y + \frac{V_{Ts}T}{2\pi}\left(\cos 2\pi \frac{t}{T} - \cos 2\pi \frac{t}{T}\right) \tag{5-2b}$$

$$s = \bar{c}\, e^{-\alpha(t-\tau)} \tag{5-2c}$$

Equation (5-1) is transformed to:

$$\frac{\partial s}{\partial t} = E_x \frac{\partial^2 s}{\partial \xi^2} + E_y \frac{\partial^2 s}{\partial \eta^2} \tag{5-3}$$

For an instantaneous injection of mass of dM at time τ, the resulting distribution of ds is

$$ds = dM \frac{\exp[-\frac{\xi^2}{4E_x(t-\tau)}]}{\sqrt{4\pi E_x(t-\tau)}} \frac{\exp[-\frac{\eta^2}{4E_y(t-\tau)}]}{\sqrt{4\pi E_y(t-\tau)}} \tag{5-4}$$

hence, $\overline{dc} = ds\, e^{-\alpha(t-\tau)}$ (5-4a)

or, using the original variables:

$$\overline{dc} = dM \frac{\exp[-\frac{[x-U_{fs}(t-\tau) + \frac{U_{Ts}T}{2\pi}(\cos 2\pi \frac{t}{T} - \cos 2\pi \frac{\tau}{T})]^2}{4E_x(t-\tau)}]}{4\pi(t-\tau)\sqrt{E_x E_y}}$$

$$\exp[-\frac{[y + \frac{V_{Ts}T}{2\pi}(\cos 2\pi \frac{t}{T} - \cos 2\pi \frac{\tau}{T})]^2}{4E_y(t-\tau)} - \alpha(t-\tau)] \tag{5-5}$$

for a continuous injection $dM = m_i d\tau$, and integrating over all values of τ:

$$\bar{c} = \int_0^t m_i \frac{\exp\left[-\frac{\left[x-U_{fs}(t-\tau)+\frac{U_{Ts}T}{2\pi}\left(\cos 2\pi\frac{t}{T}-\cos 2\pi\frac{\tau}{T}\right)\right]^2}{4E_x(t-\tau)}\right]}{4\pi(t-\tau)\sqrt{E_x E_y}}$$

$$\exp\left[-\frac{\left[y+\frac{V_{Ts}T}{2\pi}\left(\cos 2\pi\frac{t}{T}-\cos 2\pi\frac{\tau}{T}\right)\right]^2}{4E_y(t-\tau)}-\alpha(t-\tau)\right]d\tau \quad (5\text{-}6)$$

where m_i = the mass rate of injection of suspended sediments of the particular group of interest; m_i can be written as

$$m_i = \forall c_{oi} = \forall \lambda_i c_o \quad (5\text{-}6a)$$

where $\forall$ = the volume rate of injection of the seawater-sediment mixture (volume/time)

c_{oi} = the initial concentration (by mass) of sediments of the group of interest in the mixture injected

c_o = the total initial sediment concentration (by mass) in the mixture injected

λ_i = c_{oi}/c_o, the fraction of the total sediment that belongs to the group of interest.

Equation (5-6) may be brought to non-dimensional form for purposes of generality. Choosing the tidal period T as the characteristic time and the depth h as the characteristic length scale, the non-dimensional (primed) variables are defined as follows:

$$t' = \frac{t}{T}, \qquad \tau' = \frac{\tau}{T}, \qquad x' = \frac{x}{h}, \qquad y' = \frac{y}{h},$$

$$U'_{fs} = \frac{U_{fs}}{h/T}, \qquad U'_{Ts} = \frac{U_{Ts}}{h/T}, \qquad V'_{Ts} = \frac{V_{Ts}}{h/T},$$

$$E'_x = \frac{E_x}{h^2/T} \qquad E'_y = \frac{E_y}{h^2/T}, \qquad \alpha' = \alpha T, \qquad c' = \frac{\bar{c}}{\lambda_1 c_o}$$

The non-dimensional concentration c' represents the ratio of the depth-averaged concentration $\bar{c}$ at (x,y,t) to the initial concentration of the mixture for a particular group. The new form of Equation (5-6) is:

$$c' = \frac{VT}{h^3} \int_0^{t'} \frac{\exp\left[-\dfrac{\left[x'-U'_{fs}(t'-\tau') + \dfrac{U'_{Ts}}{2\pi}(\cos 2\pi t'-\cos 2\pi\tau')\right]^2}{4E'_x(t'-\tau')}\right]}{4\pi(t'-\tau')\sqrt{E'_x E'_y}}$$

$$\exp\left[-\frac{\left[y' + \dfrac{V'_{Ts}}{2\pi}(\cos 2\pi t'-\cos 2\pi\tau')\right]^2}{4E'_y(t'-\tau')} - \alpha'(t'-\tau')\right] d\tau' \qquad (5\text{-}7)$$

The integration cannot be carried out except by numerical techniques. A computer program to evaluate c' from Equation (5-7) was written and is presented in Appendix C.

The time until convergence to a quasi-steady state, as defined in Chapter 3, generally depends upon the values of the various parameters on the one hand, and the point (x,y) of interest on the other.

The two most important parameters are the decay rate, α, and the net drift. Higher values of α will cause the solution to converge more rapidly at all positions. The effect of the net drift, however, is highly related to the point (x,y) of interest. For points near the source its magnitude is not very important, but a point far from the source may not reach steady state for a long time if the net drift is small. This problem is discussed in Section 7.6, in relation to the runs made for the conditions found in Massachusetts Bay.

It must be noted that in the above solution the tacit assumption was made that the shore is not reached by the sediment "cloud", since no boundaries were considered. If the solution of Equation (5-7) shows that, in fact, no significant concentrations are found near the shore, then it is perfectly valid. Otherwise a correction can be made by means of a graphical application of the "method of images". In essence, the method assumes an imaginary source symmetric to the actual one with respect to the shoreline. The shoreline in this case has to be approximated by a straight line, since the correction would otherwise becomes too complicated. The concentrations due to the two sources are added together. This is graphically equivalent to "folding back" that part of the profile of $\bar{c}(x,y,t)$ which lies beyond the boundary. It may be recalled, however, that the model does not satisfactorily represent the conditions of the near-shore area for various other reasons (Chapter 3).

5.2 Net Drift and Tidal Velocities

With respect to circulation of coastal waters, of interest to this study are the directions and magnitudes of the tidal velocities

and any net drift. The latter is probably the most important hydrodynamic factor entering into the model, since it determines in the long run the direction and rate at which most of the sediments will move. Each area has its own characteristics in terms of geometrical configuration and prevailing meteorological conditions, both of which affect the general circulation; thus, estimates of the above parameters are usually difficult. The tidal velocity direction in an area does not vary much during the year, being approximately normal to the shoreline, while its amplitude depends primarily on tidal amplitude. By contrast, the short-term net drift is highly variable with the different seasons. The prevailing direction is usually parallel to the shoreline if wind is insignificant and the area of interest is not too far from the shore. The magnitude of the net drift, however, cannot be predicted by any simple means.

Physical as well as mathematical models are being used for studying circulation in coastal areas. It is beyond the scope of the present work to determine the velocity field in detail by using such methods.

Field measurements in the area of interest can provide valuable information about currents. There are basically two measuring techniques, current meters and drogues. Current meters give the magnitude and direction of the currents at certain points. The method is directly related to an Eulerian description of the flow field. This technique is desirable if one is interested in obtaining the flow history at specific points, for example, at the entrance to a harbor.

A current meter can be placed at any depth and is generally used for long-term measurements.

Drogues give the pathlines of water particles. This technique yields basically a Lagrangian representation of the flow field. A drogue is a fin or vane of high fluid resistance, suspended at a certain depth in the water from a flotation device. It has the measuring flexibility of the current meter in that it operates at different depths, but obviously the bottom must not be reached at any point along the drogue path. For this reason, drogues cannot be used to measure flows very close to the bottom. Because of the nature of the drogue method, long-term records are not feasible; the drogue must be followed by a vessel which monitors its position over time. Also, there is no way of keeping the drogue in a particular area of interest.

In spite of these difficulties, drogue measurements give a very valuable picture of net flows and circulations in large bodies of water. In particular with respect to the present study, the drogue movement simulates the path of a sediment particle in its lateral directions as long as there are no significant vertical currents. The spreading of a set of drogues can also provide estimates for the dispersion characteristics of the area. In fact, the results of drogue studies carried out over the last year in relation to the NOMES project were used to provide information on currents in the Massachusetts Bay, necessary for the application of the model in this area (Chapter 7).

Specifically, since the number of drogues in each study is small, (three or four), the movement of a vertical water column was examined

under the following simplifying assumptions:

1) Between drogues at different depths, the velocity changes approximately linearly.

2) Between the deepest drogue and the bottom the velocity follows a portion of a logarithmic curve.

3) Above the shallowest drogue the velocity is constant.

It can be argued that these assumptions do not agree with the logarithmic velocity profile used in Section 4.1 for the determination of the vertical diffusion coefficient ε_z and consequently with the normalized vertical distribution $\phi(\zeta)$. In fact, if the velocity profile were really logarithmic, its approximation by linear profiles over the various portions above the deepest drogue would be quite acceptable. However, the very limited field data on the vertical profile do not lead to any conclusion about its true shape. Under these circumstances, it is felt that the interpolation technique described above yields a reasonable description of the velocity profile.

The objective of the assumptions stated above is to convert the velocity profile to an equivalent step-function profile, with the values of the steps corresponding to the drogue velocities; thus, it is possible to associate with each drogue a fraction of the water column that moves on the average with the drogue velocity. Consequently, it is easy to define the mean movement of the water column at any time interval as the weighted average of the movements of the drogues at this interval, where the weights are the fractions of the column associated with every drogue (Figure 7).

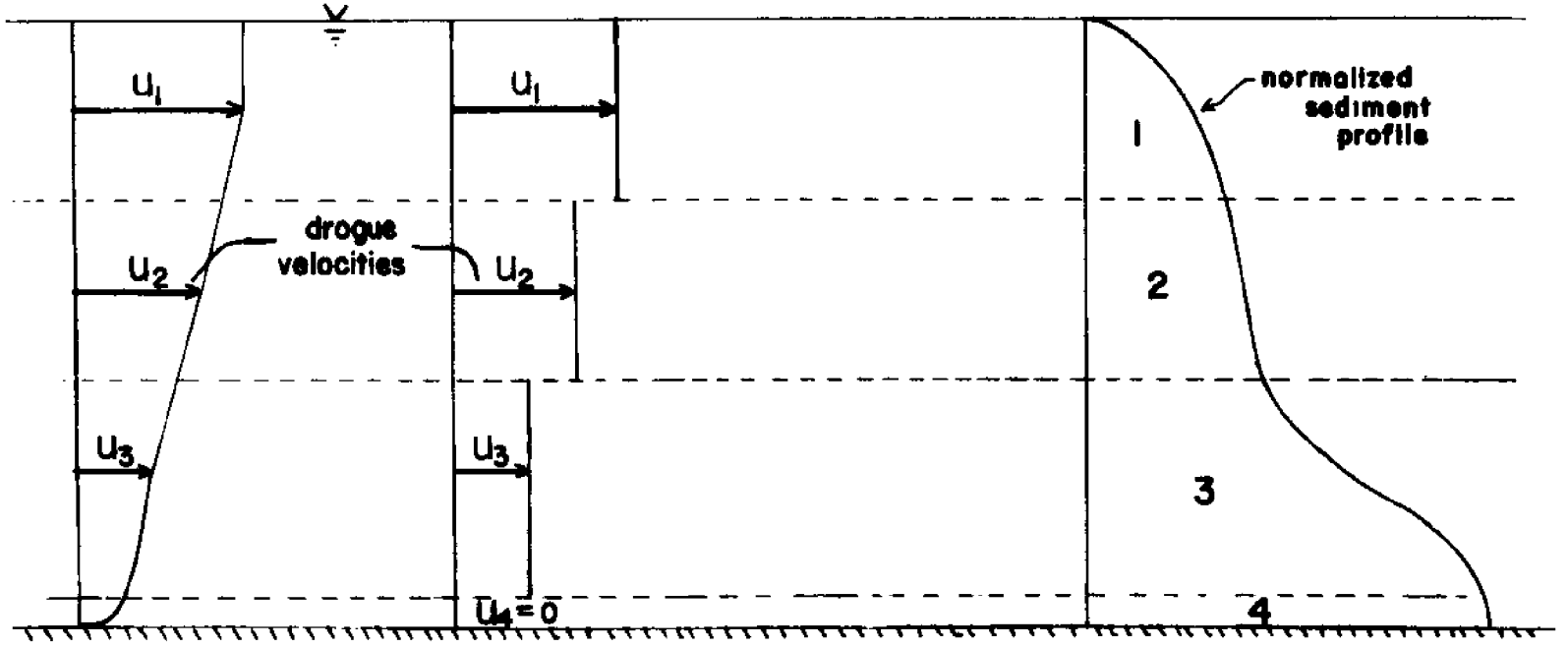

Figure 7

Schematic Representation of the Vertical Velocity Profile and the Weights Associated with the Drogues

The mean net drift over the depth can then be computed by the mean net movement of the water column over a complete tidal cycle. Any deviations from this net movement during the tidal cycle are then attributed to a sinusoidal tidal velocity. The assumption of a sinusoidal tide might be questionned. In many coastal areas the tide is not even symmetrical. Due to river discharge the ebb velocities are often higher than the flood velocities. However, most of the asymmetry of the tide can be incorporated into the net drift term. Thus, an "equivalent" sinusoidal velocity that, combined with the net drift, would move the drogues in approximately the same way as the natural currents can be evaluated. Since the interest of this study lies in the net effects of the current system in a relatively long time scale and not much in its detailed structure, the above approximation is acceptable.

Ultimately, the major interest of the study does not lie in the water velocities but, as indicated in Chapter 3, in the weighted velocities, taking into account the distribution of suspended sediments over the vertical. These velocities enter into the model as the advective terms of the dispersion Equation (5-1) for any particular group of sediments. Their estimate is quite straightforward based on the previous considerations. The drogue records can be used in the same way, the only difference being in the relative weights that each drogue is associated with. They will not depend only on the fractions of the water column as before, but rather on the areas of the normalized vertical concentration profile lying in these fractions (Figure 7).

Clearly, the weight on a drogue will be different for different sediment groups.

All these computations can be organized and performed through a computer program, which will be discussed in more detail in Chapter 7. This program is extended to provide estimates of the dispersion coefficient as will be seen in Section 5.3.

5.3 Dispersion Coefficients

Dispersion is the most difficult parameter to estimate. Values reported in the literature, mainly from one-dimensional studies, differ by as much as two orders of magnitude. Fortunately enough, the solution of dispersion equations for continuous input is not too sensitive to changes in the magnitude of this coefficient, as already indicated in Chapter 2.

It may be recalled that the dispersion coefficient is in fact a sum of two terms:

a) A horizontal turbulent diffusivity ε, due to large scale eddy motions.

b) A purely dispersive term E_d, due to velocity variations over the depth.

The value of the first at the sea surface can be predicted quite reliably by Okubo's empirical formula (22).

$$\varepsilon = 0.01\ \ell^{1.15} \quad \text{(in cm, sec units)} \tag{5-8}$$

where ℓ a characteristic length scale, initially defined as three times

the standard deviation of the concentration distribution along the axis of interest. The length scale is actually a characteristic of the region. It is not known what its relation is (if any) to the geometrical characteristics of the area considered, such as the depth h or the distance from the shore. It is conceivable, however, that the length scale should have a relation to the maximum size of eddies that can be developed around the source. For Lake Erie, Fochtman and Wnek (33) report a value of ℓ = 800 ft. for a depth of h = 27 ft., indicating a relation ℓ = 30 h. With specific information about the area of interest lacking a value of 30 to 50 h may be used for the determination of ϵ. Fochtman and Wnek further claim a slight linear decrease of ϵ with depth; the average value over the depth should be used in the model. However, the accuracy of the estimate of ϵ is not critical because its magnitude is normally much smaller than the dispersive term E_d.

This term can be derived from one-dimensional considerations, since the velocity field is assumed the same in all (x,y) positions. Thus, lateral variations do not exist and a value of E_d due to velocity variations over the vertical is appropriate. Its general form is:

$$E_d = \lambda h u_* \qquad (5\text{-}9)$$

where h = the depth

u_* = the shear velocity

λ = a constant of proportionality

Values for λ that have been reported range from as low as 6 (Elder) to

as high as 500 (Glover). Taylor's formula (2-5), modified for open channels, yields $\lambda = 20$. These lower values, derived from theoretical assumptions and tested for ideal flow conditions, represent a lower limit of the actual value of the dispersion coefficient, which is usually higher by an order of magnitude. Harleman's suggestion for doubling Taylor's coefficient to account for natural nonuniformities gives $\lambda = 40$. With respect to u_*, an average value over the tidal cycle seems appropriate. The shear velocity is related to the mean velocity and the friction factor by the expression:

$$u_* = \sqrt{\frac{f}{8}}\, U \qquad (5\text{-}10)$$

It is therefore evident that E_d is not the same in all horizontal directions but depends on the mean velocity along each axis. In fact, Equation (5-9) and Equation (5-10) indicate that E_d is proportional to the mean velocity (averaged over the tidal cycle) in a certain direction, provided that f can be considered constant throughout. For flat bed conditions it may be assumed that $f \simeq 0.02$; hence $u_* = \frac{1}{20} U$.

Okubo (23) found that for an oscillating linear velocity profile the dispersion term is

$$E_{d,o} = \frac{1}{240} \frac{V_{max}^2 h^2}{\bar{\epsilon}_z} \qquad (5\text{-}11)$$

where V_{max} = the velocity amplitude at the surface

$\bar{\epsilon}_z$ = the vertical diffusivity, assumed constant

He also found that for a steady current having a linear profile with a value at the surface equal to V_{max}

$$E_{d,s} = \frac{1}{120} \frac{V_{max}^2 h^2}{\bar{\epsilon}_z} \qquad (5\text{-}12)$$

Since the mean velocity over the depth is half the value at the surface due to the linearity of the profile

$$(u_*)_{max} = \frac{1}{2}\sqrt{\frac{f}{8}}\, V_{max} = \frac{1}{40}\, V_{max} \quad (\text{for } f = 0.02)$$

and for a sinusoidal oscillation

$$(u_*)_{max} = \frac{2}{\pi}\,\frac{1}{40}\, V_{max} = \frac{1}{63}\, V_{max}$$

Also, $\bar{\epsilon}_z$ can be taken equal to the mean value of ϵ_z over the depth: $\bar{\epsilon}_z = 0.067\, hu_*$. Substituting in Equation (5-11)

$$E_{d,o} = \frac{1}{240} \frac{V_{max}^2 h^2}{0.067\, hu_*} = \frac{1}{240} \frac{(63)^2}{0.067} hu_* \approx 250\, hu_* \qquad (5\text{-}11a)$$

Similarly, for a steady current

$$E_{d,s} = 200\, hu_* \qquad (5\text{-}12a)$$

The estimates of the dispersion coefficients by these formulas are an order of magnitude higher than Taylor's predictions. They are probably overestimating the true values since a linear profile presents

more severe velocity variations over the depth than a logarithmic profile, which was previously considered (Section 5-2) close to reality. It is proposed herein that, in case of lack of information concerning the area of interest, a value for β a little higher than Harleman's, in the range 40 to 80, may be used.

It is generally desirable to obtain some field information on the dispersion characteristics of a specific coastal area in order to model it more realistically. Measurements of the horizontal dispersion coefficient can be made by monitoring the distribution over time of some tracer injected at a point. The basic idea of the experimental measurement lies in the fact that the variance of the distribution and the dispersion coefficient along an axis are related by the following equation, assuming that the distribution of the tracer is approximately Gaussian:

$$E = \sigma^2/2t \qquad (5\text{-}13)$$

If the variance increases linearly with time, then E is constant. In reality, however, this is rarely the case. One of the reasons is that most experiments have dealt with instantaneous injections. Thus, the dispersion is expected to increase with the size of the dye patch, at least due to the diffusion term ε (Equation 5-8). The dispersion term E_d is supposedly constant (Equation 5-9). In fact, though, there is no way to have both constant velocity and constant dispersion. If the velocity is constant, the variance is increasing in proportion to t^2 and not to t. Fluctuations of the dispersion due to tidal variations

make the problem of estimating a reasonable "average" coefficient even more complicated. In the case of a continuous injection, however, the effective dispersion coefficient applicable to the whole area of interest is expected to be much more stable in terms of both tidal and real time.

It is worth noting that almost all previous experiments in the sea were carried out on the surface layer. Dye was the most common tracer used (Rhodamine B or WT). Thus, the values of the dispersion reported for various areas refer only to the diffusion term ϵ and more specifically to its value at the surface layer. Dispersion due to velocity variations over the depth could not be measured by this technique. Such measurements would require a uniform injection of dye over the depth and an exactly neutrally buoyant dye solution. The second requirement makes the application of dye techniques extremely difficult, if not impossible, in view of the slightly variable seawater density over the depth. The difficulties increase even more when it is desired to estimate dispersion of matter distributed nonuniformly over the depth.

In fact, most of the past work on dispersion coefficients was initiated in relation to the dispersion of pollutants, which are more or less neutrally buoyant and hence have a uniform concentration over the depth if injected from a vertical line source. Not much information exists on dispersion of particles having variable concentration over the depth, such as suspended sediments. For very fine sediments some approximation can be made by using the values given for uniform concentrations.

The drogues, which give values of the velocities encountered in the area, can also provide valuable, although not very accurate, information concerning dispersion characteristics. The basic requirement is that all drogues must be deployed at the same point and at the same time (at least approximately), but at different depths. The variance of their positions over time must subsequently be monitored. Since they always stay at the same depths, the variance of their positions depends on the velocity variations over the depth. The larger the number of drogues, the more accurate the estimate of the variance and therefore of the dispersion coefficient according to Equation (5-13).

In order to properly calculate the variance, the drogue positions must be appropriately weighted. The weight placed on a drogue will depend on the sediment group considered and can be found as indicated in Figure 7. The same program that computes the advective velocities can be extended to calculate the (weighted) variance of the drogues around the (weighted) mean position at various times and consequently, from Equation (5-13), the values of the dispersion coefficient at every time interval. An average value of the dispersion coefficient over a tidal cycle can therefore be calculated and used in Equation (5-1). It is evident from the above discussion that the value obtained through the drogues variance refers to the total dispersion coefficient $E = \varepsilon + E_d$. Details of the computational procedures are presented in Chapter 7, in relation to the application of the model to the Massachusetts Bay.

CHAPTER 6

SYNTHESIS OF THE MODEL COMPONENTS

6.1 Concentration Distribution of a Group of Sediments

A group of sediments is characterized by its average settling velocity, as indicated in Table 1 (Section 4.3). For such a group the normalized vertical distribution is first computed according to Equation (4.7). This distribution provides the necessary information for calculating the parameters of the differential equation (5.1) of the horizontal distribution, specifically the value of the decay factor α, through Equation (4.12). Combined with drogue measurements it also specifies appropriate values for the advective velocities and dispersion coefficients as indicated in Sections 5.2 and 5.3. The solution of the expression (5.7) for the horizontal distribution of concentrations can then be evaluated numerically. The concentration of suspended sediments for this particular group as a function of space and time is finally obtained by the relation:

$$c(x,y,z,t) = \bar{c}(x,y,t)\ \phi\ (\zeta) \qquad (6\text{-}1)$$

according to the basic model assumption.

It should be obvious that, since $\bar{c}(x,y,t)$ refers to a quasi-steady state solution, Equation (6.1) for the determination of c is strictly applicable for times after the convergence of the solution for $\bar{c}$. The solution is also not applicable for spatial coordinates very close to the shore, as indicated in Chapter 3.

If the numerical integration of the expression for $\bar{c}$ is carried out for times shorter than required for convergence to steady state, an approximation of the transient behavior of $\bar{c}$, and subsequently of $c(x,y,z,t)$, can be obtained. However, the results will be unreliable for times shorter than that necessary for vertical equilibrium, which has an upper bound of the order of $T' = h^2/\varepsilon_z$; for example, typical values in the area of interest in Mass Bay are

$h = 30$ m

$u_* = 0.5$ cm/sec

$\bar{\varepsilon}_z = 0.067\ hu_* = 0.067 \times 30 \times 0.005 = 0.01\ m^2/sec$

hence, $T' = \frac{30^2}{0.01} = 90{,}000$ sec.

This time is approximately two tidal cycles. Hence, this is the maximum time span after which reasonable transient results can be obtained.

With respect to the prediction of the concentration distribution after the end of the injection, the model can give approximate answers as long as vertical equilibrium continues to hold. Equation (6.1) is still applicable, but now the depth-averaged concentration is calculated with the integral of Equation (5.7) subject to the upper limit of the time of the end of the injection.

6.2 Total Sediment Concentration

In general, the suspended sediments introduced into the seawater have various sizes and settling velocities. For the purpose of this analysis, however, they can be classified into several discrete groups, for example into those indicated in Table 1 (Sec. 4.3). The percentage of each group forming the total sediment introduced is supposedly known, or can be found by measurements of settling velocities. These group percentages are determined in terms of settling velocities rather than of individual grain sizes. Thus, the increased settling rate of the clay fraction due to flocculation can be accounted for by including percentages of the clay material in the higher settling velocity groups. The settling tube experiments (Section 4.5) make it possible to obtain values for the assignment of the clay function to the other groups. These values will vary with such factors as the type of clay and the initial concentration of sediment.

For each group, the concentration $c(x,y,z,t)$ can be found by the model, as summarized in Section 6.1. Under the assumption that the distribution of particles of a group is independent of the presence of particles of another group, the total concentration of suspended sediments can be found as a weighted sum of the individual group concentrations at any point (x,y,z,t). The weights for this calculation are defined by the composition of the mixture introduced.

It may be noted that, even if the ideal conditions assumed in the model actually exist, an instantaneous measurement of suspended sediment concentration at some point cannot be expected to agree with the above calculated $c(x,y,z,t)$. Due to random turbulent fluctuations in velocity and concentration, the solution is considered to represent an average value of $c(x,y,z,t)$ over some period of time Δt.

6.3 Rate of Deposition

The amount of sediments deposited at the bottom is quite important from the point of view of ecological balance.

The concentration near the bottom is at any time equal to

$$c(x,y,o,t) = \phi(o)\ \bar{c}\ (x,y,t)$$

and the rate at which the particles reach the bottom is $w_s \phi(o)\ \bar{c}\ (x,y,t)$.

Recalling that A is the overall probability that a particle settling to the bottom stays there, the rate at which particles of a certain group are deposited at the bottom follows as:

$$D = A\ w_s\ \phi(o)\ \bar{c}\ (x,y,t) \qquad (6\text{-}2)$$

in units of mass/time x area, provided the sediment concentration c is expressed in mass per unit volume as a function of location and time. The spatial integration of D for any group over all x, y values should equal the rate of injection of sediment of this group, i.e.,

$$\int_{\text{all } x,y} \int D_i\ dxdy = m_i = \lambda_i \Psi c_o \qquad (6\text{-}3)$$

It is conceptually simple to find the amount of sediment deposited between times t_1 and t_2 at a particular point (x,y), more specifically in a unit area about a point. It can be computed as:

$$\int_{t_1}^{t_2} D dt = \int_{t_1}^{t_2} Aw_s \, \phi(o) \, \bar{c} \, (x,y,t) \, dt = Aw_s \, \phi(o) \int_{t_1}^{t_2} \bar{c} \, (x,y,t) \, dt \qquad (6\text{-}4)$$

provided that steady state has been reached before t_1.

The thickness of the layer of sediment deposited is

$$\delta = \frac{\int_{t_1}^{t_2} D \, dt}{\rho_e} \qquad (6\text{-}5)$$

where ρ_e is the effective density of the material, considering it to be loosely deposited, that is,

$$\rho_w < \rho_e < \rho_s - \rho_w$$

where ρ_s is the sediment density

ρ_w is the density of seawater

It is evident that the amount deposited should be calculated for each group separately and then added together to obtain the total deposition.

The computation of the amount deposited requires a further numerical integration. It can be approximated by multiplying the average steady state deposition rate, $\bar{D}(x,y)$, by the duration of dredging. This $\bar{D}$ can be obtained to the desired accuracy by averaging

the values of D for various tidal stages at a particular point. This technique is only applicable in the case of dredging of long duration, implying that the steady-state phase lasts much longer than the transient phase.

CHAPTER 7

APPLICATION OF DREDGING IN MASSACHUSETTS BAY

7.1 General Comments on the Project NOMES

In 1972, the National Oceanographic and Atmospheric Administration (NOAA) launched a three-year project to study the environmental effects of offshore mining for sand and gravel in the Massachusetts Bay as Project NOMES (New England Offshore Mining Environmental Study). Various physical, chemical and biological parameters were to be monitored before, during and after the dredging operation which was scheduled for the summer of 1974. An extensive data base was to be provided to develop mathematical models for the prediction of the environmental impact of future dredging operations and for the development of legal regulations of such activities.

The inability to find an economical use for the large amount of dredged material led to the termination of the project in the summer of 1973, after some baseline studies had been conducted.

This model was developed at M.I.T. under the belief that the experimental dredging would provide an excellent opportunity to study the dispersion of fine suspended sediments which are inevitable by-products of such operations. The model efforts were continued after the termination of the project in view of the data already obtained and of the importance of such predictive capacilities for the coastal zone.

As one of the activities of the NOMES project, an extensive dispertion experiment was carried out by NOAA's Environmental Research Laboratory in collaboration with several other institutions in June 1973, just prior to the termination of the project. A large quantity of small glass beads and sphalerite particles was dumped at the proposed dredging site and the concentrations of both were monitored for 11 days at various locations in the Mass Bay (21, 13). The injection of the particles was almost instantaneous and near the sea surface. However, the results of the experiment should be useful at least for a qualitative comparison with the model predictions. Current observations by drogues were conducted by M.I.T. during this experiment as well as earlier in the past year and provided the hydrodynamic parameters for the application of the dispersion model.

In this chapter the procedures for the collection and analysis of these data are given and the validity of the model as applied to the Massachusetts Bay is discussed.

7.2 The Sediment Source

The NOMES operation was scheduled to run for a period of six weeks with a hopper dredge having a capacity of 10-15 thousand cubic yards of sediment, to be collected in 1 1/2 to 3 hours (3). An estimated 5% of the sediments would consist of fines less than 100μ in diameter. While the sediment is pumped into the dredge, the fines are discharged back into the sea as overflow with the seawater.

It was estimated that between successive dredging periods, 6-8 non-working hours would be required by the dredge for the roundtrip to the dumping site at a desired location. With 15,000 yd^3 of sand and gravel dredged in 1 1/2 hours, the amount of fines introduced is:

$$\frac{0.05 \times 15{,}000}{1.5} = 500 \quad yd^3/hr \tag{7-1a}$$

or

$$\frac{500 \times (0.91)^3}{3600} \quad m^3/sec \simeq 0.1 \quad m^3/sec \tag{7.1b}$$

Despite the fact that the operation is intermittent, the long duration of the dredging (6 weeks) relative to non-working intervals permits to approximate the steady state actually reached as one of an "equivalent" continuous injection. With the working times of 1 1/2 hours and the intervals in between of 6-8 hours, the equivalent continuous injection of fines would result in a rate of discharge of about 20% of that calculated in (7.1) or

$$V = 0.02 \quad m^3 \text{ fines/sec} \tag{7-2}$$

This is not necessarily valid if the working hours coincide always with the same parts of the tidal cycle. However, it is reasonable to assume here that the working hours occur more or less during different parts of the tidal period.

The volume rate defined above refers to actual volume of fines. If the material were in a compact state its density would approach 2.65 gr/cm^3. Since in this case the material is loose, it is assumed herein that the concentration of the volume injected is

approximately 1 gr/cm^3 or 10^6 mg/ℓ.

The dredge site was to be located at latitude 42°21' North and longitude 70°49' West, as shown in the chart, Figure 8, and has an area of about 0.8 by 0.5 nautical miles. For the application of the model, the source is assumed to be located at the center of this area. It is also assumed that there is enough mixing caused by the nature of the injection to consider it as a uniform line source.

The bottom depth is assumed constant and equal to its value at the dredging site, i.e., 30 meters. The complex shoreline can be approximated by a set of straight lines, as also shown in Figure 8. This configuration makes it possible to deal with cases in which the sediment "cloud" reaches the shore, as discussed in Section 5.1.

7.3 Composition of the Initial Mixture

As indicated in Chapter 3, the application of the model calls for a separation of the fine sediment discharged into several groups, each characterized by its average settling velocity. The separation displayed in Table 1 will be followed.

Grain size distribution data for the fines of the dredging area are essential. In the case of Mass Bay, about 70 core samples have been obtained from various locations and depths. Grain size distributions of the fines have been obtained through hydrometer analyses at the University of New Hampshire (32). The samples indicated a very consistent composition in the range below 60μ, primarily containing inorganic clay of low plasticity and inorganic silt.

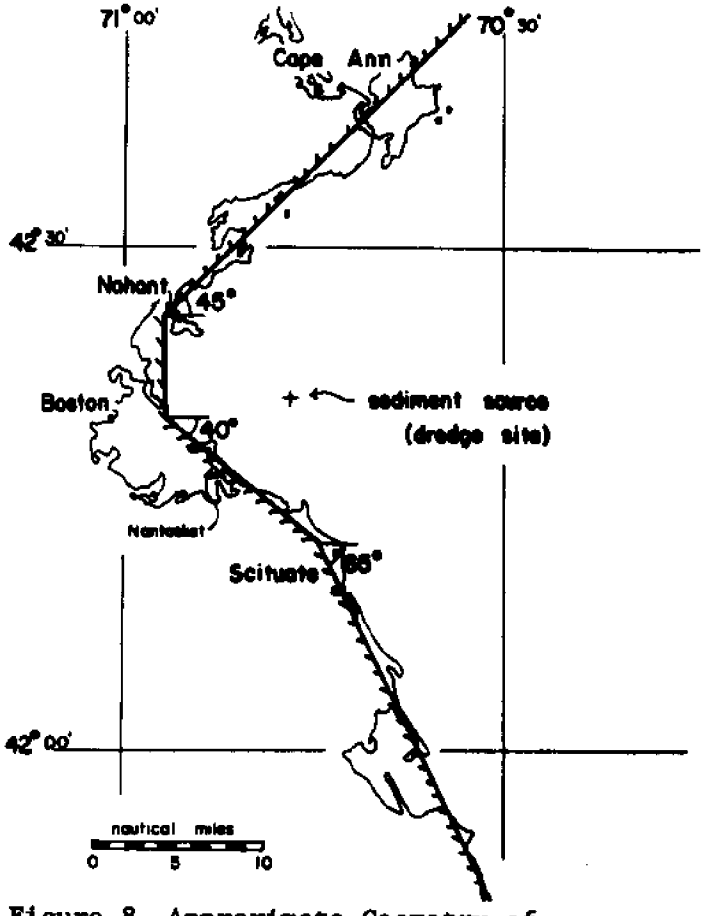

Figure 8 Approximate Geometry of Massachusetts Bay

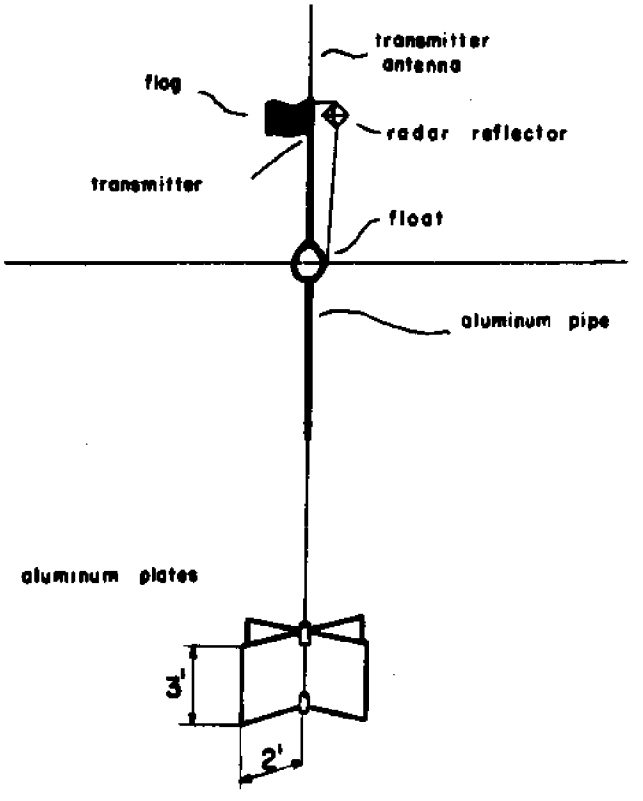

Figure 9 Drogue Used in Massachusetts Bay Current Studies

The specific gravity of the samples ranged from 2.30 to 2.90, averaging 2.60 - 2.65. This value for specific gravity indicates that Equation (4.13a), from which the settling velocities in Table 1 were derived, is valid.

The results of the UNH studies were presented in the form of classical grain size distribution curves. In terms of the 5 groups presented in Table 1, these curves yielded the following average sample composition:

fine sand	$60\mu < d < 100\mu$	10%
coarse silt	$20\mu < d < 60\mu$	13%
medium silt	$6\mu < d < 20\mu$	14%
fint silt	$2\mu < d < 6\mu$	13%
clay	$d < 2\mu$	50%

However, the grain size of the particle is not the most important quantity for the model. The critical factor is the settling velocity, w_s, which is indeed a function of grain size, but which is also influenced by other factors, such as shape, surface, and state of flocculation. Because the clay fraction of the fines is most affected by flocculation, a number of settling tube experiments on various clays were performed (Section 4.5). According to the results, the clay fraction can be distributed into different settling groups. A settling tube experiment with material from the bottom of the dredging site had been planned, but the termination of the project did not allow the necessary sampling. Based on the results

of the runs with other fine materials with 10 mg/ℓ initial concentration, as was shown in Table 2 (Section 4.5.2), it may be assumed that the clay fraction contributes to the following groups, in terms of settling rates:

$w_s = 0.68 \times 10^{-4}$ 35%

$w_s = 1.36 \times 10^{-3}$ 40%

$w_s = 1.43 \times 10^{-2}$ 25%

The results of the 10 mg/ℓ initial concentrations were used instead of the 100 mg/ℓ, because the former is more representative of the concentrations possibly predominating about the source due to the injection rate calculated in Section 7.2.

Incorporating these results with the data obtained by UNH, the resulting distribution into groups was computed and is shown in Table 3.

Table 3: Composition of Dredging Fines in Terms of Settling Velocity

Group No.	Mean Settling Velocity (cm/sec)	Percentage of Fines
1	0.462	10%
2	0.136	13%
3	$0.143 \cdot 10^{-1}$	27%
4	$0.136 \cdot 10^{-2}$	33%
5	$0.68 \cdot 10^{-4}$	17%

7.4 Background Concentrations of Suspended Sediment

Because of the nature of the mathematical model, a non-zero value of concentration, c, will be obtained at all spatial positions. Of course, very small values will be overshadowed by the "ambient" sediment concentrations existing under natural conditions. Thus, background data are needed to determine the extent of the dredging impact. Any position with a concentration increase of at least the same order of magnitude as the ambient can be considered "affected" by the dredging.

Beginning in January 1973 suspended sediment measurements were taken in Massachusetts Bay under the NOMES project. Samples were analyzed through filtering techniques and through light scattering by means of the turbidimeter described in Section 4.5. The correlation of turbidity with sediment concentrations appears rather encouraging, at least for the low concentrations encountered in the Bay, as was seen in Figure 2. Details of the procedures of monitoring turbidity and suspended sediments are given by Frankel and Pearce (10).

The measurements indicate an average suspended load in the Bay of about 1 mg/ℓ. This includes both organic and inorganic matter. Consequently, the areas of actual dredging impact are those for which the concentration increase is of the order of this value. The dredging effect can be considered minor in areas with a much smaller amount of concentration increase. In addition, the effects

of the shoreline, as discussed in Section 5.1, need not be considered if the concentrations obtained by the model are very small near the shore.

7.5 Determination of Parameters from Drogue Data

As was explained in Chapter 5, current measurements are extremely important to the model. With respect to the application of the model in the Massachusetts Bay the only suitable field data were obtained through three drogue studies carried out in the first part of 1973. The type of drogue used is shown in Figure 9. During each of these studies three or four drogues were deployed at various depths at approximately the same point. They were then tracked for at least a full tidal cycle, their positions being recorded approximately every hour. These data made it possible to obtain values of the net drift, of the tidal velocities, of the dispersion coefficients along with some information on the velocity variations over the depth. The pathlines of the drogues in these studies are given in Figures 10, 11 and 12. A full account of the methods and instrumentation used can be found in a report by the authors (4).

A computer program has been developed to carry out the evaluation of the model parameters from the drogue data and the actual computations of the model. The procedure is divided essentially into two parts. First, the drogue and sediment data are used to solve the vertical concentration distribution, to obtain average net drift and tidal velocities, and to compute the decay rate and dispersion

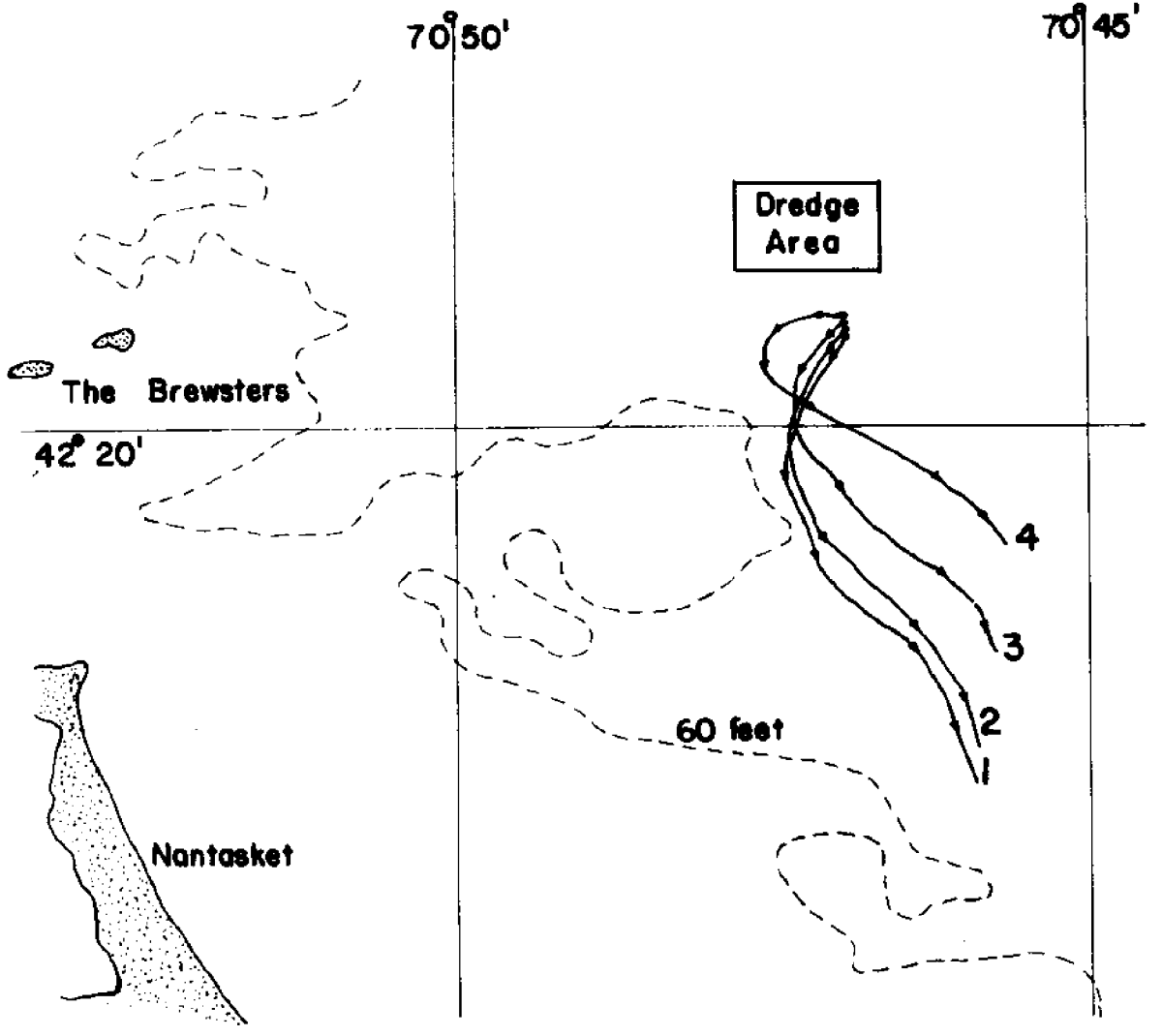

drogue depths:

#1	7 meters
#2	7 meters
#3	12 meters
#4	22 meters

meteorological cond.:

Wind calm initially, rising to 15-20 knots from NE at 0200 on 2/22 and constant thereafter. Seas calm initially, rising to 6-8 ft. by 1000 on 2/22.

1 0 1
nautical miles

Figure 10

Drogue Paths in the Study of February 21-22, 1973

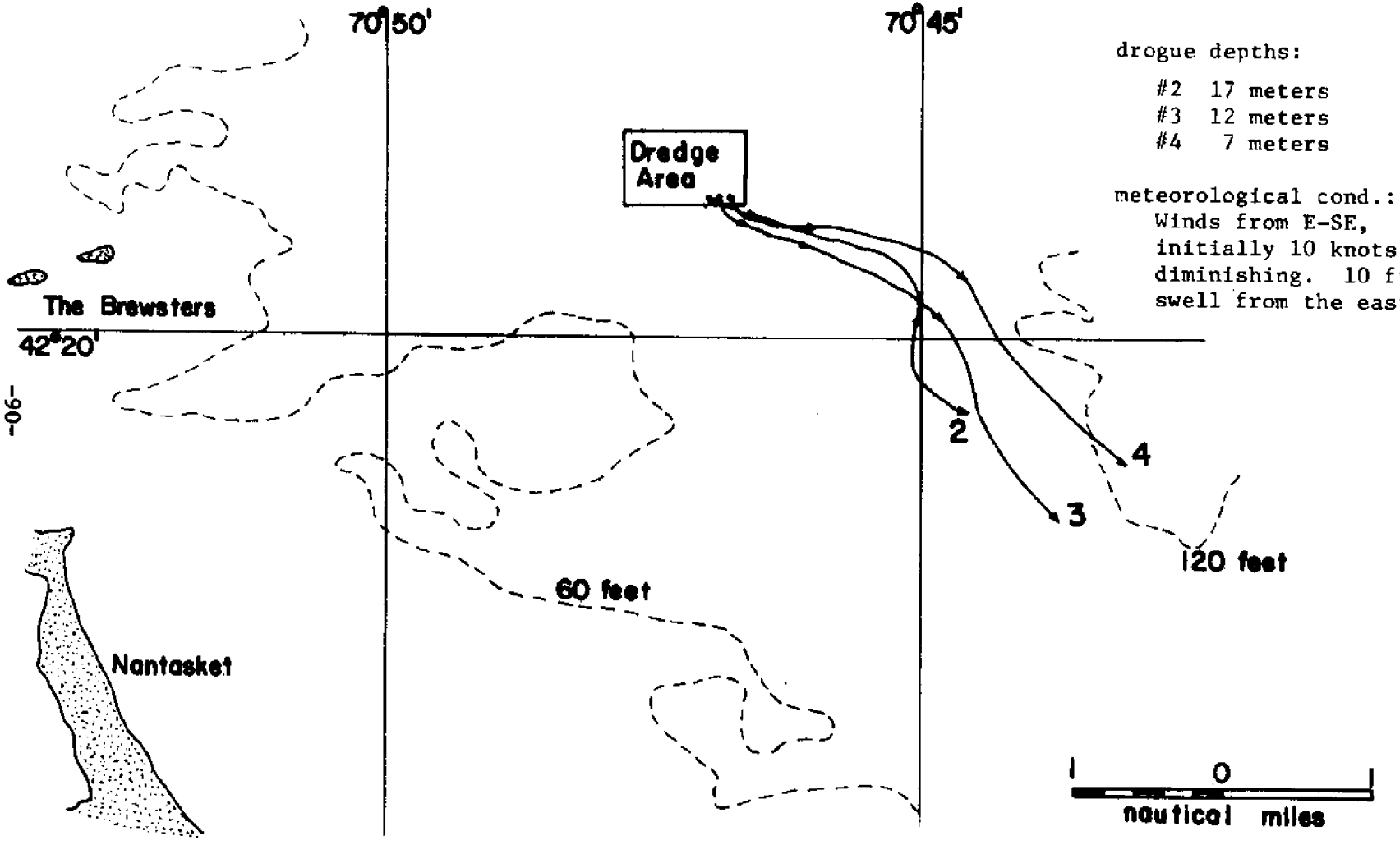

Figure 11

Drogue Paths in the Study of March 28-29, 1973

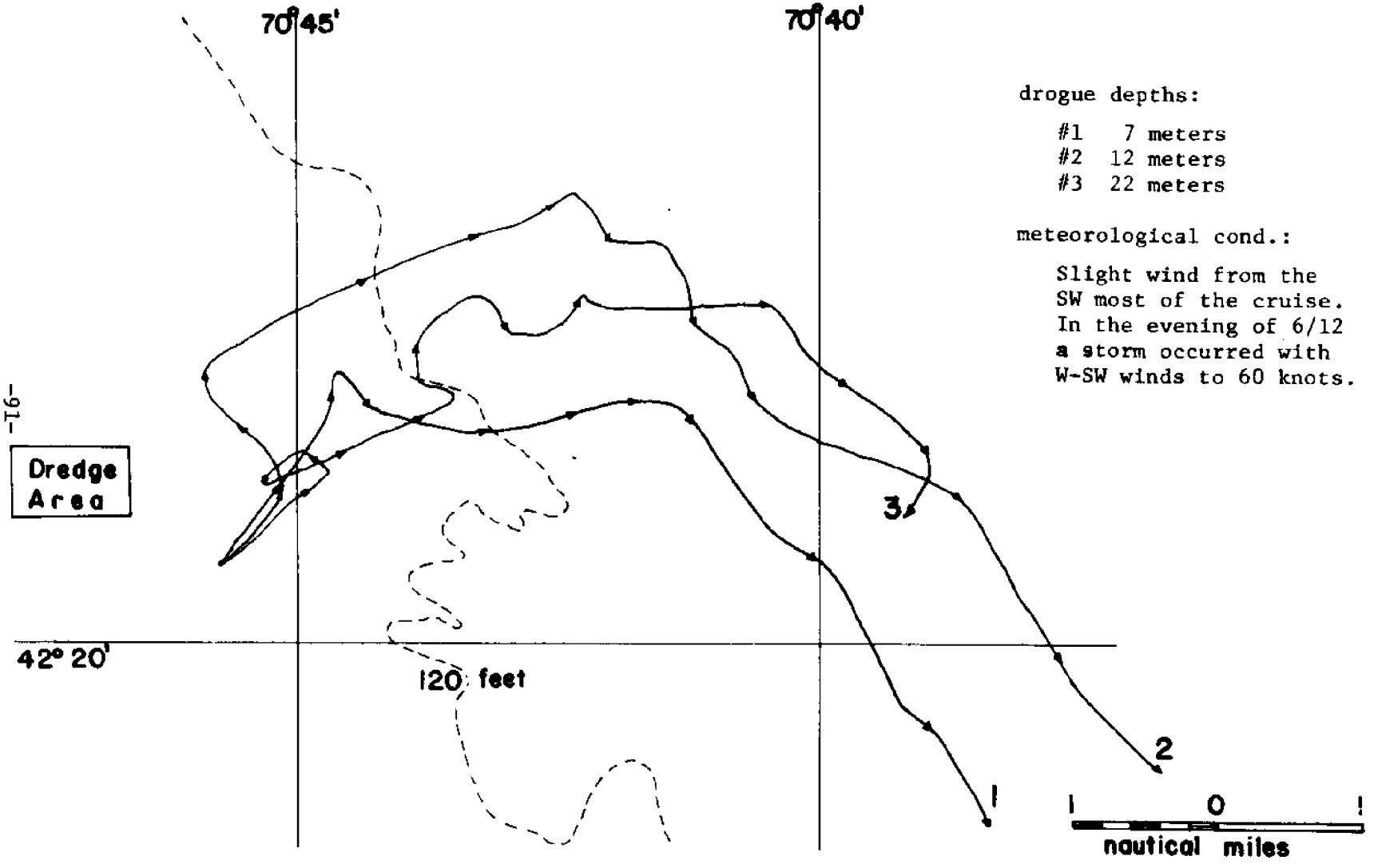

Figure 12
Drogue Paths in the Study of June 11-12-13, 1973

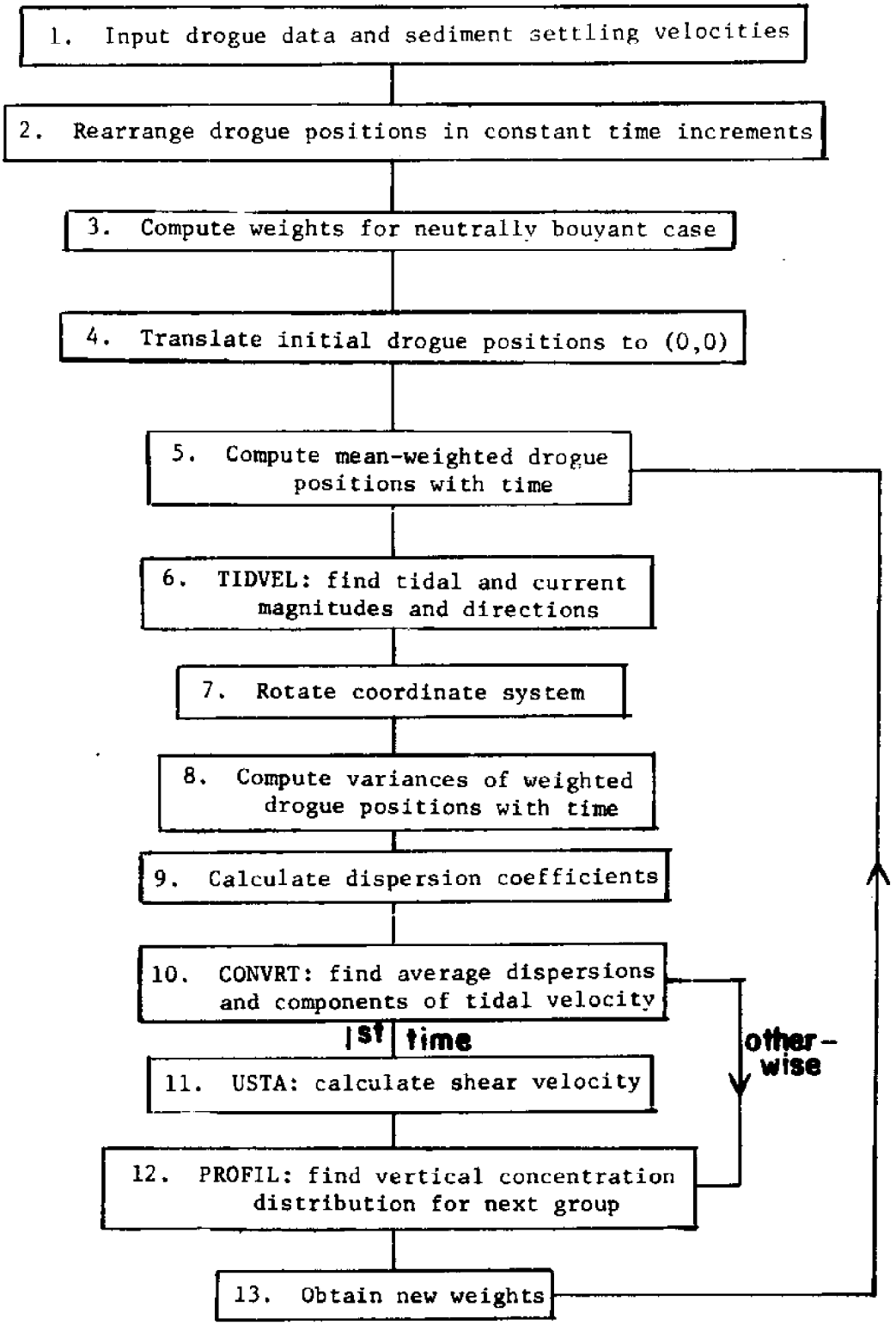

Figure 13

Flow Chart of Model Procedures

coefficients. In the second part, this information is used to solve the horizontal dispersion equation (5.7). The first part procedure is outlined in Figure 13 and described step by step below. The FORTRAN source program is listed in Appendix B.

1. The first step is the input of the drogue and sediment data along with other necessary information. For each drogue, a series of positions and times is given denoting the drogue path. The drogue depth and the mean depth of the bottom over the drogue path is also required.

The only sediment data needed are the settling velocities for each of the 5 different groups of particles shown in Table 3, with the initial concentration of each group.

Other additional information includes values for the analysis starting time and the time increment to be used in Step 2, a depth increment for the integration of the vertical sediment distribution (Step 12), and a value for Von Karman's universal constant, k.

2. The drogue data are adjusted next so that a specified time interval exists between drogue positions. This requires interpolation between the actual drogue positions, which should not introduce any significant error since there are enough actual data points in the 3 drogue studies being analyzed. The results of this operation yield a table of simultaneous drogue positions, North and East, with the corresponding times evenly spaced.

3. The weights attributed to the drogues are computed by the technique described in Section 5.2.

4. The drogue paths are all translated in space so that each drogue starts at position (0,0). This step simplifies the velocity and the dispersion calculations. It does not introduce significant error, since the initial positions of the drogues are close together in all cases.

5. The mean drogue positions at different times are calculated. (The need for the simultaneous drogue positions as computed in step 2 is now clear). The drogue positions for each time are not simply averaged, they are averaged with respect to the weighting factors computed in Step 3 or Step 13. From these, the mean-weighted velocities are calculated.

6. The Subroutine TIDVEL computes the tidal and net drift velocities. The procedure begins by selecting the drogue record covering one full tidal cycle (see Figure 14). The distance the drogue travels in this period divided by the tidal time, 12.4 hours, is denoted the net drift velocity; the direction of travel is the net drift direction. The remaining deviation about this net drift is considered to be due to the tidal current. The maximum deviation to the left and to the right of the net drift is calculated. Both distance and direction for these maxima are recorded. The difference between these two vectors is the total movement due to the tide, $2\ell_T$. (see Figure 14).

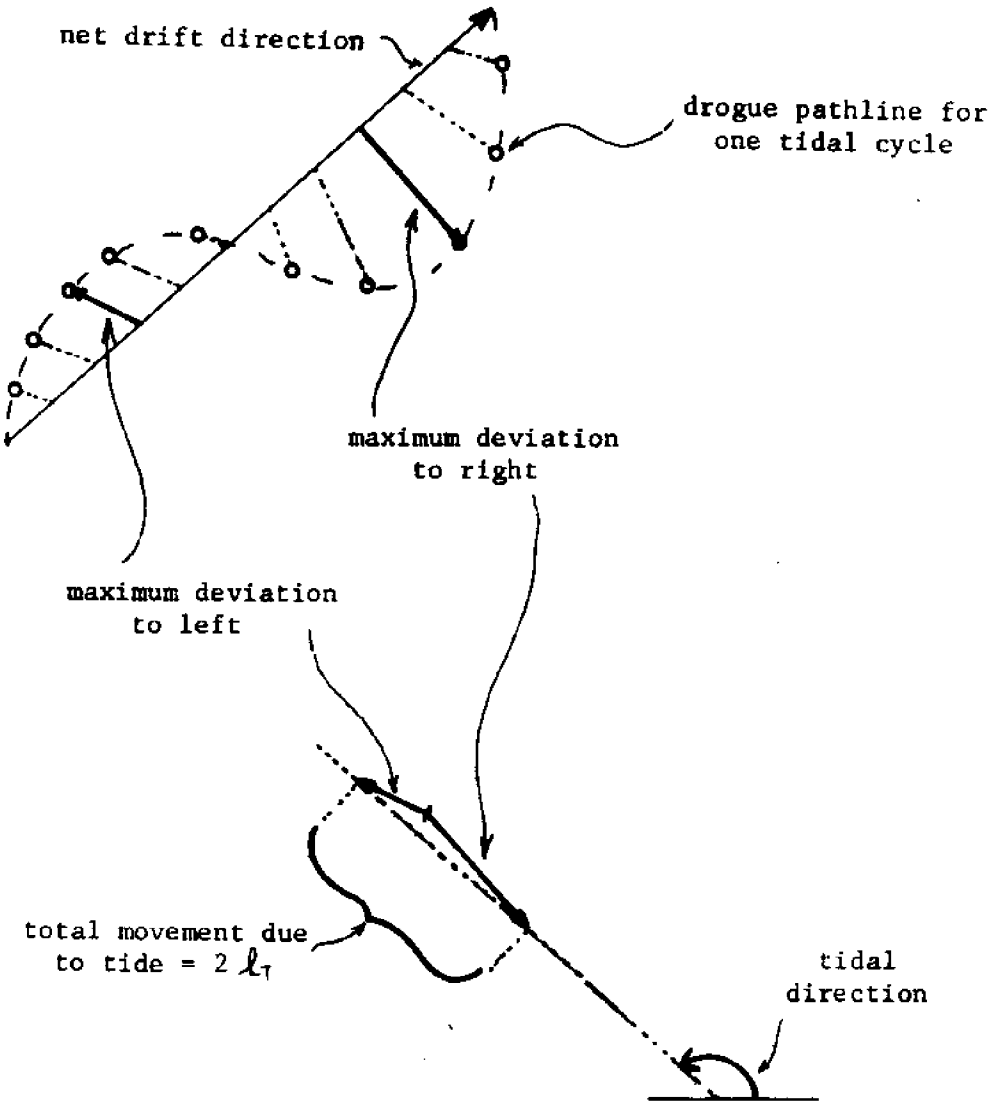

max. tidal velocity = $2\pi\ell_T/T$

Figure 14

Technique for Determining Magnitude and Direction of Tidal Velocities

An equivalent sinusoidal tide, that is, one which causes the same total movement, should have a maximum velocity given by the formula:

$$\sqrt{U_T^2 + V_T^2} = \frac{\pi}{2} \frac{2\ell_T}{T/2} = \frac{2\pi\ell_T}{T} \qquad (7\text{-}3)$$

The direction of the equivalent tide is also given by the direction of the vector $2\ell_T$.

7. The coordinate system is now rotated so the new x-axis is in the direction of the net drift.

8. The variances of the weighted drogue positions at times found in Step 2 are now calculated for both the x and y axes. (Due to the previous rotation, these variances are in the direction of the net drift and normal to the net drift).

9. From these two series of variances, the dispersions in the x and y directions are found. The formula for the determination of dispersion from the variance is

$$E = \frac{\Delta(\sigma^2)}{2(\Delta t)} \qquad (7\text{-}4)$$

where σ^2 is the variance

t is the time

From this it can be seen that the dispersion may be a function of time. It has been generally found that the dispersion increases slightly with time. This is probably due to the fact that as the drogues spread, they may enter zones of different eddy motions,

characterized by different length scales. Thus, their motion is more subject to random influences as they spread further apart. However, as mentioned, constant dispersion coefficients from averages over a tidal cycle will be used in this study.

10. In subroutine CONVRT, the average dispersion coefficients over the selected tidal cycle are calculated. Also, the components of the tidal velocity along the net drift and normal to the net drift are found.

11. In subroutine USTA the shear velocity, u_*, is found from:

$$u_* = \sqrt{\frac{f}{8}}\, U_m \qquad (7\text{-}5)$$

where f is the roughness coefficient

U_m is the magnitude of the mean water velocity

A value of the roughness coefficient, f, equal to 0.02 was used. This value is appropriate as a mean value for flat bed conditions. It should be noted that the water velocity used includes both the tidal and the net drift components of the current. In other words, the total length of the path line of the mean drogue positions over one tidal cycle divided by the tidal time constitutes the magnitude of U_m.

Up to this point, the procedure deals with purely hydrodynamic characteristics, the main purpose being to define an appropriate value of u_* for the determination of the normalized vertical sediment distribution.

12. The integration of Equation (4.8) is performed in subroutine PROFIL, to yield the solution of the normalized suspended sediment distribution in the vertical direction, $\phi(\zeta)$, for a particular settling velocity w_s.

13. In subroutine WEIGHT the normalized sediment distribution, $\phi(\zeta)$, found in Step 12, is used to compute the weights for the drogues, based on the vertical spacing of the drogues, in addition to the values of $\phi(\zeta)$ at the drogue depths. The complete computation technique was discussed in Section 5.2. For this new set of weights the procedure is repeated beginning with Step 5 but with the exception of Step 11. Instead of the mean water drift and tidal velocities, the respective mean transport rates for a certain group of sediments (identified by its settling velocity) are now calculated. Similarly, instead of the dispersion coefficients of the water body, the effective dispersions, appropriate for the various sediment groups, are found.

It may be noted that the coordinate system for each sediment group will be slightly different due to the different values of the drift direction obtained for each case. This is reasonable in view of the directional differences for the drogues at various depths and of the "heavier" particles being dominated by the velocities at lower depths. However, the "lighter" particles, being distributed more evenly over the depth, will be affected by the velocities at all depths. The values of the parameters obtained from the data of the three field trips are presented in Tables 4, 5, and 6.

Table 4

Parameters for Conditions of February 21-22, 1973

Mean depth h = 25m	Shear Velocity $u_* = 0.533$ cm/sec					
Dimensional parameters	Units	Grp 1	Grp 2	Grp 3	Grp 4	Grp 5
Net drift magnitude, U_{fs}	cm/sec	5.28	6.82	8.10	8.24	8.24
Max tidal velocity, $\sqrt{U_{Ts}^2+V_{Ts}^2}$	cm/sec	9.62	10.52	10.16	10.10	10.10
Max tide along drift axis, U_{Ts}	cm/sec	7.26	7.34	6.48	6.36	6.36
Max tide normal to drift axis, V_{Ts}	cm/sec	6.30	7.52	7.84	7.84	7.84
Dispersion along drift axis, E_x	$cm^2 10^5/sec$	1.85	1.18	0.83	0.78	0.78
Dispersion normal to drift axis, E_y	$cm^2 10^5/sec$	0.008	0.20	0.25	0.24	0.24
Average horizontal dispersion, $\sqrt{E_x E_y}$	$cm^2 10^5/sec$	0.12	0.48	0.46	0.43	0.43
Drift direction	° from E	-55	-60	-65	-66	-66
Tidal direction	° from E	-14	-14	-15	-15	-15
Angle between drift and tide	degrees	41	46	50	51	51
Dimensionless parameters						
Net drift magnitude, $U_{fs}T/h$		96	125	148	151	151
Max tidal velocity, $(\sqrt{U_{Ts}^2+V_{Ts}^2})T/h$		166	192	184	184	184
Max tide along drift axis, $U_{Ts}T/h$		132	134	118	116	116
Max tide normal to drift axis, $V_{Ts}T/h$		116	138	144	144	144
Dispersion along drift axis, $E_x T/h^2$		870	860	610	575	570
Dispersion normal to drift axis, $E_x T/h^2$		6	150	182	175	175
Decay factor, αT		101	10.1	0.32	0.025	0.001
Values for the parameters of the water itself are identical to those of group 5						

Table 5

Parameters for Conditions of March 28-29, 1973

Mean depth h = 30m	Shear Velocity u_* = 0.479 cm/sec					
Dimensional parameters	Units	Grp 1	Grp 2	Grp 3	Grp 4	Grp 5
Net drift magnitude, U_{fs}	cm/sec	2.83	6.53	8.83	9.05	9.07
Max tidal velocity, $\sqrt{U_{Ts}^2+V_{Ts}^2}$	cm/sec	2.74	5.66	6.36	6.38	6.38
Max tide along drift axis, U_{Ts}	cm/sec	1.44	2.76	2.56	2.46	2.44
Max tide normal to drift axis, V_{Ts}	cm/sec	2.32	4.94	5.84	5.88	5.88
Dispersion along drift axis, E_x	$cm^2 10^5/sec$	3.32	3.24	1.74	1.57	1.55
Dispersion normal to drift axis, E_y	$cm^2 10^5/sec$	0.001	0.036	0.14	0.15	0.15
Average horizontal dispersion, $\sqrt{E_x E_y}$	$cm^2 10^5/sec$	0.058	0.34	0.49	0.48	0.48
Drift direction	° from E	-40	-39	-37	-37	-37
Tidal direction	° from E	18	21	29	30	30
Angle between drift and tide	degrees	58	60	66	67	67
Dimensionless parameters						
Net drift magnitude, $U_{fs}T/h$		43	99	134	137	138
Max tidal velocity, $(\sqrt{U_{Ts}^2+V_{Ts}^2})T/h$		42	86	96	96	96
Max tide along drift axis, $U_{Ts}T/h$		22	42	40	38	38
Max tide normal to drift axis, $V_{Ts}T/h$		36	54	88	90	90
Dispersion along drift axis, E_xT/h^2		1680	1640	880	790	785
Dispersion normal to drift axis, E_yT/h^2		1	18	70	76	77
Decay factor, αT		87	9.3	0.27	0.021	0.001
Values for the parameters of the water itself are identical to those of group 5						

Table 6

Parameters for Conditions of June 11-12, 1973

Mean depth h = 35m	Shear Velocity u_* = 0.433 cm/sec					
Dimensional parameters	Units	Grp 1	Grp 2	Grp 3	Grp 4	Grp 5
Net drift magnitude, U_{fs}	cm/sec	2.14	4.58	6.80	7.06	7.09
Max tidal velocity, $\sqrt{U_{Ts}^2+V_{Ts}^2}$	cm/sec	3.10	5.68	6.38	6.48	6.50
Max tide along drift axis, U_{Ts}	cm/sec	3.10	5.69	6.16	6.16	6.18
Max tide normal to drift axis, V_{Ts}	cm/sec	0.14	0.22	1.70	2.02	2.06
Dispersion along drift axis, E_x	10^5 cm^2/sec	1.27	1.50	1.41	1.34	0.94
Dispersion normal to drift axis, E_y	10^5 cm^2/sec	0.002	0.22	0.84	0.93	0.94
Average horizontal dispersion, $\sqrt{E_x E_y}$	10^5 cm^2/sec	0.050	0.57	1.09	1.12	1.12
Drift direction	° from E	40	42	41	40	40
Tidal direction	° from E	43	45	57	58	58
Angle between drift and tide	degrees	3	3	16	18	18
Dimensionless parameters						
Net drift magnitude, $U_{fs}T/h$		28	60	89	92	92
Max tidal velocity, $(\sqrt{U_{Ts}^2+V_{Ts}^2})T/h$		40	74	83	84	84
Max tide along drift axis, $U_{Ts}T/h$		40	74	80	80	80
Max tide normal to drift axis, $V_{Ts}T/h$		2	4	22	26	26
Dispersion along drift axis, E_xT/h^2		470	560	525	500	495
Dispersion normal to drift axis, E_yT/h^2		1	85	315	345	350
Decay factor, αT		80.5	8.85	0.237	0.018	0.001
Values for the parameters of the water itself are identical to those of group 5						

Once the hydrodynamic parameters (mean transport rates and dispersion coefficients) and the normalized vertical concentration profiles of the sediment groups in each drogue study are determined, they are used to solve the horizontal depth-averaged dispersion equation. The decay factor, α, is computed as

$$\alpha = Aw_s \, \phi(0)/h$$

wherein A is assumed as unity. All parameters are expressed in non-dimensional form, using the depth h as the reference length and the tidal period T = 45600 sec as the reference time. Then the integration (5.7) is performed numerically, using a non-dimensional time increment of $\frac{\Delta t}{T} = 0.05$.

The lines of equal concentration for each case are plotted in Figures 15, 16, 17. This is done only for groups 3, 4, 5. Groups 1 and 2 do not yield any significant average concentrations at distances more than a mile from the source. For purposes of comparison, each figure was drawn as if the input consisted 100% from sediments of the respective group. To get the actual concentrations, the values presented must be multiplied by the percentages shown in Table 3.

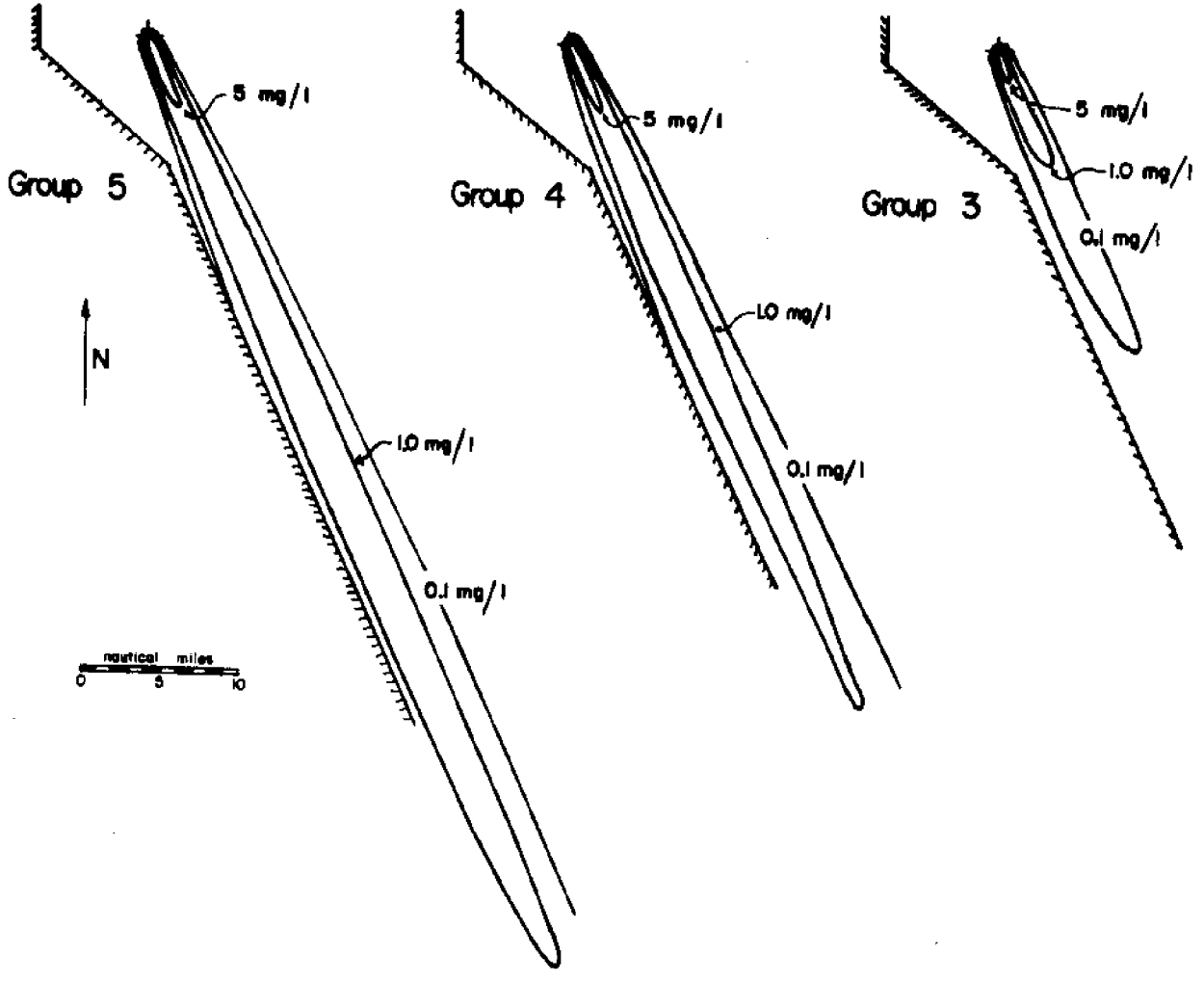

Figure 15

Distribution of Average Concentration for Conditions of February 21-22, 1973

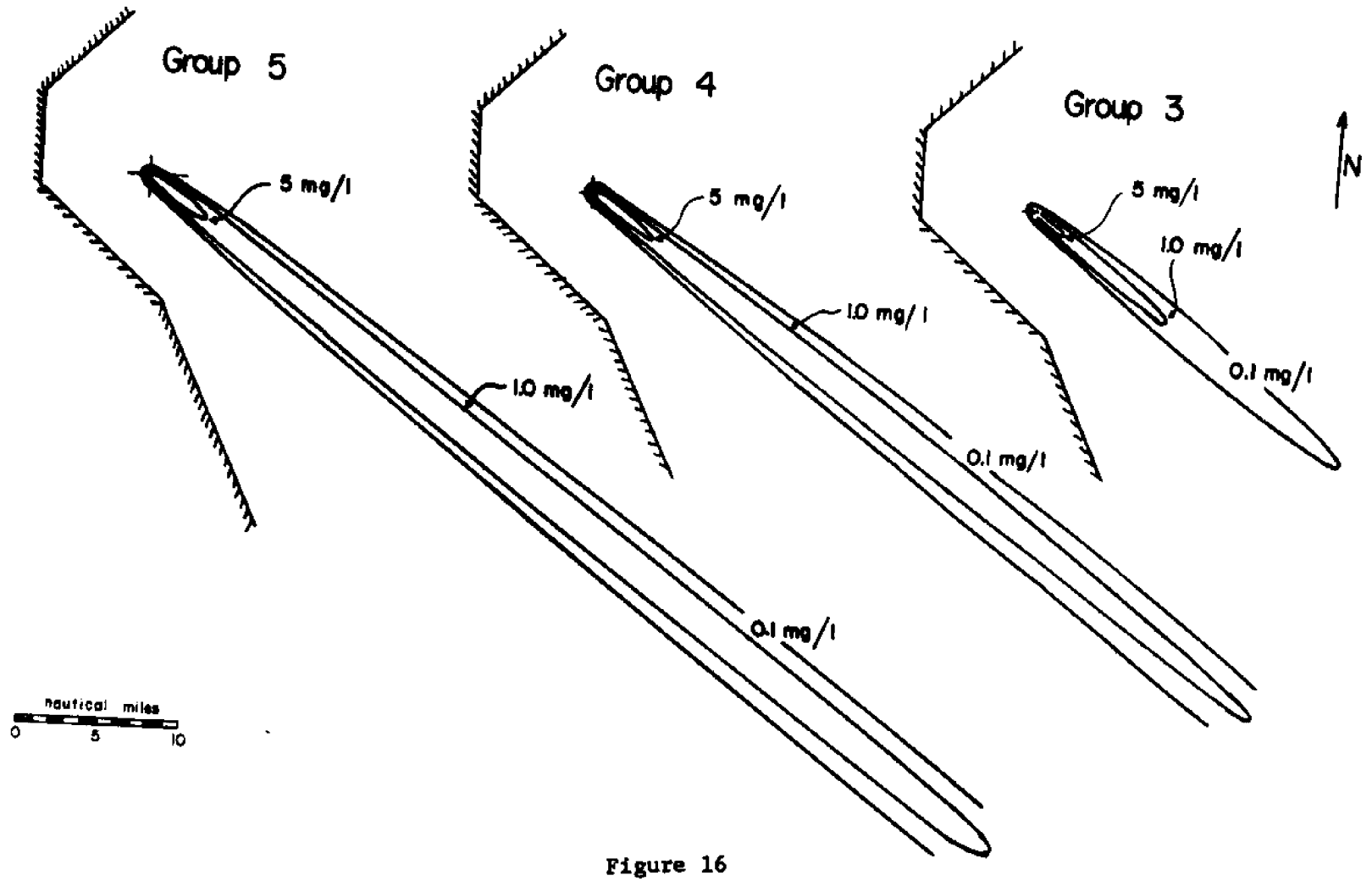

Figure 16

Distribution of Average Concentration for Conditions of March 28-29, 1973

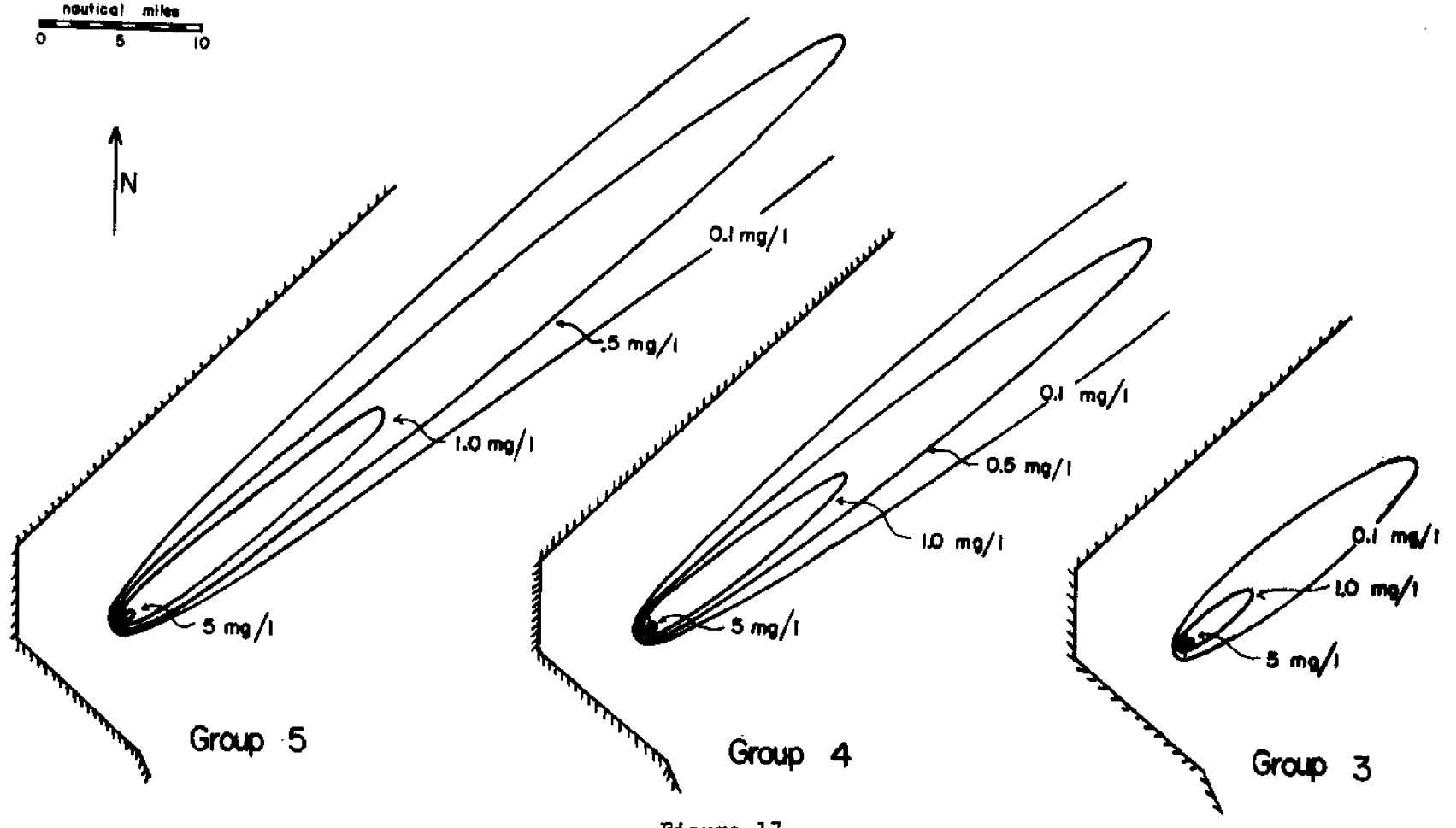

Figure 17

Distribution of Average Concentration for Conditions of June 11-12, 1973

7.6 Results and Discussion

Several things can be noted about the values of the parameters listed in Tables 4, 5, and 6.

First, there is a consistent increase of the mean transport rates both tidal and non-tidal, from group 1 to group 5. This was expected, since the lower velocities near the bottom are more heavily weighted in the first sediment groups. The differences are very slight between groups 3, 4, and 5 because of their nearly uniform vertical profiles. The tidal velocities are higher in February, when the tidal amplitude was larger. The drift velocities are generally of the same order of magnitude as those of the tides. The ratio of tidal to drift magnitudes is larger for the first groups, possibly indicating a more uniform tidal profile, with relatively high velocities near the bottom. The drift velocities of about 7-10 cm/sec for the water itself are in good agreement with values reported from other studies and discussed in more detail in another report by the authors (4).

The prevailing drift direction is SE. In June, the drogues, after moving for several hours to NE, changed direction and continued SE, which was the direction of the March and February drogues, also (Figures 10, 11, 12). The direction of transport is very much the same for all the groups, on each cruise, the difference among them being much smaller than the differences between the three cruises. This indicates that the water moves at approximately the same

direction at all depths. It should be mentioned here that the shallowest drogue is at a 7m depth, thus directional changes near the surface, due to short-duration winds, could not be measured; also, drogues were not placed close to the bottom to avoid interference with the sea bed.

The shear velocity did not change much in the three cases, having an approximate magnitude of 0.5 cm/sec.

With respect to the dispersion coefficients, it is seen that the effective value of the longitudinal dispersion (i.e., along the drift direction) decreases from group 1 to 5. This is because of the presence of high concentrations of group 1 near the bottom, where the velocity gradients are higher. By contrast, the lateral dispersion (i.e., normal to the drift direction) increases markedly from group 1 to 5. Due to the absence of any constant shear flow normal to the net drift, the nonuniform suspensions are not easily dispersed.

The average horizontal dispersion for the water body defined as the geometrical mean of the two values is remarkably similar in February and March, but twice as high in June. This increase is mostly due to the lateral dispersion. It may be due to the stratified conditions prevailing in June, in contrast to February and March. In Table 7, theoretical predictions for the eddy diffusion terms by Okubo's formula (Section 5.3) are presented for $\ell = 30h$. Also shown are the dispersion terms, following the formula $E_\alpha = \lambda h u_*$, where E_d u_* in any direction is assumed to be 1/20 of the mean velocity

Table 7

Dispersion Coefficients (10^5 cm^2/sec)

	February	March	June
Eddy Diffusivity ε	0.040	0.050	0.060
E_d along drift axis			
Elder (λ = 6)	0.092	0.106	0.132
Taylor (λ = 20)	0.305	0.350	0.430
Harleman (λ = 40)	0.61	0.70	0.85
λ = 80	1.22	1.40	1.70
Okubo (λ = 200)	3.05	3.50	4.30
Measured values	0.78	1.56	1.33
E_d normal to drift axis			
Elder (λ = 6)	0.038	0.036	0.014
Taylor (λ = 20)	0.126	0.120	0.050
Harleman (λ = 40)	0.26	0.24	0.10
λ = 80	0.52	0.48	0.20
Olubo (λ = 200)	1.30	1.20	0.50
Measured values	0.24	0.15	0.94

magnitude in that direction.

It is seen that estimates, with values of λ 40 to 80, are in most cases close to the true values; only the dispersion normal to the drift axis in June is severely underestimated.

The dispersion patterns resulting from the model for the three sets of conditions (Figures 15, 16, 17) clearly indicate that the drift direction is the most important hydrodynamic feature affecting the movement of suspended matter for the conditions investigated. Unfortunately, it is highly variable. The assumption of a constant drift is too restrictive and does not in general represent natural conditions. The drift direction changes both in time and space, as the result of wind shifts, inlets, general circulation, etc. The prevailing direction, however, for Western Massachusetts Bay, seems to be SE. Occasional changes of the drift from this direction may conceivably spread the sediments more in the lateral direction and less in the longitudinal. Thus, the model results overestimate the length but underestimate the width of a natural dispersion plume. If the drift were truely constant, the narrow isoconcentration lines would be quite reasonable. The material could not spread much due to the assumed lateral uniformity in the velocity field. The value of the dispersion coefficient normal to the drift axis becomes then the primary factor influencing the width of the isoconcentration lines. This is evident by comparison of the March and June plots (Figures 16, 17). The tide,

as will be seen later, does not materially affect the width but just moves the plume back and forth, about the drift direction. The value of the dispersion coefficient along the drift axis is, by contrast, quite insignificant in light of the very important role of the drift velocity in determining the total length of dispersion. This can be seen by comparing the lengths of the plots of February and June (Figures 15, 17).

However, the decay factor, α, a function of the sediment settling velocity, is even more important in determining the extent of the plume of the suspended matter. This is readily seen by comparing the plots for groups 3, 4 and 5 for any set of conditions, although the advective and dispersion terms are approximately the same for the three groups. The importance of A becomes now clear. If it were taken as 0.5 instead of unity, the result would be the same as if the settling velocity were divided by 2.

The time needed for the solution to reach steady state at a particular point was found to depend primarily upon the decay constant and the magnitude of the net drift. This time, expressed in number of tidal cycles, can be approximately given as

$$n = \frac{L}{T * U_f} + 4 \qquad (7\text{-}6)$$

wherein L = distance from the source

U_f = net drift velocity.

This holds, provided the decay factor is such that significant concentrations are eventually found at the point under consideration. Thus, the time to convergence for the model runs was less than 5 tidal periods for groups 1 and 2, about 12 for group 3, 20 to 25 for group 4 and more than 30 for group 5. In fact, the plots presented in Figures 15 and 16 for group 5 are for a time of 30 tidal cycles, due to restrictions in computer time. The equilibrium profiles are slightly longer. Of course, for points near the source steady state was reached much sooner for all groups.

In order to provide more specific information on the effects of a possible dredging operation, representative values for the parameters of the model, estimated from those appearing in Tables 4, 5 and 6, were used for another run of the model. The values used are listed in Table 8. The normalized vertical profiles for the 5 groups are shown in Figure 18. The decay factors were computed as $\alpha = \frac{w_s \phi(0)}{h}$, considering A = 1.

The results of the depth averaged concentration $\bar{c}$ are presented in Figure 19, in distorted scales, the x-axis being parallel to the net drift direction. The coordinates are presented in non-dimensional units, i.e., multiples of the depth. The distances to which several concentrations extend are tabulated in Table 9.

The effect of the tide, as seen in Figure 19c, is basically a shift of the isoconcentration lines along the tidal direction.

Table 8

Average Conditions

Depth h = 30m	Shear Velocity u_* = 0.5 cm/sec				
Non-dimensional Parameters	Group 1	Group 2	Group 3	Group 4	Group 5
Net drift magnitude, $U_{fs}T/h$	50	90	125	130	130
Max tidal velocity, $(\sqrt{U_{Ts}^2 + V_{Ts}^2})T/h$	80	110	120	120	120
Angle between drift and tide, degrees	50°	55°	60°	60°	60°
Dispersion along drift axis, $E_x\ T/h^2$	1000	1000	650	600	600
Dispersion normal to drift axis, $E_y\ T/h^2$	3	80	150	160	160
Decay constant, αT	87.3	8.95	0.27	0.021	0.001

Table 9

Length, in Multiples of the Depth, of Area with Concentration $\bar{c}$ Larger than Indicated

(for average conditions)

$\bar{c}$ (mg/ℓ)	Group 1	Group 2	Group 3	Group 4	Group 5
0.5	20	60	750	-	-
1.0	18	50	510	2000	3600
2.0	16	40	280	850	1080

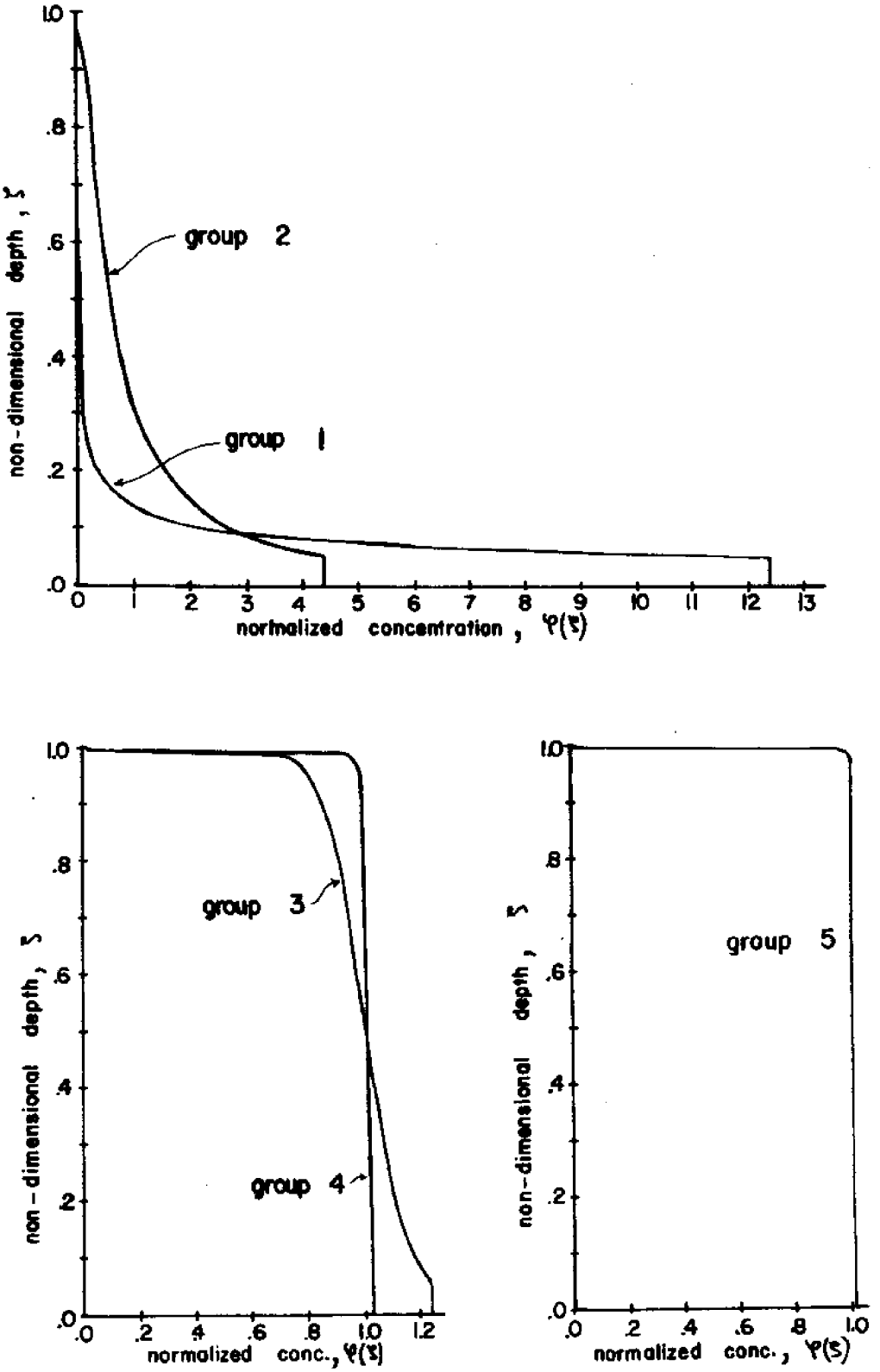

Figure 18

Normalized Vertical Profiles Under Average Conditions

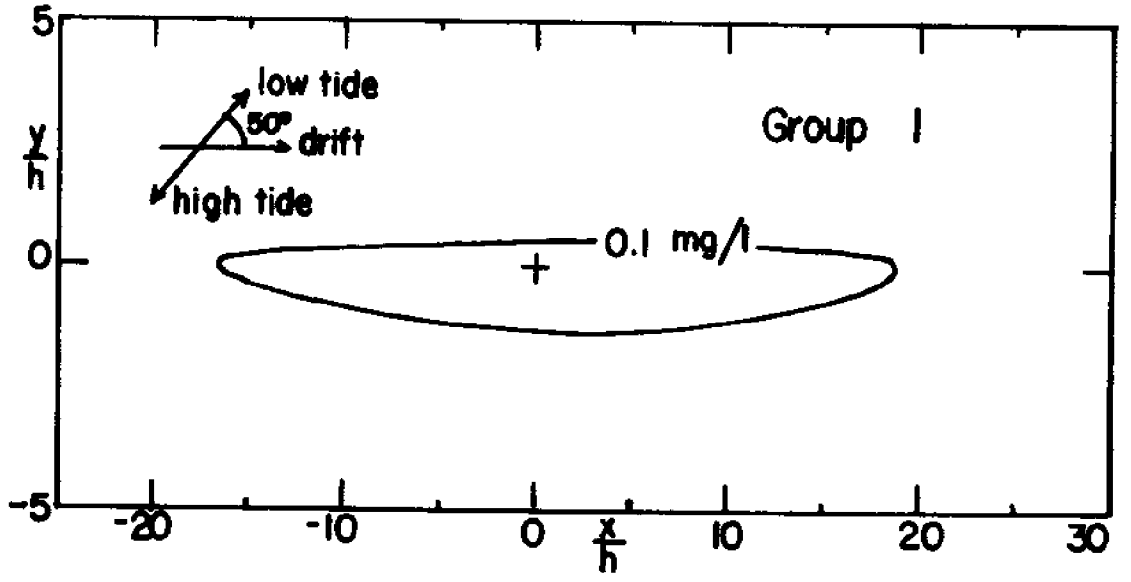

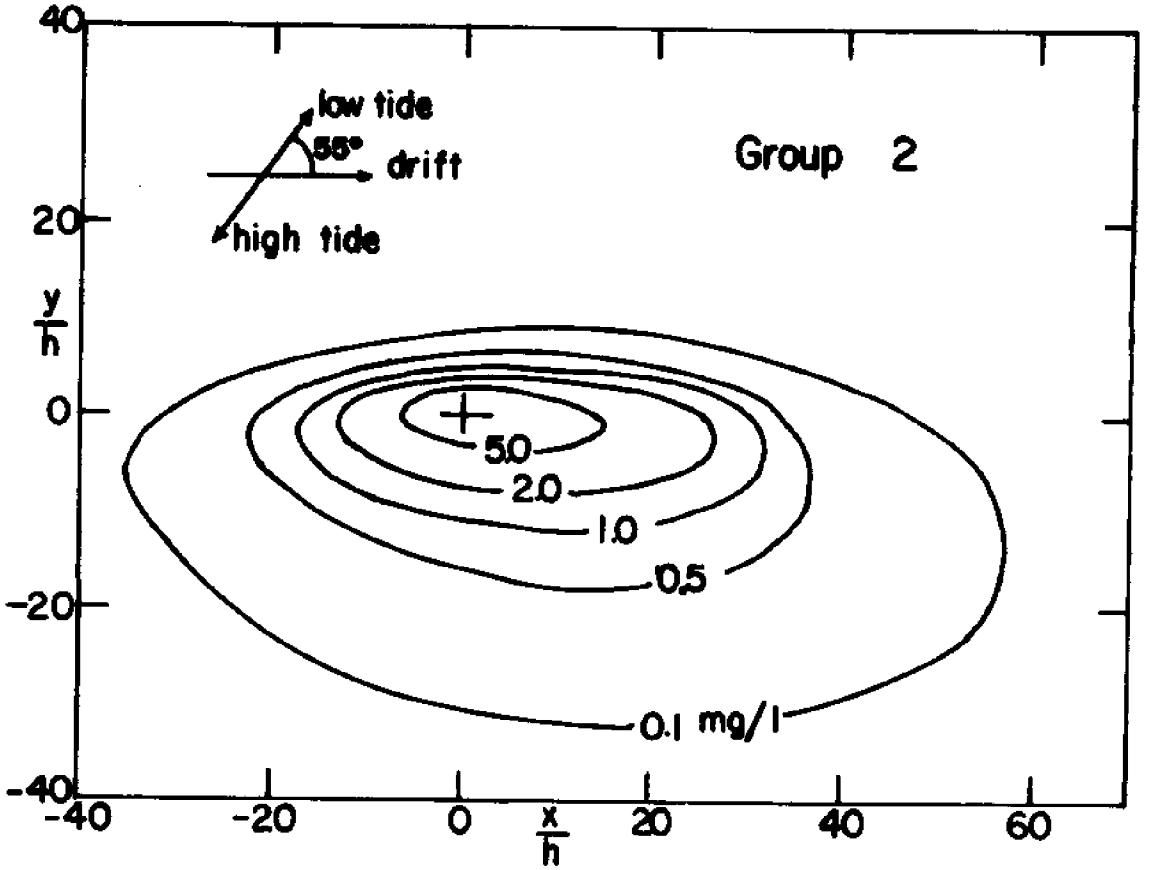

Figures 19a,b
Distribution of Average Concentration, $\bar{c}$, of Groups 1 and 2 under Average Conditions, at High Water Slack

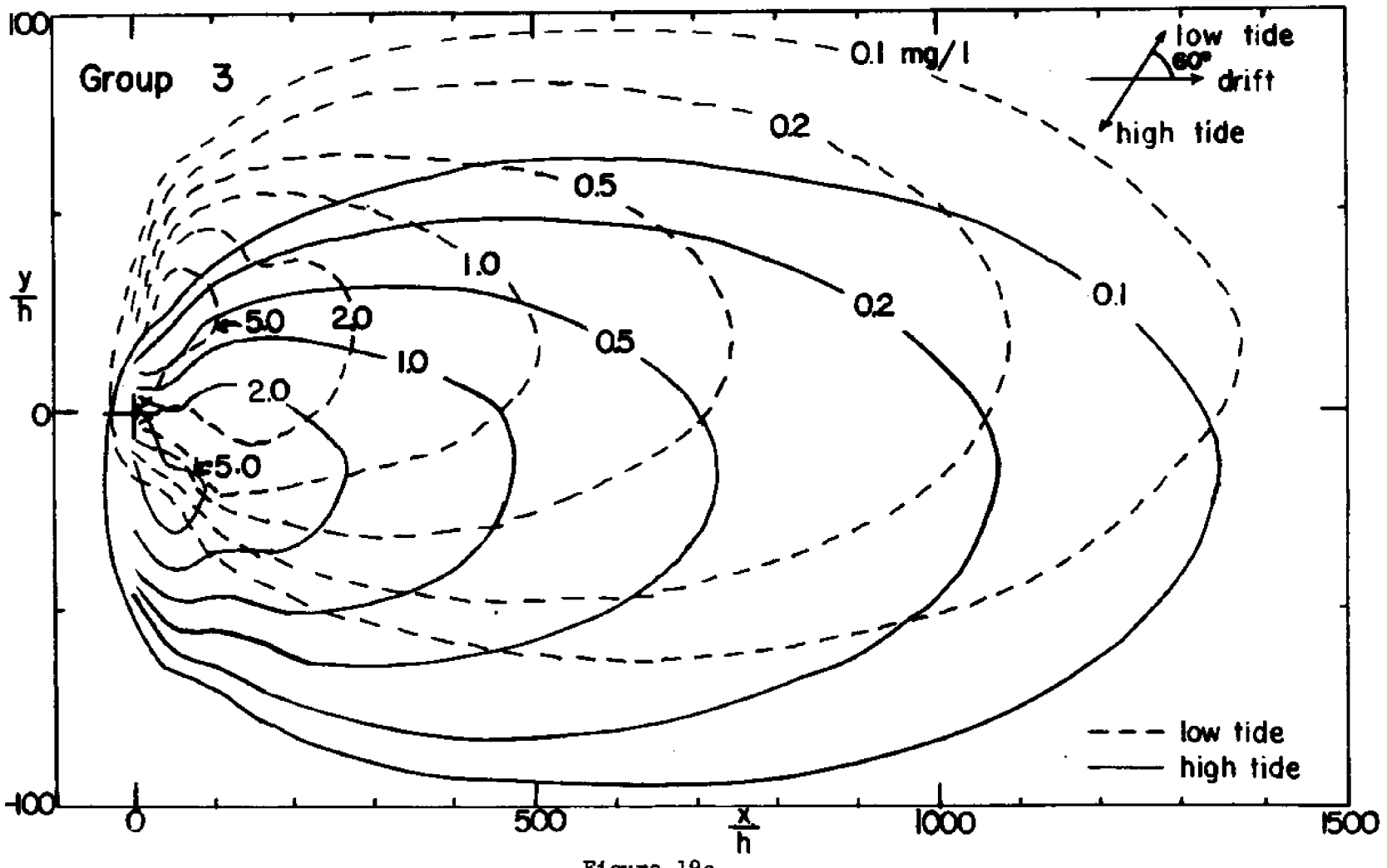

Figure 19c

Distribution of Average Concentration, $\bar{c}$, of Group 3 under Average Conditions

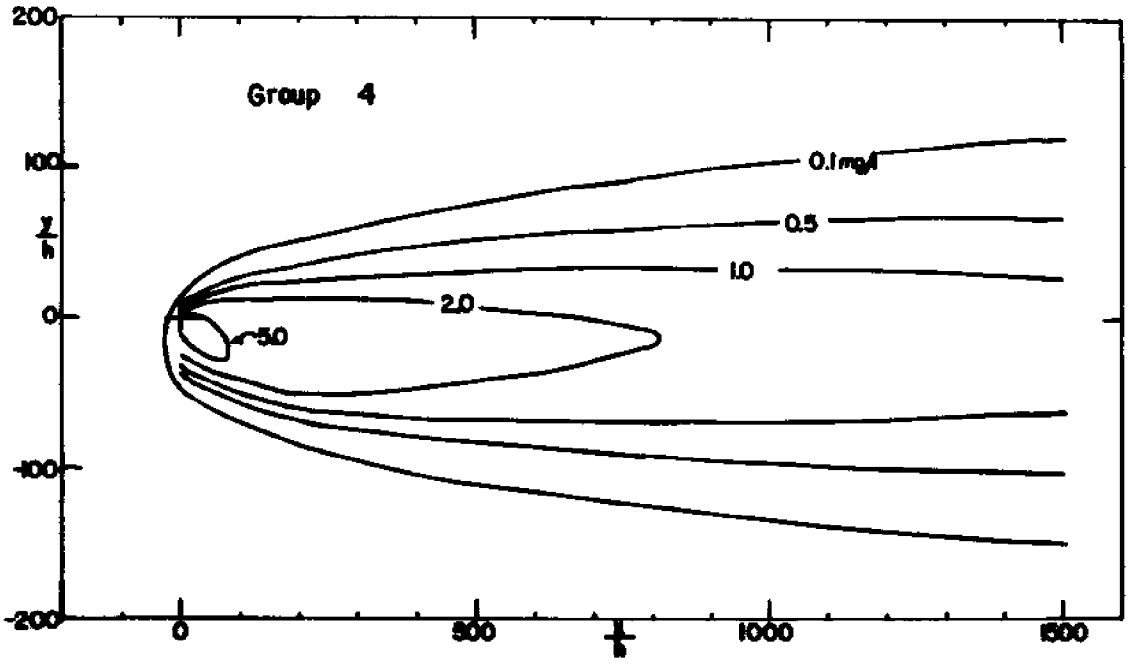

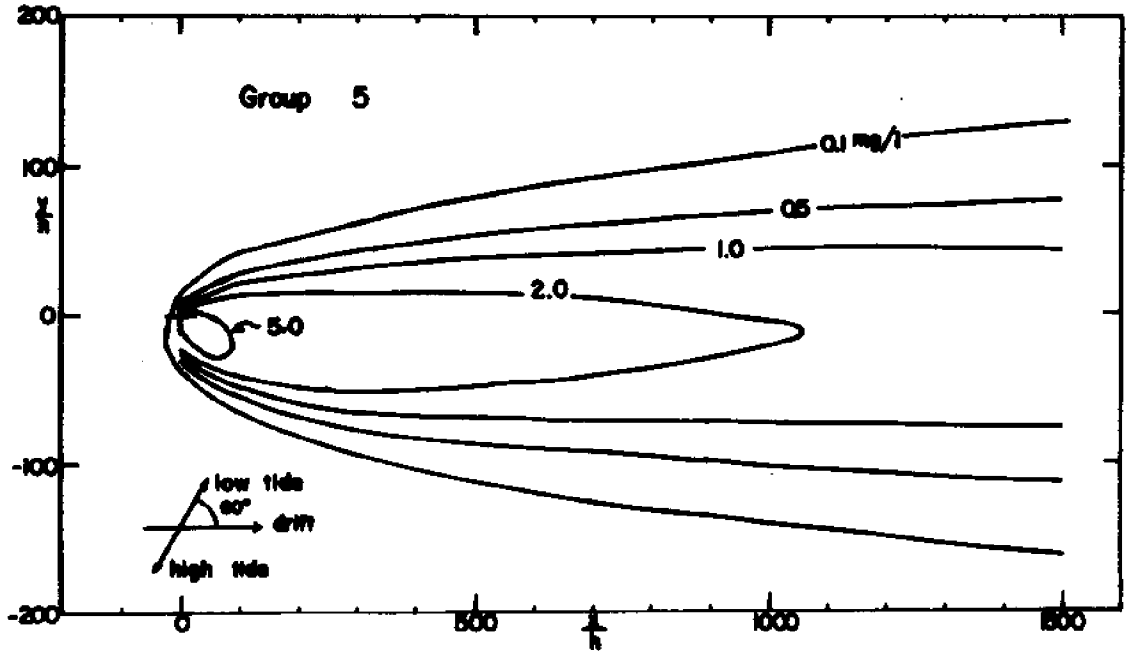

Figures 19d,e
Distribution of Average Concentration, $\bar{c}$, of Groups 4 and 5 under Average Conditions, at High Water Slack

The dependence on tidal time is more pronounced in the vicinity of the source, where the width of the plume is small. However, the model is not reliable in such small distances, as discussed in Section 3.2.

As was indicated in Section 6.3, the deposition of sediments on the bottom over a period of time can also be evaluated by the present model. Naturally, the limitations concerning the reliability of results for the suspended matter also apply to the results for the deposition. As an example, the average deposition rates (mass per unit time per unit area) are shown in Figure 20 for the sediment group 3, under the average conditions stated in Table 8. The average of the values of $\bar{c}$ at high and low water at a point was taken as a representative value over the tidal cycle. Hence, the average deposition rate was computed by multiplying this value by $w_s \phi(0)$. The resulting iso-deposition curves are almost symmetrical about the drift axis. They are valid after steady-state has been reached. By multiplying the values given on the figure by the duration of dredging, the amount of sediments deposited at various locations can be found. This amount, as well as the rate of deposition, are quite important from an ecological point of view. Nevertheless, even more important for an overall assesment of the dredging impact are the percentages of the total sediment discharge settled within a certain distance from the source.

An approximate calculation was carried out in the following way. The areas of the iso-deposition lines of Figure 20 were measured by a planimeter and, by assuming linear interpolation between the curves, the total deposition in gr/tidal cycle within each curve was computed. These quantities were related to the total amount injected which is $0.02 \times 10^6 \times 45600 = 912 \times 10^6$ gr/tidal cycle. The results are presented in Figure 21. It must be pointed out that the linear interpolation used overestimates the true percentages that are deposited within a certain area. For an accurate calculation many more iso-deposition lines between those of Figure 20 are needed.

With respect to the verification of the model, adequate information is lacking for the time being. The actual dredging operation in the summer of 1974 would have been an excellent opportunity for a quantitative evaluation of the model's weaknesses and for its improvement. The previously mentioned "glass bead study" (Section 7.1) can provide only qualitative information, mainly because it involved an instantaneous injection. At this time only preliminary data on the number of sphalerite particles found in suspension in various places in the Bay during the experiment are available (13). A total amount of 2.9×10^{15} sphalerite particles was introduced into the sea. The predominant particle size was between 1 and 8μ but their density was larger than that of the natural silt or clay, being about 4.0 gr/cm^3. Therefore their settling velocities are close to those of the sediment groups 3 and 4 considered

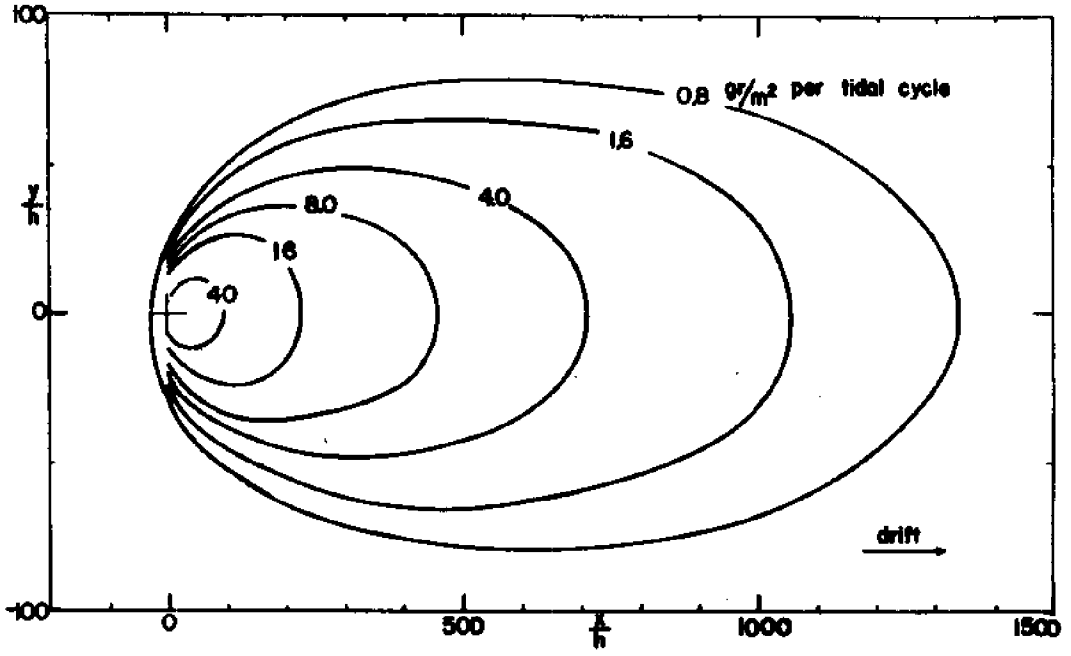

Figure 20 Deposition Rates of Sediment Group 3 Under Average Conditions

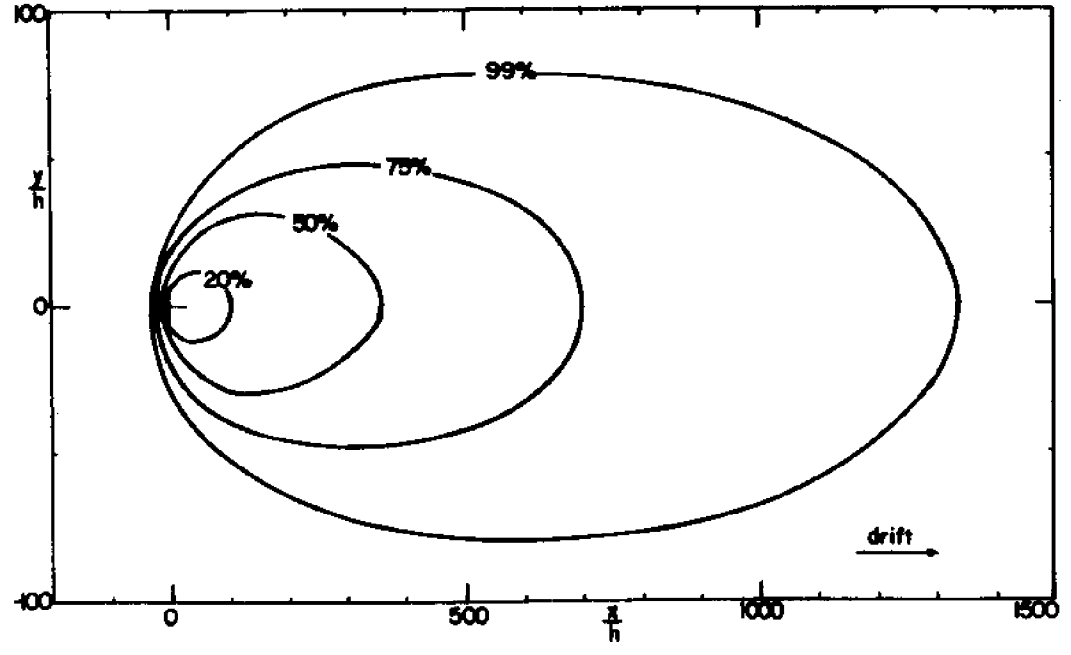

Figure 21 Percentage of Total Discharge of Group 3 Deposited Within Area Shown, Under Average Conditions

in this study. The plume closely followed the mean drogue path (Figure 12), thus confirming the primary importance of the drift direction. The particles moved initially E-NE and ultimately SE. Their spread about the mean direction was large, and apparently due to the changes in the drift with time and space. The presence of concentrations of 300 particles/liter in Cape Cod Bay 5 days or 10 tidal cycles after the injection indicates a net SE drift of about $\frac{25\text{n. miles}}{5 \text{ days}} = 5\text{n. miles/day} \simeq 10$ cm/sec, which confirms the average values obtained from the drogue studies. The drogue data cover a relatively small area around the proposed dredging site and the conclusions based on these should not be extended to the entire Bay without reservation. The drift velocity is possibly higher in the Southern part of the Bay, and a circulation pattern is probably present around Cape Cod Bay. The fact that the beads travelled all the way to Cape Cod, a distance of about 1500 times the depth, further indicates that the model predictions with respect to length of the dispersing plume are close to reality. It may be mentioned that at the time of the glass bead study such a distance of travel was quite unexpected.

CHAPTER 8

CONCLUSIONS AND RECOMMENDATIONS

The model presented herein was necessarily based on simplifying assumptions, so that an analytical solution could be found. It is basically intended to give the equilibrium distribution of suspended sediments, injected from a continuous vertical line source. The transient behavior of the dispersing sediment plume can also be estimated under certain conditions (as indicated in Section 6.1). In addition, information is provided on the deposition patterns to be expected from such a continuous source of sediments.

The relative importance of the various parameters entering into the model, investigated in Section 7.6, is established and it is shown that the net drift and the sediment settling velocity are the primary factors determining the distribution of the suspended matter around the source. Also of importance is the dispersion coefficient in a direction normal to the net drift.

A technique was developed for the analysis of drogue data to yield values for the advective and dispersion terms, taking into account the nonuniformity of the sediment distribution over the vertical. Actual data were used for determining these values for the Massachusetts Bay. However, only 3 or 4 drogues were used in each case, and the tracks covered in the field studies were relatively short. More extensive data, for longer periods of time, are needed in order to estimate the hydrodynamic parameters over the long distances that the fines are

expected to travel according to the models results. In the analysis of such long-term drogue data the change of net drift between tidal cycles can be incorporated to yield an approximate net water movement composed of a sequence of linear segments in the appropriate directions. In that case, the model could be modified and the plume adjusted so as to follow the changing net drift direction. In this way the model could be extended to any form of water movement prevailing in a certain area. The tidal component could also be similarly adjusted. The assumption of constant net drift in the present model does not reflect natural conditions in view of the resulting long dispersion patterns. If it is to be maintained, a much larger value for the lateral dispersion coefficient should probably be used in order to increase the spread of the suspended matter. With the present model the width of the sediment cloud is underestimated, while the prediction of the length is, at least, conservative.

Nevertheless, probably the most important restriction of the model is the assumption of one-layer shear flow. This assumption allowed use of the same vertical equilibrium distribution as in open channels and, furthermore, a significant simplification in the structure of the model, through independent treatment of the horizontal and vertical distributions. Secondary currents due to density variations, however, are often very important to the transport and dispersion of suspended sediments. If the suspended matter is assumed to be carried by density currents near the sea bed, the model could possibly be applied for the reduced height of that current. The non-dimensional

plots given in Figures 19, 20 and 21 would be applicable approximately although the advective and dispersion terms would have to be redefined. The main difficulty for such an extension of the model lies in the violation of the surface boundary condition.

Despite the limitations discussed so far, it is believed that the present model is a relatively simple tool that can predict to some approximation the impact of dredging or other similar activities in the coastal zone. The preliminary results of the "glass bead study" of NOMES seem, at this point, quite encouraging.

Further research is necessary to relax some of the restrictive assumptions employed in this model. A better understanding of the effects of flocculation on the settling rates of fines is very desirable. Also, the hydrodynamic characteristics must be modeled in relation to the meteorological conditions. Until such additional research produces more realistic inputs, the model developed in this study can be useful provided it is applied with full understanding of the inherent assumptions and limitations involved.

REFERENCES

1. C.S. Ahn and P.E. Smith: "The first report on a study to forecast nuclear power plants effects on coastal zones", Environmental Equipment Division, Waltham, Massachusetts, December 1972

2. ASCE Task Committee on Sedimentation: "Sediment Transportation Mechanics: D. Suspension of Sediment", J. Hydraulics Div., ASCE, No. HY 5, September 1963

3. W.R. Boehmer: "A Preliminary Exercise in Modeling the 'Rain of Fines'", Div. of Mineral Resources, Dept. of Natural Resources, Commonwealth of Massachusetts, Spring 1973

4. G. Christodoulou, W.F. Leimkuhler and B.R. Pearce: Unpublished report on current measurements by drogues in Massachusetts Bay, M.I.T., Department of Civil Engineering, September 1973

5. A.N. Diachishin: "Dye Dispersion Studies", Journal of the Sanitary Eng. Div., ASCE, Vol. 89, No. SA1, January 1963

6. W.F. Dobbins: "Effects of Turbulence on Sedimentation", Trans. ASCE, Vol. 109, Paper No. 2218, 1944

7. H.A. Einstein and R.B. Krone: "Experiments to Determine Modes of Cohesive Sediment Transportation in Salt Water", Journal of Geophysical Research, Vol. 67, April 1962

8. J.W. Elder: "The Dispersion of Marked Fluid in Turbulent Shear Flow", Journal of Fluid Mechanics, Vol. 5, May 1959

9. H.B. Fischer: "The Mechanics of Dispersion in Natural Streams", Journal of the Hydraulics Div., ASCE, Vol. 93, No. HY 6, November 1967

10. S.L. Frankel and B.R. Pearce: "Determination of Water Quality Parameters in the Massachusetts Bay (1970-1973)", Ralph M. Parsons Laboratory for Water Resources and Hydrodynamics, M.I.T., Department of Civil Engineering, Technical Report No. 174, November 1973

11. W.H. Graf: "Hydraulics of Sediment Transport", McGraw-Hill Book Company, 1971

12. D.R.F. Harleman: "One-Dimensional Models", Chapter 3 in "Estuarine Modelling: An Assessment" by TRACOR, Inc., for the Water Quality Office, EPA, February 1971

13. W.N. Hess: "Preliminary report on the NOMES glass bead experiment", NOAA Environmental Research Lab., Boulder, Colorado, July 5, 1973

14. E.R. Holley, D.R.F. Harleman and H.B. Fischer: "Dispersion in Homogeneous Estuary Flow", Journal of the Hydraulics Div., ASCE, Vol. 96, No. HY 8, August 1970

15. E.R. Holley and D.R.F. Harleman: "Dispersion of Pollutants in Estuary Type Flow", Hydrodynamics Lab., M.I.T., Department of Civil Engineering, Technical Report No. 74, January 1965

16. A.T. Ippen: "The Distribution of Suspended Material over Cross-sections of Open Channels", unpublished manuscript, 1934

17. A.T. Ippen: "A New Look at Sedimentation in Turbulent Streams", Journal of the Boston Society of Civil Engineers, July 1971

18. H.E. Jobson and W.W. Sayre: "Vertical Transfer in Open Channel Flow", Journal of the Hydraulics Div., ASCE, Vol. 96, No. HY 3, March 1970

19. H.E. Jobson and W.W. Sayre: "Predicting Concentration Profiles in Open Channels", Journal of the Hydraulics Div., ASCE, Vol. 96, No. HY 10, October 1970

20. R.B. Krone: "A Field Study of Flocculation as a Factor in Estuarial Shoaling Processes", Technical Bulletin No. 19, Committee on Tidal Hydraulics, Corps of Engineers, June 1972

21. Marine Geology and Geophysics Lab., AOML: "Preliminary Plan for the NOMES Tracer Experiment", May 15, 1973

22. A. Okubo: "Oceanic Diffusion Diagrams", Deep Sea Research, Vol. 18, 1971

23. A. Okubo: "The Effect of Shear in an Oscillatory Current on Horizontal Diffusion from an Instantaneous Source", Oceanology and Limnology, Vol. 1, No. 3, 1967

24. E. Partheniades: "A Summary of the Present Knowledge of the Behavior of Fine Sediments in Estuaries", Hydrodynamics Lab., M.I.T., Department of Civil Engineering, Technical Note No. 8, June 1964

25. E. Partheniades: "Erosion and Deposition of Cohesive Sediments", Chapter 20 in "Sedimentation - Symposium to Honor Professor H.A. Einstein", edited by H.W. Shen, Berkeley, 1971

26. H. Rouse: "Fluid Mechanics for Hydraulic Engineers", 2nd Ed., Dover, New York, 1961

27. W.W. Sayre: "Dispersion of Silt Particles in Open-Channel Flow", Journal of the Hydraulics Div., ASCE, Vol. 95, No. HY 3, May 1969

28. S.P. Sullivan and F. Gerritsen: "Dredging Operation Monitoring and Environmental Study, Kawaihae Harbor, Hawaii", J. Look Lab. of Oceanographic Engineering, Technical Report No. 25, Department of Ocean Eng., University of Hawaii, September 1972

29. W.C. Taggart, C.A. Yermoli, S. Montes and A.T. Ippen: "Effects of Sediment Size and Gradation on Concentration Profiles in Turbulent Flow", Ralph M. Parsons Laboratory for Water Resources and Hydrodynamics, M.I.T., Department of Civil Engineering, Technical Report No. 152, August 1972

30. Tennessee Valley Authority, Corps of Engineers, Dept. of Agriculture, Geological Survey, Bureau of Reclamation, Indian Service and the Iowa Institute of Hydraulic Research: "Methods of Analyzing Sediment Samples", Report No. 4 in "A Study of Methods Used in Measurement and Analysis of Sediment Loads in Streams", University of Iowa, November 1941

31. Tetra Tech, Inc.: "Further Studies on the Prediction of the Radioactive Debris Distribution Subsequent to a Deep Underwater Nuclear Explosion", Final Report, October 1969

32. P.M. Vogel: "Intermediate Grain Size Distribution Data", Campus Correspondence, University of New Hampshire, March 28, 1973

33. W.T. Wnek and E.G. Fochtman: "Mathematical Model for Fate of Pollutants in Near-Shore Waters", Illinois Inst. of Tech. Research Institute, April 1972

APPENDIX A

SETTLING TUBE MEASUREMENTS

Run No. 1
Kaolinite

Initial Concentration 100 mg/ℓ
Initial Turbidity Reading 64 FTU
Background Turbidity 0.15 FTU

Time (hrs.)	Turbidity Readings (FTU)						Percent Settled
	1	2	3	4	5	6	
1.2	47	-	53	-	55	57	18.6
17.8	18	-	-	17.5	-	18	71.8
24.8	13	-	13.0	-	-	13	79.7
41.8	9.0	-	8.7	-	-	8.4	86.5
48.5	7.2	-	7.1	-	-	7.2	89.0
64.3	5.4	-	5.6	-	-	5.5	91.5
96.8	3.6	-	3.7	-	-	3.7	94.3
160.6	2.0	-	2.0	-	-	2.1	97.0
233.0	1.3	1.3	1.3	1.6	1.3	1.3	98.2

Run No. 2
Kaolinite

Initial Concentration 10 mg/ℓ
Initial Turbidity Reading 7.0 FTU
Background Trubidity 0.40 FTU

Time (hrs.)	Turbidity Readings (FTU)						Percent Settled
	1	2	3	4	5	6	
0.8	6.1	-	6.6	-	-	6.9	6.5
2.7	6.0	-	6.1	-	-	6.4	12.7
22.9	3.3	-	3.9	-	-	3.2	52
47.3	2.2	-	2.5	-	-	2.8	68
70.5	2.0	-	1.95	-	-	2.05	76
100.6	1.5	-	1.7	-	-	1.75	80.5
149.3	-	1.3	-	1.25	-	1.6	87.1
265.8	-	0.68	-	0.67	-	0.67	95.9

Run No. 3
Illite

Initial Concentration 10 mg/ℓ
Initial Turbidity Reading 4.0 FTU
Background Turbidity 0.20 FTU

Time (hrs.)	Turbidity Readings (FTU) 1	2	3	4	5	6	Percent Settled
2.0	2.6	-	3.2	-	-	3.1	25.1
3.8	2.2	-	2.8	-	-	2.8	35.0
21.7	1.75	-	1.6	-	-	1.5	63.2
29.3	1.35	-	1.5	-	-	1.5	66.7
77.4	1.1	-	1.1	-	-	1.15	76.0
119.2	0.96	-	0.87	-	-	0.83	83.2
173.1	0.70	-	0.77	-	-	0.83	84.8

Run No. 4
Illite

Initial Concentration 100 mg/ℓ
Initial Turbidity Reading 36 FTU
Background Turbidity 0.20 FTU

Time (hrs.)	Turbidity Readings (FTU) 1	2	3	4	5	6	Percent Settled
0.6	24	29.5	33.5	-	35	36	10.2
3.3	17	-	23	-	-	32	29.5
27.7	7.6	-	8.0	-	-	8.1	78.5
47.0	4.75	-	5.0	-	-	5.0	86.7
142.0	1.6	-	1.5	-	-	1.5	96.2

Run No. 5
Boston Harbor Mud

Initial Concentration 10mg/ℓ
Initial Turbidity Reading 5.0 FTU
Background Turbidity 0.25 FTU

Time (hrs.)	Turbidity Readings (FTU) 1	2	3	4	5	6	Percent Settled
1.7	2.4	-	3.4	-	-	3.5	37.2
4.6	2.1	-	2.9	-	-	3.1	46.3
17.4	2.0	-	2.0	-	-	2.5	60.0
23.8	1.75	-	1.9	-	-	2.15	64.5
65.8	1.1	-	1.3	-	-	1.6	78.7
124.1	0.88	-	0.92	-	-	0.88	86.3
189.9	0.62	-	0.62	-	-	0.65	91.7

Run No. 6
Boston Harbor Mud

Initial Concentration 100 mg/ℓ
Initial Turbidity Reading 52 FTU
Background Turbidity 0.15 FTU

Time (hrs.)	Turbidity Readings (FTU) 1	2	3	4	5	6	Percent Settled
0.6	35.5	-	43.5	-	-	47	17.2
2.9	23	-	33	-	-	39	33.3
6.1	16	-	25	-	-	28	53.8
22.7	5.8	-	7.2	-	-	9.7	82.7
45.3	1.9	-	3.3	-	-	5.5	93.2
99.0	1.95	-	2.15	-	-	1.9	96.4
169.1	0.98	-	1.01	-	-	1.02	98.5
244.3	0.50	-	0.54	-	-	0.51	99.3

APPENDIX B

COMPUTER PROGRAM FOR ANALYSIS OF DROGUE DATA

```
0001                DIMENSION  T(5,50), X(5,50), Y(5,50),DEPTH(6),W(6),DST(50)
0002                DIMENSION  XX(5,50), YY(5,50),XXMEAN(50),YYMEAN(50),XXVAR(50)
0003                DIMENSION YYVAR(50),EX(50),EY(50),PHI(6I),CUM(6I),Z(6I),VXX(50)
0004                DIMENSION VYY(50),SEP(6)
0005                DIMENSION WS(5)
0006                READ (5,300) NO
0007          300   FORMAT(I3)
0008                DO 299 IJK=1,NO
0009                NUMWT=0
0010                READ(5,40)STT,TINT,BOTDEP
0011          40    FORMAT(F8.0,F7.0,F5.0)
0012                READ(5,301) CAPPA,NSTEP,NCYC
0013          301   FORMAT(F4.2,I4,I3)
0014                READ(5,308) NWS
0015          308   FORMAT(I2)
0016                READ(5,309)(WS(I),I=1,NWS)
0017          309   FORMAT(5F12.7)
0018                I=1
0019                M=1
0020          3     READ(5,10) N,IDEP,IH,IM,IS,IY,IX
0021          10    FORMAT(I3,11X,I3,I3,I2,I2,I8,I8)
0022                IF(N+1) 12,4,5
              C
              C     SIGNAL ALL UNUSED ELEMENTS OF ARRAY WITH
              C     NEGATIVE NUMBER
              C
0023          4     DO 1 III=I,50
0024                T(M,III)=-10000000.
0025          1     CONTINUE
0026                I=1
0027                M=M+1
0028                GO TO 3
              C
              C     PUT INTEGER INFORMATION INTO REAL ARRAYS
              C
0029          5     T(M,I)=FLOAT(3600*IH+60*IM+IS)
0030                X(M,I)=FLOAT(IX)
0031                Y(M,I)=FLOAT(IY)
0032                DEPTH(M)=FLOAT(IDEP)
0033                I=I+1
0034                GO TO 3
              C
              C     SIGNAL UNUSED ELEMENTS OF LAST ARRAY AS WITH OTHERS
              C
0035          12    DO 13 III=I,50
0036                T(M,III)=-10000000.
0037          13    CONTINUE
              C
              C     MAKE TIME CORRECTIONS SO THAT TIME IS ALWAYS INCREASING
              C
0038                DO 30 K=1,M
0039                DO 25 KK=1,49
0040                Q=T(K,KK+1)-T(K,KK)
```

```
0041                    IF(Q) 17,25,25
0042            17      DO 23 KKK=KK,49
0043                    T(K,KKK+1)=T(K,KKK+1)+86400.
0044            23      CONTINUE
0045            25      CONTINUE
0046            30      CONTINUE
                C
                C       SET UP DESIRED TIME ARRAY
                C
0047                    DST(1)=STT
0048                    DO 32 J=1,49
0049                    DST(J+1)=DST(J)+TINT
0050            32      CONTINUE
0051                    JJ=50
                C
                C       ASSOCIATE X AND Y VALUES WITH DESIRED TIME ARRAY
                C
0052                    DO 60 L=1,M
0053                    I=1
0054                    J=1
0055            33      IF(DST(J)-T(L,I)) 50,35,35
0056            35      IF(DST(J)-T(L,I+1)) 42,42,55
0057            42      DT=(DST(J)-T(L,I))/(T(L,I+1)-T(L,I))
0058                    XX(L,J)=X(L,I)+(X(L,I+1)-X(L,I))*DT
0059                    YY(L,J)=Y(L,I)+(Y(L,I+1)-Y(L,I))*DT
0060            50      J=J+1
0061                    GO TO 33
0062            55      I=I+1
0063                    IF (T(L,I)+1) 57,57,35
                C
                C       LENGTH USED IS THAT OF THE SMALLEST ARRAY
                C
0064            57      IF(JJ-J) 60,58,58
0065            58      JJ=J-1
0066            60      CONTINUE
0067                    MP=M+1
0068                    MZ=M-1
0069                    DO 80 L=1,MZ
0070                    IF(L-1) 65,65,68
0071            65      F2=0
0072                    GO TO 73
0073            68      F2=(DEPTH(L-1)+DEPTH(L))*0.5
0074            73      F1=(DEPTH(L)+DEPTH(L+1))*0.5
0075                    W(L)=(F1-F2)/BOTDEP
0076            80      CONTINUE
0077                    DFAC=1.-DEPTH(M)/BOTDEP
0078                    W(M+1)=DFAC/(9.*ALOG(DFAC))
0079                    W(M)=1.-W(M+1)-(DEPTH(M-1)+DEPTH(M))/(2.*BOTDEP)
0080                    WRITE(6,310)
0081            310     FORMAT(1H1)
0082                    WRITE(6,119)
0083            119     FORMAT(3X,'FOR NEUTRALLY BOYANT PARTICLES')
0084                    WRITE(6,120) (W(L),L=1,MP)
```

```
0085          120   FORMAT(2X,' WEIGHTS',1X,10F6.3)
0086                XX(M+1,1)=XX(M,1)
0087                YY(M+1,1)=YY(M,1)
0088                DO 82 J=1,JJ
0089                XX(M+1,J)=XX(M+1,1)
0090                YY(M+1,J)=YY(M+1,1)
0091          82    CONTINUE
0092                DO 86 L=1,MP
0093                DO 88 J =2,JJ
0094                XX(L,J)=(XX(L,J)-XX(L,1))*30.5
0095                YY(L,J)=(YY(L,J)-YY(L,1))*30.5
0096          88    CONTINUE
0097                XX(L,1)=0.
0098                YY(L,1)=0.
0099          86    CONTINUE
0100                DO 96 J=1,JJ
0101          96    DST(J)=DST(J)-STT
0102          87    DO 84 J=1,JJ
0103                XXMEAN(J)=0.
0104                YYMEAN(J)=0.
0105                XXVAR(J)=0.
0106                YYVAR(J)=0.
0107          84    CONTINUE
0108                DO 90 J=1,JJ
0109                DO 89 L=1,MP
0110                XXMEAN(J)=XXMEAN(J)+XX(L,J)*W(L)
0111                YYMEAN(J)=YYMEAN(J)+YY(L,J)*W(L)
0112          89    CONTINUE
0113          90    CONTINUE
0114                DO 92 J=2,JJ
0115                VXX(J)=(XXMEAN(J)-XXMEAN(J-1))/TINT
0116                VYY(J)=(YYMEAN(J)-YYMEAN(J-1))/TINT
0117          92    CONTINUE
0118                CALL TIDVEL(NCYC,JJ,DST,XXMEAN,YYMEAN,TINT,DRIFMG,DRIFDR,UT,
                   1TIDEDR,LAST)
0119                WRITE (6,130)
0120          130   FORMAT(    '   TIME',5X,'MEAN X',5X,'MEAN Y',8X,'C VAR',8X,'N VAR',
                   19X,'DISP C',8X,'DISP N',7X,'VEL X',5X,'VEL Y')
0121.               WRITE(6,131)
0122          131   FORMAT(3X,'(SEC)',6X,'(CM)',6X,'(CM)',7X,'(CM2/SEC)',5X,'(CM2/SEC)
                   1',5X,'(CM2/SEC)',5X,'(CM2/SEC)',4X,'(CM/SEC)',2X,'(CM/SEC)',/)
0123                ST=SIN(DRIFDR)
0124                CT=COS(DRIFDR)
0125                DO 95 J=1,JJ
0126                XM=XXMEAN(J)*CT+YYMEAN(J)*ST
0127                YM=-XXMEAN(J)*ST+YYMEAN(J)*CT
0128                DO 94 L=1,MP
0129                XXX=XX(L,J)*CT+YY(L,J)*ST
0130                YYY=-XX(L,J)*ST+YY(L,J)*CT
0131                XXVAR(J)=XXVAR(J)+W(L)*(XXX-XM)**2
0132                YYVAR(J)=YYVAR(J)+W(L)*(YYY-YM)**2
0133          94    CONTINUE
0134          95    CONTINUE
```

```
0135                    DO 195 J=2,JJ
0136                    EX(J)=(XXVAR(J)-XXVAR(J-1))/(2.*TINT)
0137                    EY(J)=(YYVAR(J)-YYVAR(J-1))/(2.*TINT)
0138              195   CONTINUE
0139                    DO 141 J=2,JJ
0140                    WRITE (6,140) DST(J),XXMEAN(J),YYMEAN(J),XXVAR(J),YYVAR(J)
                       1,EX(J),EY(J),VXX(J),VYY(J)
0141              140   FORMAT (3F10.0,4E14.5,2F10.3)
0142              141   CONTINUE
0143                    CALL CONVRT(NCYC,LAST,DRIFNG,DRIFDR,UT,TIDEDR,EX,EY)
0144              293   IF(NUMWT)294,294,295
0145              294   CALL USTA (NCYC,JJ,VXX,VYY,DST,USTAR,TINT)
0146              295   NUMWT=NUMWT+1
0147                    IF(NWS-NUMWT)299,83,83
0148              83    WS1=WS(NUMWT)
0149                    WRITE (6,315)WS1
0150              315   FORMAT('1',3X,'NORMALIZED VERTICAL PROFILE FOR SETTLING VELOCITY',
                       1F12.7,2X,'CM/SEC',/)
0151                    CALL PROFIL(PHI,CUM,Z,WS1,USTAR,CAPPA,NSTEP,BOTDEP)
0152                    CALL WEIGHT(W,SED,DEPTH,CUM,M,BOTDEP,Z,NSTEP)
0153                    GO TO 87
0154              299   CONTINUE
0155                    CALL EXIT
0156                    END
```

```
0001                  SUBROUTINE TIDVEL(NCYC,JJ,DST,XXMEAN,YYMEAN,TINT,DRIFMG,DRIFDR,
                     1UT,TIDEDR,LAST)
                      C
                      C     THIS ROUTINE COMPUTES THE MEAN WEIGHTED TIDAL AND NET DRIFT
                      C     VELOCITIES GIVEN THE MEAN WEIGHTED DROGUE MOTION (XXMEAN,YYMEAN)
                      C
0002                  DIMENSION DST(50),XXMEAN(50),YYMEAN(50)
0003                  WRITE(6,311)
0004                311 FORMAT(1H1)
0005                  PI=3.14159
0006                  NDST=45600./TINT
0007                  REM=45600.-NDST*TINT
0008                  LAST=NCYC+NDST
0009                  IF(LAST-JJ)15,15,14
0010                14  WRITE(6,301)
0011                301 FORMAT(//,'  TIDAL CYCLE OVERRUNS RECORD IN TIDVEL
                     1_COMPUTATIONS MADE ON REDUCED AVAILABLE CYCLE')
0012                  LAST=JJ
0013                  REM=0.
0014                  XXMEAN(LAST+1)=XXMEAN(LAST)
0015                  YYMEAN(LAST+1)=YYMEAN(LAST)
0016                15  XLAST=XXMEAN(LAST)+(XXMEAN(LAST+1)-XXMEAN(LAST))*REM/TINT
0017                  YLAST=YYMEAN(LAST)+(YYMEAN(LAST+1)-YYMEAN(LAST))*REM/TINT
0018                  XDRIF=XLAST-XXMEAN(NCYC)
0019                  YDRIF=YLAST-YYMEAN(NCYC)
0020                  CYCDUR=DST(LAST)-DST(NCYC)+REM
0021                  DVELX=XDRIF/CYCDUR
0022                  DVELY=YDRIF/CYCDUR
                      C
                      C     DIRECTION OF NET DRIFT
                      C
0023                  DIRECT=ATAN(YDRIF/XDRIF)
0024                  IF(XDRIF)20,25,25
0025                20  IF(YDRIF)21,22,22
0026                21  DIRECT=DIRECT-PI
0027                  GO TO 25
0028                22  DIRECT=DIRECT+PI
0029                25  DRIFDR=DIRECT
003C                  DEGDIR=DRIFDR*(180./PI)
0031                  DRIFMG=SQRT((XDRIF)**2+(YDRIF)**2)/45600.
0032                  WRITE(6,303) DRIFMG,DEGDIR
0033                303 FORMAT(/,3X,'NET DRIFT=',F10.3,2X,'CM/SEC',10X,'DIRECTION FROM
                     1 EAST',F10.3)
0034                  DEVM1=0.
0035                  DEVM2=0.
0036                  XDEV1=0.
0037                  YDEV1=0.
0038                  XDEV2=0.
0039                  YDEV2=0.
004C                  NP=NCYC+1
0041                  DO 98 LL=NP,LAST
0042                  XO=DVELX*TINT*(LL-NCYC)+XXMEAN(NCYC)
0043                  YO=DVELY*TINT*(LL-NCYC)+YYMEAN(NCYC)
```

```
0044                DEVM=SQRT((XXMEAN(LL)-XD)**2+(YYMEAN(LL)-YD)**2)
0045                CALL TEST(NTEST,XXMEAN(NCYC),YYMEAN(NCYC),XXMEAN(LL),YYMEAN(LL),
                   1DIRECT)
0046                IF(NTEST)31,31,34
0047          31    IF(DEVM1-DEVM)32,38,38
0048          32    XDEV1=XXMEAN(LL)-XD
0049                YDEV1=YYMEAN(LL)-YD
0050                DEVM1=DEVM
0051                GO TO 38
0052          34    IF(DEVM2-DEVM)35,38,38
0053          35    XDEV2=XXMEAN(LL)-XD
0054                YDEV2=YYMEAN(LL)-YD
0055                DEVM2=DEVM
0056          38    CONTINUE
0057                XDEV=(XDEV1-XDEV2)
0058                YDEV=(YDEV1-YDEV2)
0059                TIDDIR=ATAN(YDEV/XDEV)
0060          185   TIDEDR=TIDDIR
0061                TIDDEG=TIDEDR*(180./PI)
                    C
                    C     MAX. TIDAL VEL. = DISP. OVER 1/2 CYCLE * PI/TIME OF CYCLE
                    C
0062                DEVT=SQRT(XDEV**2+YDEV**2)
0063                UT=DEVT*3.14159/CYCDUR
0064                WRITE (6,304) UT,TIDDEG
0065          304   FORMAT(/,3X,'MAX TIDAL VELOCITY=',F10.3,2X,'CM/SEC',10X,
                   1'DIRECTION FROM EAST',F10.3,/)
0066          999   RETURN
0067                END
```

```
0001                SUBROUTINE TEST(NTEST,X0,Y0,X1,Y1,DIRECT)
0002                PI=3.14159
0003                X=X1-X0
0004                Y=Y1-Y0
0005                DIREC1=ATAN(Y/X)
0006                IF(X)20,25,25
0007          20    IF(Y)21,22,22
0008          21    DIREC1=DIREC1-PI
0009                GO TO 25
0010          22    DIREC1=DIREC1+PI
0011          25    CONTINUE
0012                IF(DIRECT-DIREC1)30,38,30
0013          30    IF(DIRECT-DIREC1-PI)  36,36,38
0014          36    NTEST=1
0015                GO TO 99
0016          38    NTEST=-1
0017          99    RETURN
0018                END
```

```
0001                  SUBROUTINE  CONVRT(NCYC,LAST,DRIFMG,DRIFDR,UT,TIDEDR,EX,EY)
0002                  DIMENSION EX(50),EY(50)
0003                  EXS=0.
0004                  EYS=0.
0005                  NNCYC=NCYC+1
0006                  DO 190 J=NNCYC,LAST
0007                  EXS=EXS+EX(J)
0008                  EYS=EYS+EY(J)
0009            190   CONTINUE
0010                  AVEX=EXS/(LAST-NCYC)
0011                  AVEY=EYS/(LAST-NCYC)
0012                  THETA=ABS(DRIFDR-TIDEDR)
0013                  TIDEC=UT*COS(THETA)
0014                  TIDEN=UT*SIN(THETA)
0015                  WRITE(6,191) TIDEC,TIDEN
0016            191   FORMAT(/,3X,' TIDE ALONG DRIFT AXIS',F10.3,2X,'CM/SEC',10X,
                     1' TIDE  NORMAL TO IT',F10.3,2X,'CM/SEC')
0017                  WRITE(6,192) AVEX,AVEY
0018            192   FORMAT(/,3X,'AVERAGE DISPERSION COEF. ALONG DRIFT AXIS',E12.5,2X,
                     1'CM2/SEC,',10X,'NORMAL TO IT',E12.5,2X,'CM2/SEC')
0019                  RETURN
0020                  END
```

```
0001                  SUBROUTINE USTA (NCYC,JJ,VXX,VYY,DST,USTAR,TINT)
                C
                C     THIS ROUTINE COMPUTES THE SHEAR VELOCITY FROM A TWO
                C     DIMENSIONAL TRACK OF DROGUE POSITIONS, USING THE VELOCITY
                C     MAGNITUDES
                C
0002                  DIMENSION DST(50),VXX(50),VYY(50)
0003                  CVEL=C.
0004                  NDST=45600./TINT
0005                  LAST=NCYC+NDST
0006                  LLAST=LAST-1
0007                  IF(JJ-LAST)41,42,42
0008            41    WRITE(6,341)
0009            341   FORMAT(/,2X,'RECORD TOO SHORT FOR TIDAL CYCLE DESIRED IN USTA')
0010                  LLAST=JJ-1
0011            42    DO 115 LLL=NCYC,LLAST
0012                  CVEL=CVEL+SQRT(VXX(LLL+1)**2+VYY(LLL+1)**2)
0013            115   CONTINUE
0014            117   VELAV=CVEL/(LLL-NCYC+1)
                C
                C     ASSUMING THAT FRICTION COEFFICIENT, F, =.02
                C
0015                  USTAR=VELAV/20.
0016                  WRITE(6,331) USTAR
0017            331   FORMAT(/,3X,'USTAR=',F10.3,2X,'CM/SEC',/)
0018                  RETURN
0019                  END
```

```
0001                SUBROUTINE PROFIL(PHI,CUM,Z,WS,USTAR,CAPPA,NSTEP,ROTDEP)
                C
                C     THE PROGRAM COMPUTES THE NORMALIZED VERTICAL CONCENTRATION
                C     PROFILE FO A GIVEN DEPTH, SHEAR VELOCITY, AND SETTLING RATE.
                C
0002                DIMENSION PHI(61),S2(61),CUM(61),Z(61)
0003                Q=WS/(USTAR*CAPPA)
0004                Z(1)=0.
0005                RSTEP=NSTEP
0006                DZ=1./RSTEP
0007                CUM(1)=0.
0008                N=NSTEP+1
0009          20    DO 50 I=1,N
0010                IF(Z(I)-.05) 25,25,30
0011          25    ZZ=.05
0012                GO TO 40
0013          30    ZZ=Z(I)
0014          40    S2(I)=((1./ZZ-1.)/19.)**Q
0015                IF (I-N) 42,43,43
0016          42    Z(I+1)=Z(I)+DZ
0017          43    IF(I-1)50,50,45
0018          45    S3=.5*(S2(I)+S2(I-1))*DZ
0019                CUM(I)=CUM(I-1)+S3
0020          50    CONTINUE
0021                S5=1./CUM(N)
0022                WRITE(6,448)
0023          448   FORMAT(5X,'Z',10X,'PHI')
0024                DO 60 I=1,N
0025                PHI(I)=S5*S2(I)
0026                WRITE(6,450) Z(I),PHI(I)
0027          450   FORMAT(2X,F8.3,5X,E12.5)
0028          60    CONTINUE
0029                RETURN
0030                END
```

```
0001                SUBROUTINE WEIGHT(W,SEP,DEPTH,CUM,M,BOTDEP,Z,NSTEP)
0002                DIMENSION SEP(6),W(6),CUM(61),DEPTH(6),Z(61),ZZ(61),WT(6),DCUM(61)
0003                MP=M+1
0004                MZ=M-1
0005                DO 65 L=1,MZ
0006                SEP(L)=.5*(DEPTH(L+1)+DEPTH(L))/BOTDEP
0007          65    CONTINUE
0008                DFAC=1.-DEPTH(M)/BOTDEP
0009                SEP(M)=1.-DFAC/(9.+ALOG(DFAC))
0010                L=1
0011                NN=NSTEP+1
0012                DO 66 I=1,NN
0013                ZZ(I)=1.-Z(I)
0014                DCUM(I)=CUM(NN)-CUM(I)
0015          66    CONTINUE
0016                DO 70 I=1,NN
0017                IF(ZZ(NN-I+1)-SEP(L))70,68,68
0018          68    SFAC=(SEP(L)-ZZ(NN-I+2))/(ZZ(NN-I+1)-ZZ(NN-I+2))
0019                WT(L)=(DCUM(NN-I+2)+SFAC*(DCUM(NN-I+1)-DCUM(NN-I+2)))/CUM(NN)
0020                L=L+1
0021                IF(L-M)70,70,72
0022          70    CONTINUE
0023          72    DO 80 L=1,M
0024                IF(L-1)75,75,77
0025          75    W(L)=WT(L)
0026                GO TO 80
0027          77    W(L)=WT(L)-WT(L-1)
0028          80    CONTINUE
0029                W(M+1)=1.-WT(M)
0030                WRITE(6,120) (W(L),L=1,MP)
0031         120    FORMAT(/,2X,'WEIGHTS',1X,10F6.3)
0032                RETURN
0033                END
```

APPENDIX C

COMPUTER PROGRAM FOR THE HORIZONTAL DISTRIBUTION OF AVERAGE CONCENTRATION

```
0001            3     READ(5,8) IH,ITT,VOLR
0002            8     FORMAT(I2,I6,F6.3)
0003                  H=IH
0004                  TT=ITT
0005                  IF(H)1,2,2
0006            2     DO 70 K=1,5
0007                  READ (5,10) IXS,IYS,IXL,IYL,ID,T,T1,DT
0008           10     FORMAT(I3,I4,I4,I4,I4,F6.2,F6.2,F6.3)
0009                  XS=IXS
0010                  YS=IYS
0011                  XL=IXL
0012                  YL=IYL
0013                  D=ID
0014                  READ(5,11) IED,IEN,IUD,IVT,IVN,A,ANG
0015           11     FORMAT(2I7,3I5,F7.3,F7.2)
0016                  ED=IED
0017                  EN=IEN
0018                  VT=IVT
0019                  UD=IUD
0020                  VN=IVN
0021                  P=3.14159
0022                  WRITE(6,9) K
0023            9     FORMAT('1',2X,'FOR SEDIMENT GROUP NO.',I3)
0024                  WRITE(6,19) ANG
0025           19     FORMAT('  DRIFT DIRECTION IS',F8.2,'  DEGREES FROM EAST')
0026                  WRITE(6,12)
0027           12     FORMAT(//,' DIMENSIONLESS PARAMETERS:')
0028                  WRITE(6,13) IUD,IVT,IVN
0029           13     FORMAT('   NET DRIFT VELOCITY',I5,5X,'MAX TIDAL VELOCITY ALONG DRI
                     1FT AXIS',I5,5X,'NORMAL TO IT',I5)
0030                  WRITE(6,14) IED,IEN
0031           14     FORMAT('  DISPERSION COEFFICIENTS-',5X,' ALONG DRIFT AXIS',I7,5X,
                     1'NORMAL TO IT',I5)
0032                  WRITE(6,16) T,T1,DT
0033           16     FORMAT(2X,'TIME= ',F6.2,5X,'END OF INJECTION AT', F6.2,5X,'STEP OF
                     1 INTEGRATION',F6.3)
0034                  WRITE(6,17) A
0035           17     FORMAT('  DECAY FACTOR',F10.4)
0036                  WRITE(6,18)
0037           18     FORMAT(/,'     X       Y           C(BAR)/CO',/)
0038                  M=XL/D
0039                  N=YL/D
0040                  M1=(M+1)/2
0041                  N1=(N+1)/2
0042                  M2=2*M1+1
0043                  N2=2*N1+1
0044                  X=XS-M1*D
0045                  Y=YS-N1*D
0046                  ANG=P*ANG/180.
0047                  DO 60 I=1,M2
0048                  DO 65 J=1,N2
0049                  XPRIME=X*COS(ANG)+Y*SIN(ANG)
0050                  YPRIME=-X*SIN(ANG)+Y*COS(ANG)
```

```
0051                T2=0.
0052                Q1=0.
0053                Q3=0.
0054          49    IF(T1-T2) 100,51,51
0055          51    S1=(XPRIME-UD*(T-T2)+(.5*VT/P)*(COS(2*P*T)-COS(2*P*T2)))**2
0056                R1=4*ED*(T-T2)
0057                F1=S1/R1
0058                S2=(YPRIME+(.5*VN/P)*(COS(2*P*T)-COS(2*P*T2)))**2
0059                R2=4*EN*(T-T2)
0060                F2=S2/R2
0061                F3=A*(T-T2)
0062                F=F1+F2+F3
0063                R=4*P*(T-T2)*SQRT(ED*EN)
0064                Q=Q1
0065                IF(F-100.) 55,55,56
0066          55    Q1=(EXP(-F))/R
0067                GO TO 57
0068          56    Q1=0.
0069          57    T2=T2+DT
0070                IF(T2-DT) 49,49,52
0071          52    Q2=.5*(Q+Q1)*DT
0072                Q3=Q3+Q2
0073                GO TO 49
0074         100    CB=VOLR*TT*Q3/(H**3)
0075                WRITE(6,20) X,Y,CB
0076          20    FORMAT(F8.1,F9.1,4X,E10.3)
0077                Y=Y+D
0078          65    CONTINUE
0079                X=X+D
0080                Y=YS-N1*D
0081          60    CONTINUE
0082          70    CONTINUE
0083                GO TO 3
0084           1    CALL EXIT
0085                END
```